CHAPTER ONE

INTRODUCTION

1.1 Background of the Study

Wireless communication technologies having evolved over the years are faced with diverse challenges which the wireless service providers must proffer technical solutions to improve quality of service delivery. The desire of wireless service providers to establish additional base stations have been driven by the need to [1]:

i. Provide coverage to a geographic region where the service provider has not previously served.
ii. Fill in “dead spot” and areas where existing signals are weak or non-existence.
iii. Allow for the reuse of channels or spectrum bandwidth to support a larger number of mobile users.
iv. Meet the higher speed requirements of emerging technologies.

The demand to meet these needs had led to the proliferation of new cell towers which are capital intensive, pose environmental health hazards and distorts the beauty of the environment. Possible solution to the proliferation of cell towers is the placement of a number of Radio Frequency (RF) transceiver antennas at close proximity to one another, a concept known as co-location [2]. Co-location has been an aspect of interest in the fields of wireless communication; government and armed forces in the United States were the first to adopt the

strategy. They required different wireless platforms to share a small site because of the mobile nature of their equipment (e.g. battleships, aircraft and expeditionary fighting vehicles [3,4].

Co-location is globally accepted as a reliable way of lowering capital and operating expenditure, to improve the network quality and efficient network deployment for operators in telecommunication industry [5]. It promotes economic efficiency and completes quick network rollouts. With high cost of acquiring licenses in some countries like Nigeria, network operators have welcomed the possibility of sharing the cost of establishing cellular network infrastructures. Therefore it is practically proven that the cost of sharing facilities in a joint location is reasonably reduced compared to the cost of building one's own infrastructure [6]. Furthermore, it promotes a faster return on investment and an opportunity to focus more on the core business of the companies by providing telecommunication services [7]. It also encourages operators to pursue a cost-oriented policy with the added effects of reduction in the tariffs chargeable to consumers [8]. In a co-located setting, base station receivers have to receive weak desired signals in the presence of high-power transmit signals on single antenna mast, resulting to major interference [9].

Telecommunication infrastructure sharing (co-location) is of two types, namely; passive and active components sharing [10]. Active sharing involves sharing of electronic components and facilities such as base station,

microwave radio equipment, switches, antennas and receivers while passive sharing involves sharing of non-electronic components and facilities such as towers, shelters, electric supply, easements and ducts. The infrastructure sharing technique considered in this work is mainly on passive component sharing.

The benefits of passive infrastructure sharing include [6]:

a) To optimize savings on operators' Capital Expenditure (CAPEX) and Operating Expenditure (OPEX) required for site infrastructure development.
b) To ensure that unnecessary duplication of infrastructure is minimized or completely avoided so as to enhance sharing and to maximize the use of network facilities including but not limited to network capacity and capabilities, base station sites, backbone, towers etc.
c) To protect the environment by reducing the proliferation of infrastructure and consequently protect the beauty of environmental landscape.
d) To promote fair competition through equal access being granted to the installations and facilities of operators on mutually agreed terms.
e) To ensure that the economic advantages derivable from the sharing of facilities are harnessed for the overall benefit of all telecommunications stakeholders.

f) To promote the availability of a broad range of high quality, efficient, cost effective and competitive telecommunications and broadcasting services throughout the country by ensuring optimum utilization of telecommunications resources

g) To reduce barriers of entry into the telecommunications and broadcasting markets in an effort to increase competition in these markets through the provision of reasonable cost alternatives for network infrastructure.

h) To ensure that harmful interference (health hazard) is significantly reduced through the implementation of best practices in installation and safety precautions.

i) To ensure that new projects and developments should be catered for the unserved and the underserved areas to be in line with the Nigeria Communication Commission's (NCC) Policy.

Sequel to these benefits and developments, new operators seeking to expand their services in the city by building new cell sites are thus regulated and managed by the Nigerian Communication Commission licensed service vendors such as the IHS Plc, the Swap technologies, the MTI and the Helios Tower for rent of cell sites and infrastructure sharing to Nigeria telecommunication operators [11,12]. The practical validation of this new development will boost the economic situation and equally promote fair

competition among telecommunication licensees in Nigeria. The drive in this co-location reform though has guaranteed lots of benefits to the industry, pose quality service challenges to the network operators and the end user equipment, due to the presence of interference by the co-located interfering network. Hence required necessary mitigation approach.

Interference in radio frequency may be defined as the unwanted signals generated from other transmitters which interfere with the desired signal [13]. It is a key factor affecting the network quality in terms of call quality, call drop, handoff, conversation quality, network coverage, and capacity [14]. Radio Frequency Interference (RFI) in mobile communication network may be caused by such factors as: an original dedicated radio system occupying an existing frequency resource, improper network configurations by different operators and problematic configuration in the transmitter. Others include: cell overlapping, Electromagnetic Compatibility (EMC) and intentional interference [15]. Primary forms of interference to mobile communication systems mainly consist of common frequency interference, adjacent channel interference, out-of-band emission, inter-modulation emission and receiver blocking interference. Interferences between the transmitted signals and the received signals depend on factors such as the number of active channels at the site; the interval between the working frequency ranges of the two systems; the spatial separation between the receiver and transmitter (relative placement of

the antennas) and the characteristics of the technology including base station equipment [16].

Factors affecting the potential for interference between wireless operators have been accelerated by industry trends, including the auctioning of frequency bands, development of new broadband and multi-channel technologies and the antenna-to-antenna isolation between antennas which increased the probability of shared site interference [16,17].

Radio frequency interference basically consists of interference caused by natural phenomenon such as lightning, sun spots and man-made sources which are external and non-external interference [18].

External interference originated from sources such as; the repeater, radar, analog BaseTransciever Station (BTS), high power broadcast systems like TV and AM/FM radio. Others include a 2-way radio system, mobile telephone networks, emergency and public safety communications systems. There are also unintentional emitters that are classified among the sources of external interference. They consist of electric power lines, transformers, medical equipment, electro-mechanical switches, microwave ovens, Bluetooth devices, wireless video cameras, outdoor microwave links, wireless game controllers, Zigbee devices, fluorescent lights and other communication equipment [18].

Non-external interference comes from the self-interference which may be caused by illegal terminals, parameter setting problems, BTS faulty equipment and interference generated by co-located systems which primarily include: the transmitter noise (or sideband noise), the intermodulation distortion and the receiver blocking interference[18].

This work predominantly investigated the characteristic of the transmitter noise radiation from the co-located CDMA 2000 network on the overall performance of the WCDMA receiver system. The study also focused on finding a lasting solution to the sideband noise and considered the applications of Band Pass Filter (BPF) and Adaptive Noise Cancellation (ANC) techniques. The CDMA-2000 network used for this research study is owned by Visaphone network operator and the WCDMA network is owned by Mobile Telecommunication Network (MTN) operator. The two networks are co-located and administered by the IHS co-location Vendors.

The Transmit noise is the lowest continuous wideband emission which occurs when a transmitter radiates energy on its operating frequency as well as frequencies above and below the assigned frequency. They manifest as sideband noise signals that operate outside the transmit frequency band [19]. This mostly occurs when power amplifiers generate a significant amount of emission during its active mode and create a high level of non-linearity. This

undesired noise energy could fall within the pass band of a nearby receiver even if the receiver's operating frequency is several megahertz away

The co-located measurement environment considered for this research is located at plot 5 Peace close Federal Housing Estate Trans Ekulu, Enugu state, while the unco-located measurement environment is situated at Independent Layout opposite Brown and Brown Hotel, New Haven, Enugu. The two scenarios are characterized by free space propagation. This is because the propagation loss between the co-located CDMA2000 and WCDMA antennas is very small. The co-located environment was primarily considered owing to the fact that no mitigation technique(s) had previously been implemented on the reference network. The interference mitigation technique(s) developed from the research could serve as a mitigation approach to other co-located networks in Nigeria with the same characteristic features.

1.2 Problem Statement

In the near future, relative to the trend in rapid wireless development, various digital networks in the wireless world shall soon converge to become a unique system with a high data rate (e.g. the four generation technology (4G)), with low percentage level of interference. The need to achieve the goal necessitated the introduction of new and modified techniques. The research study was developed based on the salient network challenges and unforeseen-interference issues facing co-located networks, involving the downlink frequency of

CDMA-2000 and the uplink frequency of WCDMA networks operating at 1.9GHz within close frequency bands.

The following challenges conspicuously might result at the WCDMA receiver channel when the two networks are co-located on a single mast:

a. Received signal strength degradation.
b. Increase in system total noise floor level
c. High call blocking probability
d. Overall system capacity reduction.

This research work became necessary to develop a mitigation technique comprised Band Pass Filter (BPF) and Adaptive Noise Cancellation (ANC).

1.3 Aim and Objectives of the Study

The aim of the study is to mitigate the sideband noise in a WCDMA receiver front end caused by a co-located CDMA-2000 network using a hybrid of BPF and ANCT.

The specific objectives of the research include:

1. To determine using mathematical analysis, the performance effects of the interfering power of the CDMA 2000 transmitter on the WCDMA received signal stengthfrom the parametric values obtained in field measurements.
2. To evaluate the characteristic effects of the system noise floor levels and the percentage Carrier-to-Interference (C/I) ratio on the overall system performance and its significant impact on the co-located receiver channel using empirical data and mathematical analysis.

3. To determine the Normalized Frequency Specifications (NFS) and the Magnitude Specifications (MS) for the Band Pass filter design using Filter Modeling Technique (FMT) and specifications.
4. To obtain by simulation, the performance characteristics of the Magnitude response, phase response, group delay, impulse and pole/zero responses for the Band Pass digital Filter using Filter Design and Analysis Tool (FDATool) in MATLAB.
5. To develop an Adaptive Noise Cancellation Technique (ANCT) to demonstrate theoretical perfect error cancellation performance using MATLAB-Simulink test bed set-up.
6. To evaluate the characteristic performance at 52dB attenuation in terms of Amplitude Imbalance, Phase Error and Delay Mismatch using Noise cancellation performance criteria.
7. To compare the cancellation performance levels (dB) of the proposed research techniques using graphical representations.

1.4 Significance of the Study

The relevance of this research contributes towards network performance improvement in a co-located system involving CDMA2000 and WCDMA networks. Some of the benefits include:

a. Capacity and coverage maximization in a co-located network
b. Guaranteed optimum network availability
c. Rapid expansion of customer base services

d. Reduction in the proliferation of towers
e. Reduction in capital expenditure and more revenue generation

1.5 Scope and Limitations of Research

Interference could be generated by sources at a shared site (co-located scenario) and also by sources located some distances away from a shared site (co-existence scenario) [20]. The research investigation is exclusively on the sideband noise generated by sources at the shared site involving CDMA 2000 and WCDMA networks. The operating frequencies of interest in the study are 1920-1980MHz frequencies in the uplink for WCDMA network and 1960-1990 MHz frequencies in the downlink for CDMA2000 network. Relevant existing models were considered in the research.

The idea of increase in antenna-to-antenna isolation beyond the standard specifications of 50dB by NCC for co-located networks involving Personal Communication System (PCS) and Digital Communication System (DCS) at 1.9GHz was not relevant for the study.

The limitations of the research are as follows:

a. The study could not address the issue of intermodulation distortion and the Receiver Blocking effects which are among the primary interference issues faced in a co-located networks due to the huge time and cost required to embark on the experiments and analysis.

b. The research failed to utilize a real-life scenario hardware application for the ANC experimental test set-up due to the cost of the relevant equipment.
c. The research could not also utilize the actual conceptual simulation framework for the ANC test-bed analysis due to the unavailability of some basic parameters in the MATLAB-Simulink tool box such as the vector modulator (in-phase and quadrature-phase) and the directional couplers. User defined functions in the MATLAB-Simulink library browser were considered an alternative.

1.6 Thesis Structure

This thesis is outlined as follows: the background of the study, the problem statement, aims and objectives of the study, significance of the study, scope and limitations of the study are detailed in chapter one. Chapter two discussed some basic concepts required for the thesis which include: interference analysis, third generation wireless network, antenna isolation, radio frequency bands, band pass filters and adaptive cancellation systems. Theoretical background of the problem and the related literature reviews were also presented in chapter two. Chapter three described the proposed techniques, the characterization of the system and analysis, the measurement test-bed environment and configuration, and the proposed theoretical concept of adaptive noise cancellation techniques (ANCT). Chapter four performed the system configuration, experiment measurement, data collection and filter calculation procedure. It also addresses the filter design requirements and procedure, design specifications and implementation with the corresponding

graphical representations. The test-bed Matlab-simulink model build-up for the adaptive noise cancellation systems, the simulated performance results and the simulink generated graphs were demonstrated. Various cancellation performance models for amplitude imbalance, phase error and delay mismatch were exploited using graphical illustrations. Finally, chapter five summarizes the key outcomes, thesis contribution and research recommendations.

CHAPTER TWO

LITERATURE REVIEW

2.1 Mechanisms in Radio Frequency Transmission Pathway

Radio frequency (RF) front-ends are integral parts of wireless communication systems. In the transmitter front-end, the baseband modulated signals are up-converted to RF using a mixer and then power amplified before radiation through the antenna system [21]. The receiver front-end accordingly uses a low-noise amplifier to boost the weak received signals intercepted by the antenna and down-converts them to baseband signals using a mixer. Power amplifiers, low-noise amplifiers and mixers exhibit nonlinearity when operating at RF frequencies [21]. They introduce unwanted signal components or nonlinear distortions which add noise into the system.

In this chapter, the theoretical background of the problem and the summary of some related works by different authors and scholars on radio frequency interference are discussed.

2.2 Interference in Wireless Networks

Interference problems associated with mobile communications equipment are due to the problem of time congestion within the electromagnetic spectrum [21, 22, 23]. It is one of the limiting factors in the performance of cellular systems. It can occur from the jamming of the transmitted signal of one mobile station (MS) with another MS in the same cell (intra-cell interference) or because of a call in the adjacent cell (inter-cell interference). There can be

interference between the base stations operating at same frequency band or any other non-cellular system's energy leaking inadvertently into the frequency band of the cellular system (co-channel interference) [21]. If there is interference in the voice channels, cross talk will appear as noise between the users. The interference in the control channels leads to missed and drop calls. Interference on voice channels causes background noise and results in poor voice quality. It is more severe in urban areas because of the greater RF noise and greater density of mobile stations and base stations [23]. Fundamentally, interference is the major bottleneck in increasing capacity of a cellular network.

In addition, frequency of an interfering signal is the most common parameter leading to the identification of the interfering source [22]. Thus, an interference problem can often be categorized by its frequency characteristics. It should be noted that whether the interfering signal is in-band or out-of-band, the signal is almost certainly coming through the antenna, down the cable, and into the affected receiver. Hence, Interference generally affects receiver performance. Although it is possible that a source of interference can be physically close to a transmitter, the characteristics of the transmitted signal will not be affected [19] .

The first step in recognizing if interference has corrupted a receiver system is to understand the characteristics of the signal that the affected system is intended to receive while the second step requires determining the level of the

interfering power that affects the amplitude of the received signal [22]. By analyzing the frequency domain using a spectrum analyzer, the signal frequency, power, harmonic content, modulation quality, distortion, noise or interference can easily be measured. If interference is overlapping the intended receiver signal, it will be relatively shown on the spectrum analyzer display. A displayed interference "fingerprint" contains important identification characteristics. A modulated signal will equally have unique characteristics depending on the type of modulation used. Interference in cellular network can be characterized as either being wideband noise (WBN) or intermodulation related [23]. The major types of system generated cellular interference are Co-Channel Interference (CCI) and Adjacent Channel Interference (ACI). Others include; intermodulation interference, transmitter noise, out of band emission, in-band emission and receiver blocking. This section discussed basically the interference issues that occur in a co-located scenario. These comprised (a) the intermodulation interference, (b) transmitter noise, (c) in-band and out-of-band interference and (d) the receiver blocking.

(a) Intermodulation Interference (IMI)

Intermediation interference (IMI) occurs when two or more signals occupy the same transmission paths as in full duplex systems [24]. When the signals mix, a non-linear response called intermodulation interference manifests itself as bi-products of the fundamental frequency. These unwanted signals typically show up in the receive band and can block a channel. All semiconductors inherently exhibit a degree of non-linearity, even those which are biased for "linear"

operation. The spurious products which are generated due to the non-linearity of a device are mathematically related to the original input signals. The frequencies of the two-tone intermodulation products can be computed using equation (2.1) [25].

$$Mf_a \pm Nf_b \tag{2.1}$$

where M, N = 0, 1, 2, 3, ... The order of the distortion product is given by the sum of M + N. The second order intermodulation products of two signals at f_a and f_b would occur at $f_a + f_b$, $f_b - f_a$, $2f_a$ and $2f_b$. Third order intermodulation products of the two signals, f_a and f_b, would be: $2f_a + f_b$, $2f_a - f_b$, $f_a + 2f_b$, $f_a - 2f_b$, where $2f_a$ is the second harmonic of f_a and $2f_b$ is the second harmonic of f_b. Mathematically the $f_b - 2f_a$ and $f_a - 2f_b$ intermodulation product calculation could result in a "negative" frequency. The absolute value of $f_a - 2f_b$ is the same as the absolute value of $2f_b - f_a$. It is common to talk about the third order intermodulation products as being $2f_a \pm f_b$ and $2f_b \pm f_a$ [25].

There are two basic categories of Intermodulation Interference. They are; receiver produced and transmitter produced [25]. Transmitter produced intermodulation interference is the result of one or more transmitters impressing a signal in the non-linear final output stage circuitry of another transmitter, usually via antenna coupling. The intermodulation product frequency is then re-radiated from the transmitter's antenna. Receiver

produced intermodulation interference is the result of two or more transmitter signals mixing in a receiver RF amplifier or mixer stage when operating in a non-linear range.

(b) Transmitter Noise

The transmitter noise is defined as the lowest continuous wideband emission which occurs when a transmitter radiates energy on its operating frequency as well as frequencies above and below the assigned frequency [19]. The energy radiated above and below the transmitting frequency is known as sideband noise energy and extends for several Megahertz on either side of the operating frequency [19]. They manifest as wideband signals that operate outside the transmit frequency band. When this noise energy falls within the pass-band of a nearby receiver, it reduces the receiver sensitivity, leading to reduced coverage radius and increases the noise floor level thereby reducing the channel capacity. This mostly occurs when power amplifiers generate a significant amount of emission during its active mode and also create a high level of non-linearity [19]. This undesired noise energy can fall within the pass band of a nearby receiver even if the receiver's operating frequency is several megahertz away. The transmitter noise appears as channel noise interference. It is on the receiver's operating frequency that the noise competes with the desired signal, which in effect degrades the operational performance. The noise caused by the transmitter (Tx) cannot be reduced with the radio frequency planning alone. It is related to the noise figure of the transmitter

chain, hence requires other mitigation measures. The wideband radio frequency noise is also referred to as sideband noise. The major part of this noise is generated in the amplified and the transmitter output stages [19, 24].

(c) In-Band and Out-of-Band Emission

Often, transmitters cause a degree of interference into every receiver especially when operating in a close proximity [24]. Interference is attenuated by the separation between the transmitter and receiver in the geographic and frequency domains. It is therefore often useful to categorize interference into two types: In-Band Interference and Out-of-Band Interference [26].

(i) In-Band Interference: This occurs when there is frequency overlap between the transmitter and receiver operating bandwidths [26]. In-band interference sources are the intra-cell interference due to multiple access or users operating in the same cell, and the inter-cell interference is due to users or base station operating in the same band but placed different cells apart. Typically for both to be able to operate without excessive interference, this implies a degree of geographic separation or co-ordinated time/code sharing. In-band emissions received out-of-band due to imperfections in the filtering of the receiver.

(ii) Out-of-band interference: Out-band interference source is the adjacent channel interference (ACI) generated by other cellular signals in the adjacent frequency bands [26]. This results when there is no overlap in frequency between the transmitter and receiver's bandwidth, but the geographic

separation is sufficiently small that there can be appreciable interfering signal [26]. Out-of-band emissions received in-band interference due to imperfections in the filtering of the transmitter. Figure 2.1 illustrates the in-band and out-of-band interference paths. For the geographic region 1, the transmitter and the receiver are operating in different frequencies. The transmitter is operating at frequency band 1 and the receiver is operating in frequency band 2, but the geographic separation is quite close, causing out-of-band interference. While for geographic region 2, the transmitter and the receiver are operating at the same frequency (frequency band 1), resulting to in-band interference [26].

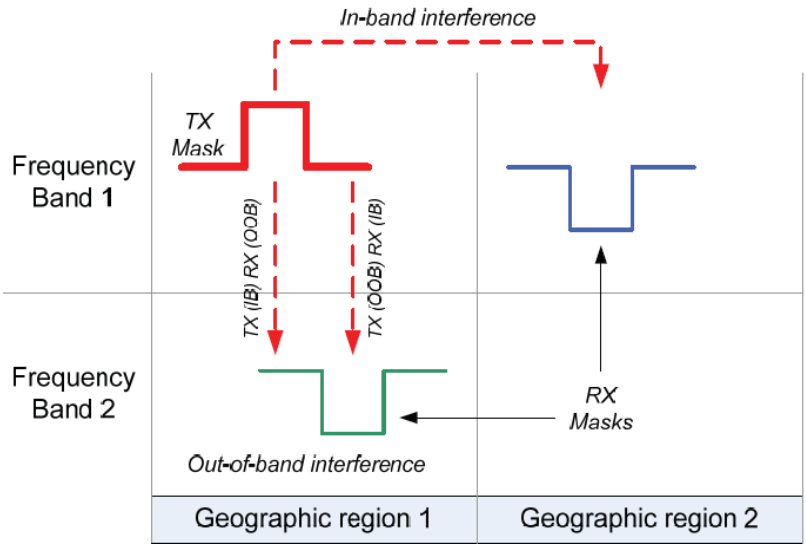

Fig 2.1: In-band and Out-of-band Interference Paths[26]

(d) Spurious emissions

International Telecommunication Union Recommendation (ITU-R), defines spurious emission as ‘emission on frequencies which are outside the necessary bandwidth 12.5MHz below the first carrier and 12.5MHz above the last carrier transmitted by a base station [26]. Within this frequency, a spectrum emission

mask is defined for the measurement of out-of-band emissions. The emission is caused by unwanted radiations generated by the interference source (transmitter) in the working frequency band of the interfered receiver. Spurious emissions include harmonic emissions, parasitic emissions, inter-modulation products and frequency conversion products but exclude out-of-band emissions [24]. ITU defines spurious emissions limit for CDMA far offset from carrier as -13dBm/1MHz. Table 2.1 shows the transmitter spurious emission limits.

Table 2.1: Limits of spurious emissions level defined by 3GPP2 protocol

For $\lvert\Delta f\rvert$ within the range	**Applies to multiple carriers**	**Emission limit**
885kHz to 1.25MHz	No	-45dBc/30kHz
1.25 to 1.98MHz	No	More stringent of -45dBc/30KhZ or -9dBm/30kHz
1.25 to 2.25MHz (MC tests only)	Yes	-9dBm/30kHz
1.25 to 1.45 MHz (Band class 6 only)	Yes	-13dm/30kHz
1.45 to 2.25 MHz (Band class 6 only)	Yes	$-\lvert 13+17x(\Delta f - 1.45MHz)\rvert dBm/30KHz$
1.98 MHz to 2.25MHz	No	-55dBc/30kHz; pout≥33dBm -22dBm/30kHz; 28dBm≤pout<33dBm -50dBc/30kHz; pout<20dBm
2.25MHz to 4.00MHz	Yes	-13dBm/1MHz
>4.00MHz (ITU category A only)	Yes	-13dBm/1kHz; 9kHz<f<150kHz -13dBm/10kHz; 150kHZ<f<30MHz -13dBm/100kHz; 30MHz<f<1GHz -13dBm/1MHz; 1GHz<f<5GHz

Source: (3GPP2)[24]

(e) Receiver Blocking

Receivers usually work in linear form [24]. When a strong interference enters a receiver, it may overdrive the receiver to work in non-linear state or even worse (in saturation mode) as the out of band suppression ratio of the receiver may be limited [24]. Any receiver can be completely blocked by an off-channel interfering signal that is strong enough [27]. Receiver blocking interference occurs when an undesired signal from a nearby "off-frequency transmitter is sufficiently close to a receiver's operating frequency [27]. If this undesired signal is of sufficient amplitude, the receiver's critical voltage and current levels are altered and the performance of the receiver is degraded at its operating frequency [27].

If the interference frequency is far removed from the receiver frequency, the receiver blocking interference will be sufficiently rejected. However, if the transmitter is too close to the receiver as in a co-located scenario, its wide band noise can be so great that it blocks the front-end of the receiver even if the channel separation is relatively large [27]. Receiver blocking is therefore an effect greatly influenced by the proximity of interfering transmitter to the receiver. The blocking interference reduces the receiver gains and increases the noise floor level [27]. This effect led to a reduced signal to noise ratio at the receiver, given rise to degradation on the system performance. Figure 2.2 illustrates the receiver blocking interference.

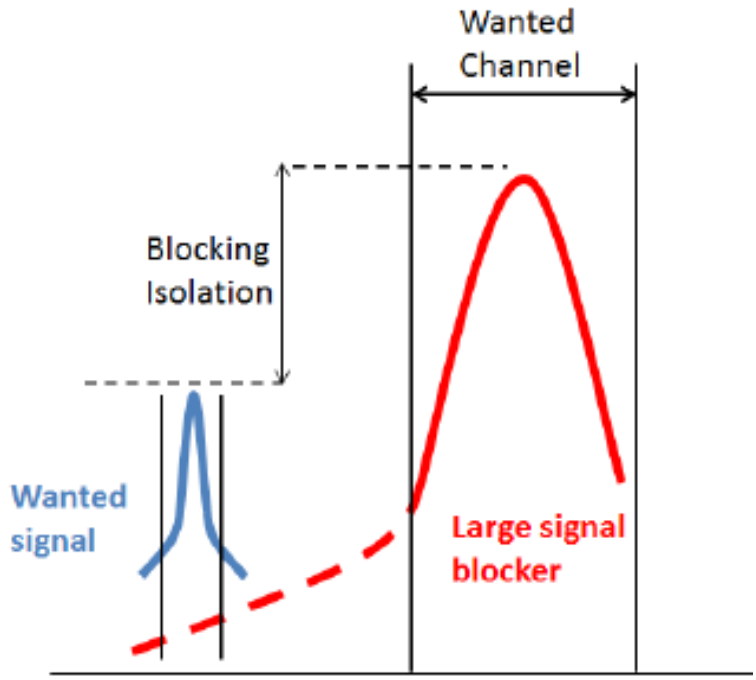

Figure 2.2 Receiver blocking interference [27].

In Figure 2.2, the blocking effect of interfering power within the transmission channel was illustrated. A strong unwanted signal (large signal blocker), prevents the receiver from detecting a wanted signal by driving the receiver into overload or in saturation mode [27]. This effect significantly leds to total signal blockage at the victim receiver front end resulting to high call blocking rates. This interference can occur irrespective of the received signal level because of the high transmitting power. The effect is not as frequency selective as out of band interference and could also occur when the unwanted signal is many channels away [27]. It could be reduced by increasing the isolation between the offending transmitter and the victim receiver.

2.3 Multiple Access Technologies in Wireless Network

In wireless communication systems, it is often desirable to allow the subscriber to send simultaneously information to the base station while receiving information from the base station. A cellular system divides any given area into cells where a mobile unit in each cell communicates with a base station. The main aim in the cellular system design is to ensure an increase and optimized performance in the channel capacity i.e. to handle as many calls as possible in a given bandwidth with a satisfactory level of quality of service [28].

Multiple access networks are mostly used to allow many mobile users to share simultaneously a finite amount of radio spectrum [29]. The sharing of spectrum is required to achieve high capacity by simultaneously allocating the available bandwidth (or the available amount of channels) to multiple users [29]. For high quality communications, this must be done without severe degradation in the performance of the system.

There are several different multiple radio access technologies defined within ITU, based on either Code Division Multiple Access (CDMA) or Time Division Multiple Access (TDMA) technology [30]. The three generation (*3G)* wireless system is currently split into two groups: the Universal Mobile Telecommunication System (*UMTS)* group (i.e third Generation Partnership Project (3GPP)) and the CDMA-2000 group (3GPP2). ITU approved a family

of three 3G standards, which are part of the 3G framework known as IMT-2000: (a) W-CDMA (b) CDMA-2000 (c) TD-SCDMA. Europe, Japan, and Asia have agreed upon a 3G standard called the Universal Mobile Telecommunications System (UMTS), which is WCDMA operating at 2.1 GHz. UMTS and WCDMA are often used as synonyms. This section principally elaborates on the WCDMA and CDMA-2000 access techniques which are of relevance to the research.

2.3.1 3G W-CDMA (UMTS)

WCDMA is based on Direct Sequence Code Division Multiple Access (DS-CDMA) technology in which user-information bits are spread over a wide bandwidth (much larger than the information signal bandwidth) by multiplying the user data with the spreading code. The chip rate (symbol rate) of the spreading sequence is 3.84 Mcps, which, in the WCDMA system deployment is used together with the 5-MHz carrier spacing. The processing gain term is referred as the relationship between the signal bandwidth and the information bandwidth [31]. Thus, the name wideband is derived to differentiate it from the 2G CDMA (IS-95), which has a chip rate of 1.2288 Mcps. In a CDMA system, all users are active at the same time on the same frequency and are separated from each other with the use of user specific spreading codes.

The wide carrier bandwidth of WCDMA allows supporting high user-data rates and also has certain performance benefits such as, increased multipath diversity. The actual carrier spacing to be used by the operator may vary on a

200-kHz grid between approximately 4.4MHz and 5MHz, depending on spectrum arrangement and the interference situation [31]. In WCDMA, each user is allocated frames of 10 ms duration, during which the user-data rate is kept constant. WCDMA supports two basic modes of operation: FDD and TDD. In the FDD mode, separate 5-MHz carrier frequencies with duplex spacing are used for the uplink and downlink, respectively, whereas in TDD only one 5-MHz carrier is time shared between the uplink and the downlink. WCDMA uses coherent detection based on the pilot symbols and/or common pilot. WCDMA allows many performance- enhancement methods to be used, such as transmit diversity or advanced CDMA receiver concepts [31]. Table 2.2 summarizes the main WCDMA parameters.

Table 2.2: Main WCDMA parameters [31]

Multiple access method	DS-CDMA
Duplexing method	Frequency division duplex/time division duplex
Base station synchronization	Asynchronous operation
Chip rate	3.84Mcps
Frame length	10ms
Service multiplexing	Multiple services with different quality of service requirements multiplexed on one connection
Multi-rate concept	Variable spreading factor and multicode
Detection	Coherent using pilot symbols or common pilot
Multi-user detection, smart antennas	Supported by the standard, optional in the implementation

UMTS or W-CDMA, assures backward compatibility with the second generation GSM, IS-136 and PDC TDMA technologies, as well as all 2.5G

TDMA technologies. The network structure and bit level packaging of GSM data is retained by W-CDMA, with additional capacity and bandwidth provided by a new CDMA air interface.

The network architecture of *UMTS* is divided into the radio access network (*RAN*) and the core network [32] as shown in Figure 2.3. The *RAN* contains the User Equipment (*UE*), which includes the Terminal Equipment (*TE*) and Mobile Terminal (*MT*), and the *UMTS* Terrestrial Radio Access Network (*UTRAN*), which includes the Node-B and Radio Network Controller (*RNC*). The core network (focused on packet domain) includes two network nodes: the Serving General Packet Radio Services (GPRS) Support Node (*SGSN*) and the Gateway *GPRS* Support Node (*GGSN*). The *SGSN* monitors user location and performs security functions and access control. The *GGSN* contains routing information for packet-switched (*PS*) attached users and provides inter-working with external *PS* networks such as the packet data network (*PDN*). The *WCDMA* technology is network asynchronous, meaning that there is no synchronization between base stations. This implies that no additional source of synchronization is needed (as in CDMA 2000).

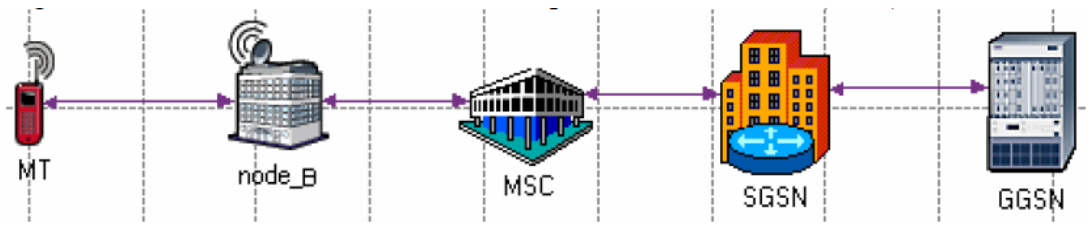

Figure 2.3: The Third Generation Wireless Network (UMTS)

2.3.2 3G CDMA 2000

Code Division Multiple Access 2000 (CDMA 2000) is the natural evolution of IS-95 (CDMA-One). It includes additional functionality that increases its spectral efficiency and data rate capability. CDMA is a mobile digital radio technology where channels are denied with codes (PN sequences). CDMA permits many simultaneous transmitters on the same frequency channel. Since more phones can be served by fewer cell sites, CDMA-based standards have a significant economic advantage over TDMA- or Frequency Division Multiple Access (FDMA)-based standards. This standard is being developed by Telecommunications Industry Association (TIA) of US and is standardized by 3GPP2. It is another wireless standard designed to support *3G* services as defined by the *ITU* and its *IMT*-2000 [33]. CDMA 2000 can support mobile data communications at speeds ranging from 144 kbps to 2 Mbps as *WCDMA* technology[34]. The *CDMA 2000* uses the same baseline chip rate of 1.2288 Mcps as *CDMA-One* [31]. Each of the individual carriers is modulated with a separate orthogonal code and has an optional overlay mode. This coding distinguishes the *CDMA-One* and the *CDMA-2000* users. The main CDMA-2000 standards are: CDMA-2000 1xRTT, CDMA-2000 1xEV and CDMA-2000 EV-DV,DO and CDMA 3xRTT. The *CDMA-2000-1*x*RTT* (Radio Transmission Technology) is technically known as *G3G-MC-CDMA-1*x and supports twice as many users as *2G CDMA* with data rates up to 153.6 Kbps

(or 614.4 Kbps if all supplemental channels are used). The *CDMA-2000-1*x*EV* is a High Data Rate (*HDR*) packet standard originally developed by Qualcomm, Inc. [34]. The *CDMA-2000 1*x*EV-DO* is obtainable to suit demanding applications such as video streaming and large file downloads. The *CDMA-2000-3*x*RTT* is a future standard that will use 3, 1.25 MHz radio channels simultaneously to create a "super channel" and provide outstanding data rates (3.09 Mbps) for every user. These are the approved radio interfaces for the ITU's IMT-2000 standard. In the following, a brief discussion about all these standards is given. CDMA-2000 1xRTT: The designation "1x", meaning "1 times Radio Transmission Technology", indicates the same RF bandwidth as IS-95.The main features of CDMA-2000 1x are as follows:

a. Supports an instantaneous data rate up to 307kpbs for a user in packet mode and typical throughput rates of 144kbps per user, depending on the number of user, the velocity of user and the propagating conditions.
b. Supports up to twice as many voice users as the 2G CDMA standard
c. Provides the subscriber unit with up to two times the standby time for longer lasting battery life.

- **CDMA-2000 EV**: This is an evolutionary advancement of CDMA with the following characteristics [34]:

a. Provides CDMA carriers with the option of installing radio channels with data only (CDMA-2000 EV-DO) and with data and voice (CDMA-2000 EV-DV).

b. The CDMA-2000 1xEV-DO supports greater than 2.4Mbps of instantaneous high-speed packet throughput per user on a CDMA channel, although the user data rates are much lower and highly dependent on other factors.
c. CDMA-2000 EV-DV can offer data rates up to 144kbps with about twice as many voice channels as IS-95B.

- **CDMA-2000 3x** (known as EV-DO Rev B) is a multi-carrier evolution [34].

a. It has higher rates per carrier (up to 4.9 Mbit/s on the downlink per carrier). Typical deployments are expected to include 3 carriers for a peak rate of 14.7 Mbit/s. higher rates is possible by bundling multiple channels together. It enhances the user experience and enables new services such as high definition video streaming.
b. Uses statistical multiplexing across channels to further reduce latency, enhancing the experience for latency-sensitive services such as gaming, video telephony, remote console sessions and web browsing.
c. It provides increased talk-time and standby time.
d. The interference from the adjacent sectors is reduced by hybrid frequency reuse and improves the rates that can be offered, especially to users at the edge of the cell.
e. It has efficient support for services that have asymmetric download and upload requirements (i.e. different data rates required in each direction) such as; web browsing, and broadband multimedia content delivery.

2.4 Antenna Isolation

Antenna isolation is one of the utmost factors that must be considered before dealing with interference analysis in co-located and co-existing networks. Antenna isolation is defined as the pathloss between a Transmitting (Tx) antenna connector and a Receiving (Rx) antenna connector [35]. It could also be defined as the loss between two co-located antennas ports [36]. Antenna-to-antenna isolation is normally expressed in terms of decibel (dB) of attenuation. The isolation is often called antenna coupling loss, or antenna decoupling.

Physical separation of antenna can to an extent increase the antenna-to-antenna isolation. Other techniques include: separation of frequency band, selection of antenna gain, size and beamwidth, radiation pattern of the antennas, polarization, and the conducting properties of the antenna tower and the use of filters [36]. The distance required for the physical separation of antenna used for the mobile co-location service cannot be accurately deduced by calculation because the co-located antennas are in the “near field” than the “far field”. For these reasons, the exact isolation is best determined by site measurement using the measuring kits. The site-by-site measurement technique is achieved by aligning the antenna azimuths between the affecting and affected antenna. At the point where the azimuth did not overlap, measurement is taken using the RF network analyzer and then utilizes it to calculate the distance based on the antenna characteristics. However, such measurement campaigns may be too

costly and time-consuming and even pose accessibility issue [35]. As an alternative, different method of analytical modeling is proposed which include vertical antenna isolation and horizontal antenna isolation. If the antennas are located on the same tower, then the isolation must be calculated for vertical separation. If the antennas are located on separate towers, then the formula for horizontal separation is applied. The attenuation formula for free space propagation calculates the amount of isolation provided by horizontal separation unlike in vertical separation because of the short distance. Antennas are either exactly vertically separated or exactly horizontally separated. The isolation will be better (more like vertical) if each antenna is not in the other antenna's beamwidth. However, antenna isolation is primarily a function of the wavelength, antenna types (omnidirectional vs directional), antenna characteristics (downtilt, gain, radiation patterns, etc.) and relative spatial configurations as mentioned before.

2.4.1 Isolation Technique

When several different radio systems are co-located or co-existed, the antenna isolation concept can be brought into consideration in the calculation of interference between them as explained above, such as the isolations of horizontal (HI), vertical (VI) and slant (SI) antenna configurations [35]. The isolation between systems is given by the interference attenuation between the transmitter (Tx) and the receiver (Rx). The illustration in Figure 2.4 shows the disturbance between the two base transceiver stations (BTS).

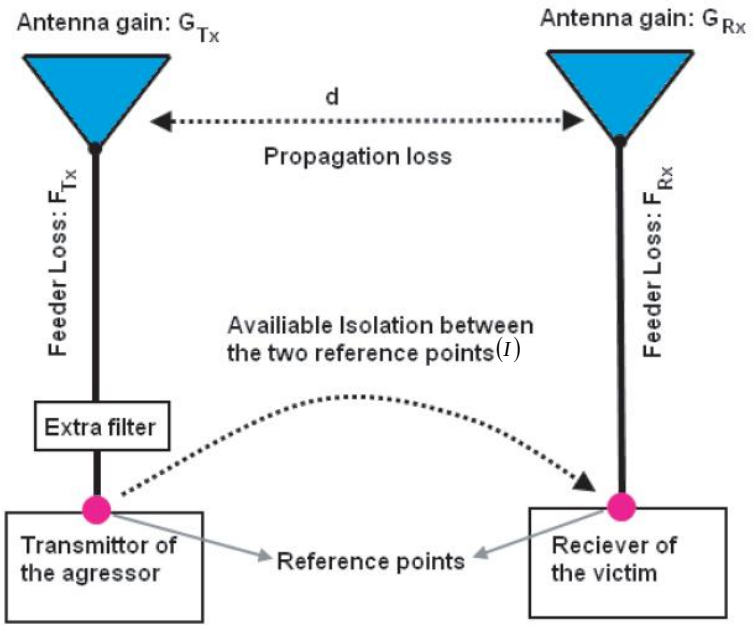

Figure 2.4 : Isolation requirement between Transmitter and Receiver of a co-existence networks [35].

The parameter I is the isolation between the transmitter of the aggressor and the receiver of the victim, given by equation (2.2) [35];

$$I = (F_{TX} - G_{TX}) + (F_{RX} - G_{RX}) + P_L + A \tag{2.2}$$

Where F_{TX}, F_{RX} are the feeder loss of the Transmitter and Receiver; G_{TX}, G_{RX} are the transmitter and receiver antenna gain; P_L, propagation loss and A, extra attenuation provided by special filter. It follows that if for distances 'd' more than 10m, the propagation loss between the two antennas is small, so the channel may be described by a free space propagation model. By using filters in the *Tx* and or *Rx*, could cancel or at least reduce the effect of the interference caused by the co-existence of various mobile networks. It is important to note that the choice of the appropriate filters varies in terms of the

frequency of operation, attenuation requirement and distance between the co-existence antennas.

2.4.2 Vertical Antenna Isolation

To calculate the amount of isolation for vertically separated antennas, the following formula should be used.

Antenna isolation for vertical distance (Av) can be computed using equation (2.3) [39]

$$Av = 28 + 40\log\left(\frac{d_v}{\lambda}\right) \tag{2.3}$$

Where,

$$\lambda = \frac{v}{f} = \frac{300x10^6}{centrefrequency(MHz)}$$

Av is the isolation between vertically separated transmitter and receiver antennas in dB. λ is the wavelength of the interfered signal with system frequency band (center frequency) and d_v is the vertical tip-to-tip distance from the interferer antenna to the interfered with receiver antenna, measured from radiation center-to-radiation center in meters as shown in Figure 2.5.

In order to achieve a maximum isolation, the antennas should be exactly collinear (one directly in a vertical line with the other). Equation (2.3) does not take into account any tower coupling that might decrease the amount of isolation between the two antennas. Separation is measured from center-to-

center frequencies on the antennas. Figures 2.5a and 2.5b below illustrate vertical antenna isolation placement.

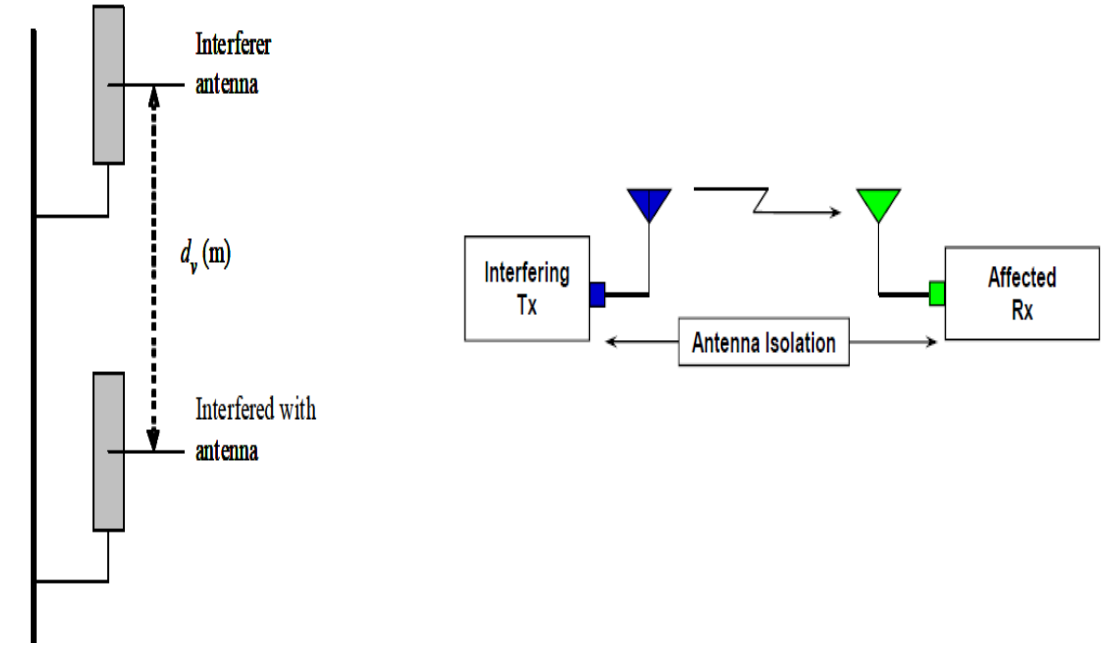

(a) (b)

Figure 2.5 Vertical Antenna Isolation

2.4.3 Horizontal Antenna Isolation

Horizontal Separation distance (A_H) can be calculated approximately from equation (2.5) [39]:

$$A_H = 22 + 20\log\left(d_H / \lambda\right) - \left(G_{Tx}(\alpha) + G_{Rx}(\beta)\right) \tag{2.5}$$

where d_H = Horizontal distance between the centerlines of antennas (m); λ = wavelength (m); $G_{TX}(\alpha)(dBi)$ is the gain of the transmitter antenna 1 at the relative angle α, to antenna 2; $G_{RX}(\beta)(dBi)$ is the gain of the receiver antenna 2 at the relative angle β, to antenna 1. Figure 2.6 illustrates horizontal isolation of the antennas.

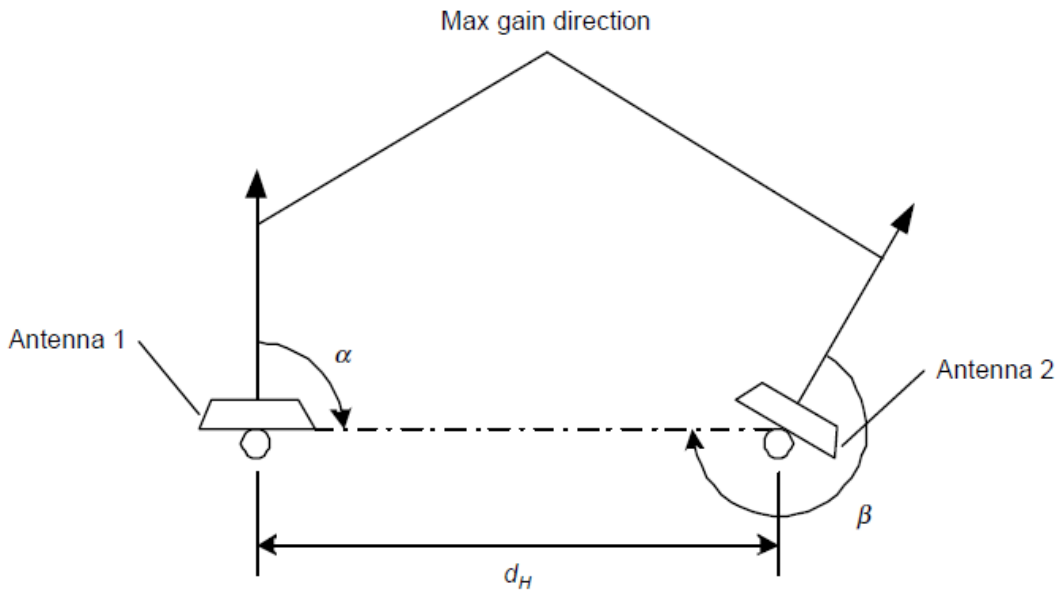

Figure 2.6: Horizontal Isolation of the antennas

Equation 2.5 can further be elaborated by showing the influence of antenna azimuthally, considering the gain of the side-lobe with respect to the main-lobe of the transmitter antenna and the gain of the side-lobe with respect to the main-lobe of the receiver antenna as shown in Figure 2.7. The horizontal free space antenna isolation for a scenario can be computed by using equation (2.6) [39]:

$$I_H(dB) = 22 + 20\log\left(\frac{d_h}{\lambda}(m)\right) - \left(G_{Tx} + G_{Rx}\right)(dBi) - \left(SL(\rho)T_x + SL(\theta)R_x\right)(dB) \qquad (2.6)$$

Where d_h between two antennas satisfies the following approximate far-field condition [38]. $d_h(m) \geq 2D^2/\lambda(m)$, D expressed in meters, is the minimum dimension of the largest of the transmitter or receiver antennas; $I_H(dB)$ is isolation between horizontally separated transmitter and receiver antennas;

$d_h(m)$ is the horizontal distance from the center of interfere antenna to that of the interfered with receiver antenna; $\lambda(m)$, the wavelength of the interfered with system frequency band; $G_{Tx}(dBi)$, the maximum gain of the transmitter antenna with respect to an isotropic antenna (dBi); $G_{Rx}(dBi)$ is the maximum gain of the receiver antenna with respect to an isotropic antenna (dBi); $SL(\rho)_{Tx}(dB)$ is the gain of the side-lobe with respect to the main-lobe of the transmitter antenna (negative value) while $SL(\theta)_{Rx}(dB)$, is the gain of the side-lobe with respect to the main-lobe of the receiver antenna (negative value) as shown in Figure 2.7

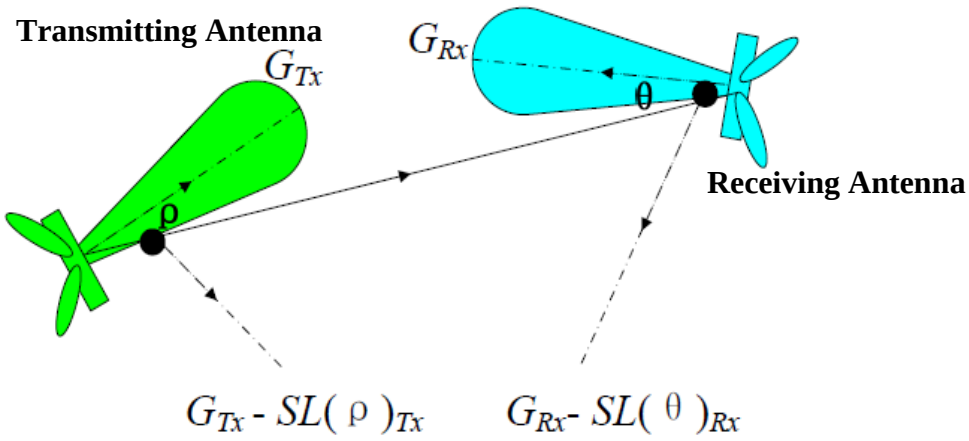

Figure 2.7: Influence of antenna azimuthal angle

2.5 Frequency Band Evaluation

This is one of the essential considerations when analyzing a co-located network with the aim centered on evaluating the original assigned frequency bands between the two co-located networks, whether the frequency of the two networks are adjacent to each other or overlaps.

2.5.1 Spectrum Allocation by the International Telecommunication Union (ITU)

Figures 2.8 and 2.9 showed the intended frequency bands, frequency overlap and likelihood of interference occurrence for Digital Communication System (DCS), Personal Communication System (PCS) and the Universal Mobile Telecommunication System (UMTS) at 2.1GHz respectively [24].

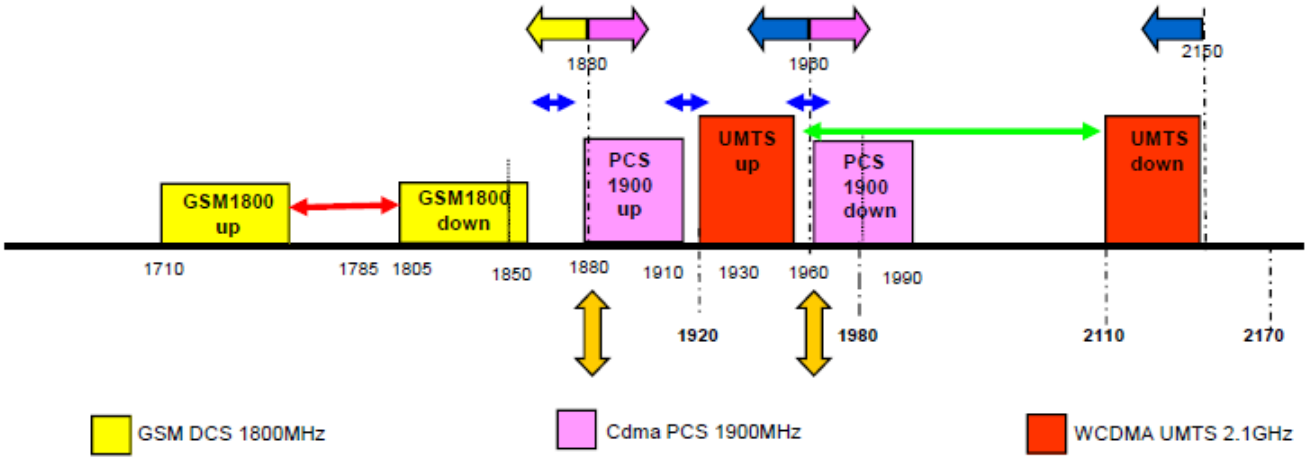

Figure 2.8: Intended frequency band
Source: NCC 2008 [24]

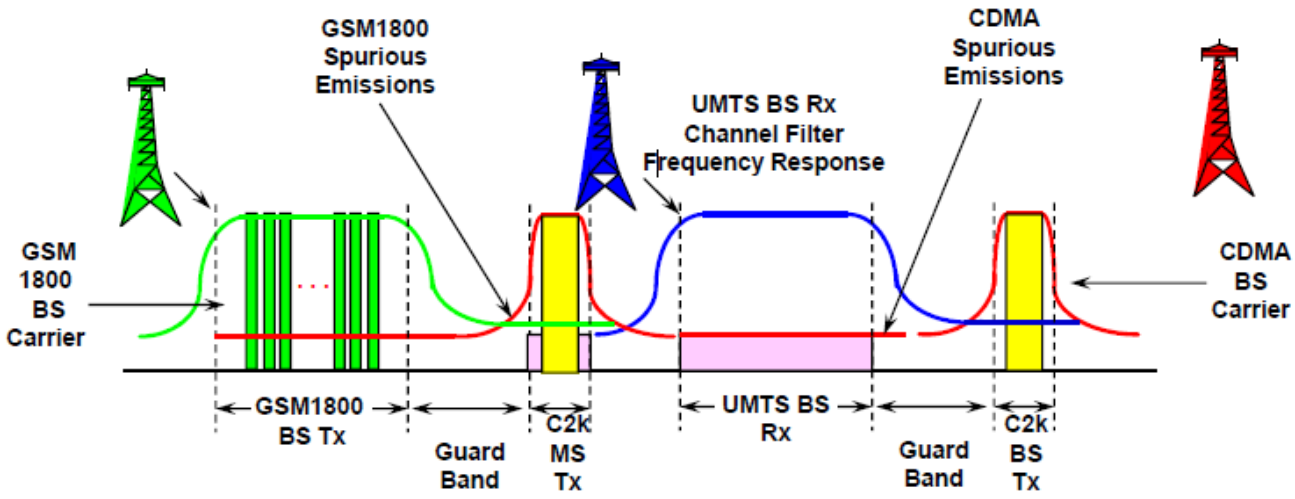

Figure 2.9: Interference overview
Source: NCC 2008 [24]

Figures 2.10 and 2.11 conversely, showed the spectrum allocation by the International Telecommunication Union (ITU) and the re-banded spectrum by Nigerian Communication's Commission (NCC) between CDMA-2000 downlink and WCDMA uplink.

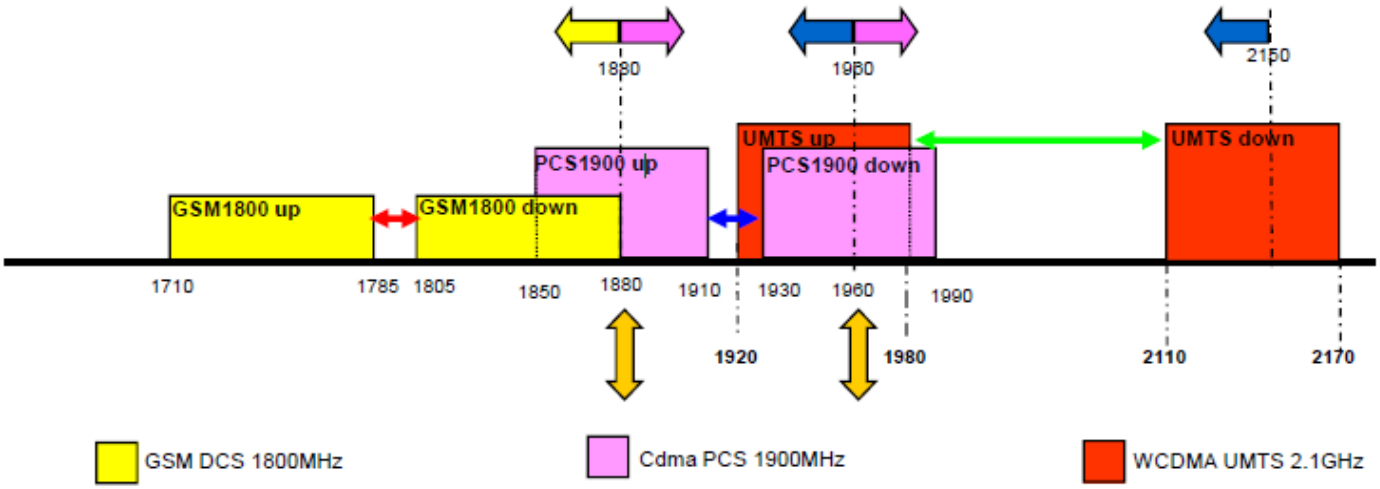

Figure 2.10: Spectrum allocation by ITU
Source: NCC 2008 [24]

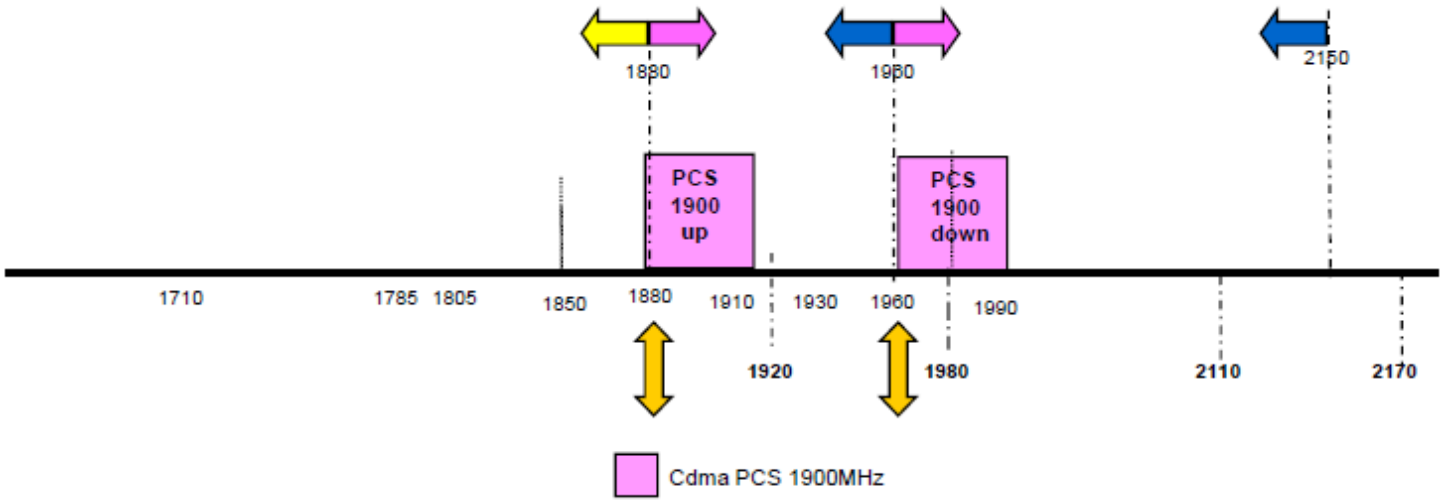

Figure 2.11: Spectrum Allocation by NCC (After Re-banding)
Source: NCC 2008 [24]

Figure 2.10 explained the spectrum allocation overview by the global wireless communication standard, the International Telecommunication Union (ITU). The frequency band allocation for CDMA-2000 downlink is between 1930 and 1990MHz and that of WCDMA uplink is between 1920 and 1980MHz. In Figure 2.10, CDMA-2000 downlink frequency overlaps with the WCDMA uplink frequency by 50MHz. This frequency band already was allocated prior to the implementation of co-location strategy. Based on the critical circumstances foreseen between these two networks for the benefit of co-location, NCC, re-banded the frequency between the two networks as shown in Figure 2.11. Therefore, CDMA-2000 downlink new frequency band operates between 1960-1990MHz, with the new frequency overlap between 1960-1980MHz. The frequency re-band by NCC reduces the overlap from 50MHz to 20MHz, given rise to about 60 percentage reduction on overlap, which further provided significant reduction on the interference effect. The WCDMA uplink frequency band still maintains the frequency band between 1920-1980MHz. Despite the re-banding methodology by NCC, interference was still apparent. For this reason, the research study was embarked-upon finding a lasting solution to the imperative issue. Figure 2.12 shows the new frequency allocation for the UMTS and CDMA-2000 [24].

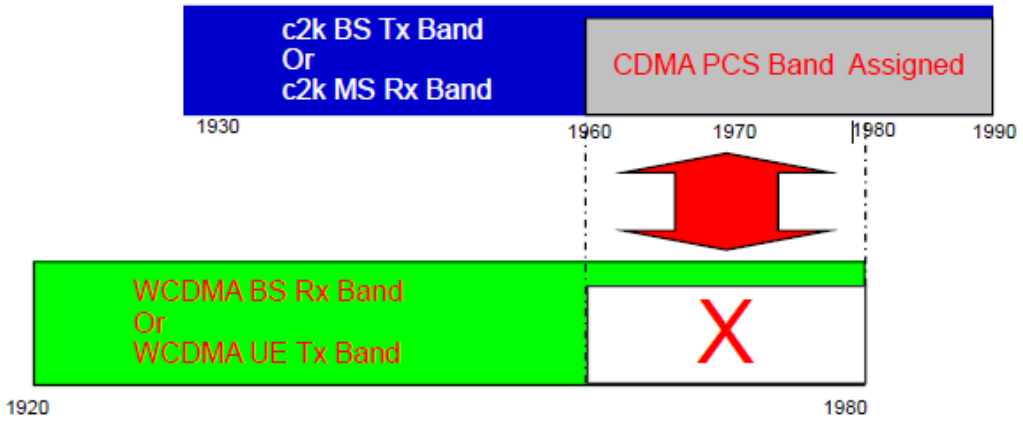

Figure 2.12; UMTS and CDMA-2000 Spectrum Allocation in Nigeria
Source: NCC 2008 [24]

The PCS band spectrum has been assigned to different operators. CDMA-2000 PCS Tx band overlaps 20MHz on WCDMA UMTs Rx band, so CDMA-2000 Tx will interfere UMTS Base station (Bs) Rx. There is no interference between UMTS Bs Tx and CDMA-2000 Bs Rx because of large frequency band isolation as shown in Table 2.3. UMTS downlink frequency is between 2110-2170MHz while that of CDMA-2000 uplink is between 1850-1910MHz; the frequency isolation is 200MHz, therefore no interference.

Table 2.3: Frequency spectrum for CDMA-2000 AND WCDMA [24]

Wireless access technology	Mobile station transmitter (MHz) (Uplink)	Base station Transmitter(MHz) (downlink)	Duplex separation (MHz)
CDMA 2000	1850-1910	1960-1990	80
WCDMA	1920-1980	2110-2170	190

Table 2.4: Comparison of Typical parameters for CDMA-2000 and WCDMA

Technology	IF bandwidth (channel BW)MHz	Signal Bandwidth MHz	Noise Coefficient (i.e. Noise figure)	Theoretic Received signal stength(dbm)
CDMA 2000	1.25	1.23	4	-125
WCDMA	5	3.84	5	-122

Source: Huawei Technology[39]

Table 2.3 shows the frequency spectrum range for CDMA 2000 and WCDMA and Table 2.4 shows various parametric comparisons of the CDMA-2000 and the WCDMA systems [39]. The frequency gaps between Tx and Rx band of CDMA-2000 for mobile station transmitter (uplink) and base station transmitter (downlink), that is, the Guard band is 20MHz while that of WCDMA mobile station transmitter and base station transmitter (downlink), the guard band is 130MHz respectively.

2.6 Adaptive Noise Cancellation

The usual method of estimating a signal corrupted by additive noise is to pass it through a filter that tends to suppress the noise while leaving the signal relatively unchanged. The design of such filters is the domain of optimal filtering, which originated with the pioneering work of [40] and was extended and enhanced by [41]. Filter used in direct filtering can be either fixed or adaptive.

1. **Fixed Filters**: The design of fixed filters requires a priori knowledge of both the signal and the noise, i.e. if the characteristics of the signal and

noise are known beforehand, a filter that passes frequencies contained in the signal and rejects the frequency band occupied by the noise can be designed.

2. **Adaptive Filters**: Adaptive filters, on the other hand, have the ability to adjust their impulse response to filter out the correlated signal in the input. They require little or no prior knowledge of the signal and noise characteristics. If the signal is narrowband and noise broadband, which is usually the case, or vice versa, no priori information is needed; otherwise, they require a signal (desired response) that is correlated in some sense to the signal to be estimated). Moreover, adaptive filters have the capability of adaptively tracking the signal under non-stationery conditions[42]. Figure 2.13 shows a simple illustration of an adaptive filter.

Noise cancellation is a variation of optimal filtering that involves producing an estimate of the noise (ň) by filtering the reference input (n) and then subtracting this noise estimate from the primary input containing both signal and noise (s+n).

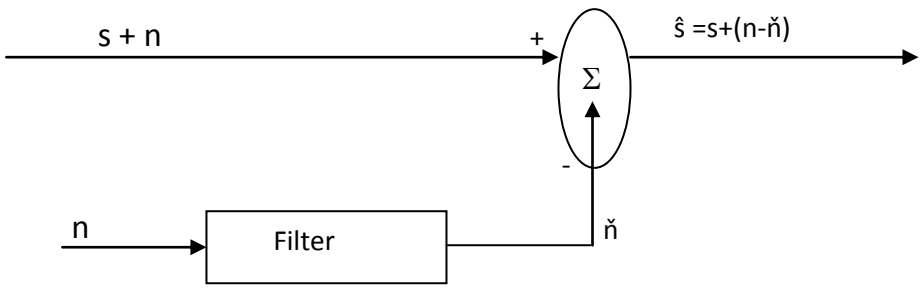

Figure 2.13: A simple Adaptive filter illustration

It makes use of an auxiliary or reference input which contains a correlated estimate of the noise to be cancelled. The reference can be obtained by placing one or more sensors in the noise field where the signal is absent or its strength is weak enough [42]. Subtracting noise from a received signal involves the risk of distorting the signal and if done improperly, it may lead to an increase in the noise level [42]. This requires that the noise estimate ň should be an exact replica of n. If it were possible to know the relationship between n and ň, or the characteristics of the channels transmitting noise from the noise source to the primary and reference inputs, it would be possible to make ň a close estimate of n by designing a fixed filter. However, since the characteristics of the transmission paths are not known and are unpredictable, filtering and subtraction are controlled by an adaptive process. Hence an adaptive filter is used that is capable of adjusting its impulse response to minimize an error signal, which is dependent on the filter output. The adjustment of the filter weights, and hence the impulse response, is governed by an adaptive algorithm [42]. With adaptive control, noise reduction can be accomplished with little risk of distorting the signal. In fact, adaptive noise canceling makes possible attainment of noise rejection levels that are difficult or impossible to achieve by direct filtering. The error signal to be used depends on the application. The criteria to be used may be the minimization of the mean square error, the temporal average of the least square errors etc. Different algorithms are used for each of the minimization criteria e.g. the Least Mean Squares (LMS)

algorithm, the Recursive Least Squares (RLS) algorithm etc [41]. The minimum mean-square error criterion (MMSE) is mostly used to understand the concept of adaptive noise cancellation,. The steady-state performance of adaptive filters based on the MMSE criterion closely approximates that of fixed Wiener filters. Hence, Wiener filter theory provides a convenient method of mathematically analyzing statistical noise canceling problems [40].

2.7 The Concept of Adaptive Cancellation System

Adaptive cancellation technique has been applied and driven by military applications in the past. [43, 44], obtained a patent in 1972 for an adaptive interference cancellation system that can be used to ease co-location of high power transmitters and receivers. The same type of system has been suggested for use in electromagnetically dense platforms such as ships and aircrafts that contain many co-located transmitters and receivers [45]. In these systems, the interfering signal is sampled using an auxiliary antenna oriented in the direction of arrival of the interference signal or directly from the source such as the output of the power transmitter. The sampled signal is then used to subtract the interference present in the main antenna path of the affected receiver [46].

The most basic type of adaptive noise cancellation technique has a signal controller. The signal controller is the core of the noise cancellation system. The signal controller must be able to produce a counter-interference signal

having a wide instantaneous bandwidth and wide dynamic range [47]. The main component of a signal controller is a vector modulator which is a cascade of amplitude attenuation and phase shifter or other components capable of modifying the relative amplitude and phase of the signal passing through. An amplifier is contained in the signal controller in the case where there is too much loss in the cancellation path to match the amplitude of the interference signal present in the main path. In a basic adaptive cancellation system, the delay is matched at the point of implementation by tuning a delay line manually or using a delay element. However, the signal controller contains some means of fine tuning the electrical delay of the RF signal [48].

Figure 2.14 shows a prototype of a basic Adaptive Cancellation System (ACS) that uses a 'primary' input transducer to receive the noise corrupted desired signal and a 'reference' transducer to acquire noise that is correlated in some way to the primary input's noise [46]. The reference input is adaptively filtered and subtracted from the primary input to obtain the actual desired signal.

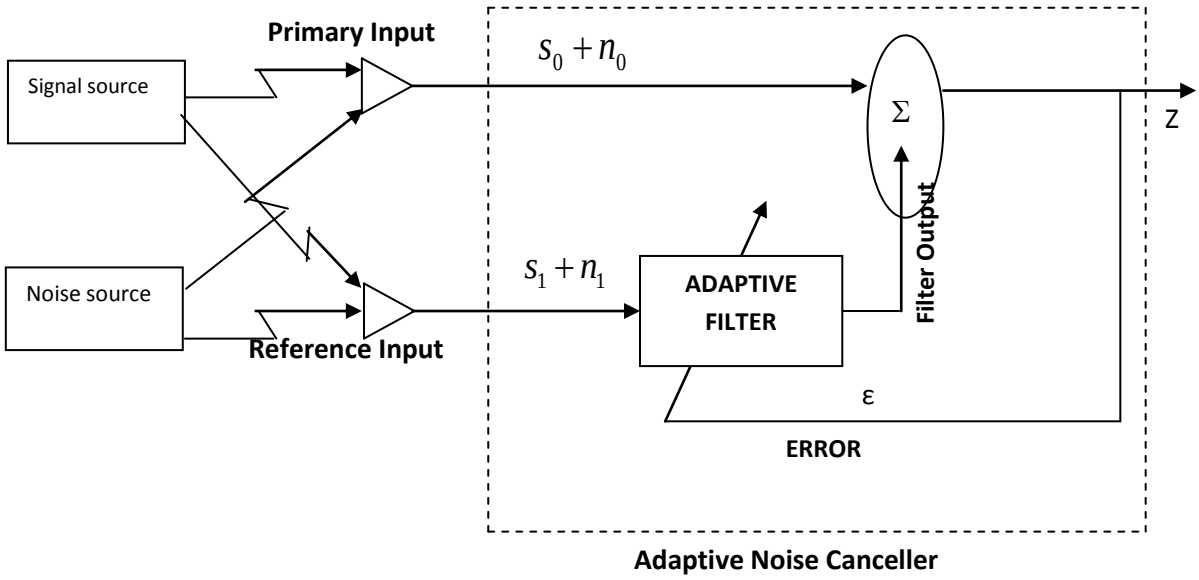

Fig: 2.14 The Adaptive Noise canceling concept []46

2.8 Review of Related Works

In [49], the authors focused on the study of *Adjacent Channel Interference (ACI) and its Effects on the Overall Capacity of the System*. They studied the ACI by using a static simulator. On the basis of the results, the authors identified the best strategy for frequency deployment within the available spectrum. When defining the UMTS system, a bandwidth of 5MHz was considered for each radio channel and the channels allocated were positioned beside each other in uplink (UL) and downlink (DL) bands separated by 190MHZ. The strategy designed to reduce the interference, thus achieving the highest possible capacity, required identifying optimal spacing between carriers in the radio spectrum available for use. Hence a specific frequency arrangement was considered, as it may vary from country to country. Possible ways of measuring the interference leakage between connections operating on different carriers were considered. As the filter is not perfect, when transmitting in its own channel, one carrier will send part of its power into adjacent channels. This effect was measured as the Adjacent Channel Leakage Ratio (ACLR). On the other hand, the receiver filter was unable to receive only the desired signal alone, which was why the rejection of the adjacent channel signal was measured as Adjacent Channel Selectivity (ACS). When considering the existence of two carriers which interfere with each other, the total interference was given as an Adjacent Channel Interference Ratio (ACIR) and determined from equation 2.7.

$$ACIR = \frac{1}{1/ACLR + 1/ACS} \tag{2.7}$$

Their work was based on the study of rural and urban environments. When simulating two operators, Base Stations (BSs) working with adjacent carriers were uniformly distributed over a map. In order to simulate a worst case situation, the sites of both operators were not co-located, being the interoperator spatial offset equal to the cell radius. It was found that the inter-frequency interference impact on the capacity was minimal, when compared with the intra-frequency interference. The reason for this result lies in the fact that there were too many BSs from the same carrier interfering with each other. The next step taken was to identify scenarios where the ACI played a significant role, at least as important as the interference from the connections working on the same carrier. Following simple scenarios, where just a few BSs and two carriers were considered, the analysis developed to encompass broader environments simulating urban centers with many antenna sites and three carriers. The simulator used to achieve this analysis was static, using a Monte-Carlo evaluation method. By examining many static situations, referred to as snapshots, network capacity was estimated through the average number of users served. Two types of antennas were chosen to simulate macro and micro BS: for the macro BS, tri-sectorized antennas (18 dBi), and for the micro BS, omni-directional antennas (4 dBi). Two different propagation models were considered to calculate the path loss according to the

characteristics of the environment (both for outdoor propagation). For rural scenarios, the COST 231 Hata model was used. The main input parameters for the model were the UE antenna heights, 1.5 m, and BS antenna heights, 35 m. For the urban environment the propagation model applied was COST 231 Walfish-Ikegami. The main parameters used were the User Equipment (UE) antenna heights, 1.5 m, BS antenna heights, between 10 and 25 m (depending if they are macro or micro), street width, 20 m, building separation, 40 m, and building height, 12 m. From the result obtained, it was observed that the main interference source was not ACI, but the interference from the neighbouring BSs working on the same channel.

The reviewed work specifically focused on investigating the source of adjacent channel interference within the co-existing network, but failed to evaluate the different levels of interfering power effects on the victim receiver and the overall system performance. This research work bridged the gap by evaluating the degree of interfering power effects on the victim receiver front end. The result(s) obtained from the evaluation was utilized in the design of the specific mitigation system.

The authors in [50], emphasized on the emerging heterogeneous multi radio networks, focusing on interference issues due to simultaneous operation of multiple radios. The work was based on the sources of co-existing interference including transmitter noise, receiver blocking and intermodulation distortion.

Various co-existing techniques and relevant standardization efforts were studied, which included the Physical Technique (PHY) and the Media Access Control (MAC). Also the ongoing IEEE standards relating to co-existing and how to improve the system performance of a multi-radio device by making air-interface adapt to co-existing interference were also enumerated. The physical technique comprised of *Spectrum Masking* and *Antenna Isolation*, which are applied to increase the coupling loss between antennas, *Shielding* which aids in adding further isolation between the radio circuitries. Others include; The *Band Pass or Low Pass RF filter,* which is often used to reduce harmonic emission and out-of-band emissions at the transmitter output, *Beam Forming* and *Interference Cancellation,* which aids in removing interference from the output involving the application of spatial diversity and or signal processing.

The second technique (MAC) provided protection which included the applications of dynamic frequency selection (DFS), transmission power control (TPC) and time sharing (TS). DFS, allows a radio to dynamically select a channel with the least interference, TPC, forces a radio to operate at its lowest transmit power subject to link budget measurement and calculation while TS, schedules multiple radio in time domain to avoid overlap with each other. The standard technique involved the IEEE standard related to coexistence which include 802.19 and P1900.2. These standards focused on analysis and evaluation methodology while 802.15.2, 802.16.2, 802.11h and

802.16h aimed at providing solutions or facilitations to enable coexistence. A Media Independent Co-existing Service (MICE) layer was proposed and suggested that the performance of a multi-radio system can be further improved if necessary support and modifications were added to individual wireless technology. Packet traffic arbitration technique was used for the co-existing. The proposed co-existing adaptation achieved up to 50% improvement of the transmission efficiency in a Wifi/Bluetooth dual-radio device using 802.15.2.

The reviewed work emphasized on theoretical suggestions on the various techniques to reduce interference in a co-existing network. The inherent weakness observed in this work was that other necessary procedures required for adequate design and implementation, for example either the use of adaptive or fixed filter technique as a mitigation approach was lacking. Also antenna-to-antenna isolation that was considered in the paper is adequate but owing to achieving maximized coverage; antenna isolation is not required to increase beyond standard specifications. This specification has to do with the environment or country of research interest (for example in Nigeria, 50dB antenna-to-antenna isolation for co-located networks remained the standard specification by NCC for PCS, DCS, AND UMTS) [23]. Hence this option was not considered a primary approach. This research improved on the limitations by extensive evaluation and characterization of the environment of

interest (the signals and noise characteristics) to obtain the specifications required for the filter design.

Another author [51] characterized transmitter and receiver performance based on lab tests conducted on commercial equipment for both UMTS 900 and GSM 900MHz terminals and base stations. The impact of GSM Mobile Stations (MS) and UMTS node B and user end with GSM BTS on receiver performance as a function of frequency offset and coupling loss between interfering transmitter and victim receiver were assessed. The result obtained showed that the limiting factor was the interference caused by the GSM MS to the UMTS Node B and that as little as 4.2MHz of GSM spectrum can be cleared and allocated to one UMTS carrier with satisfactory system performance. Also they studied the required guard band between UMTS 900 and GSM 900MHz in coordinated and uncoordinated operation using lab test measurement with commercial GSM BTs, UMTS node B and dual mode handset. It described the transmitter and receiver characteristics and the calculation of adjacent channel interference rejection (ACIR) using the sensitivity degradation measurements in the laboratory. They further presented how the sensitivity of victim receiver was degraded based on the interferer strength and coupling loss between the interferer and the victim. Mutual interference between GSM MS and UMTS UE and GSM BTs were studied. It was concluded that in coordinated deployment, 2.2MHz frequency offset from

UMTS center can be satisfied for requirement when the operator can tolerate slight capacity and coverage loss (i.e. UMTS 900 center is allocated 4.2MHz). Also when the operator has enough frequency resource or cannot tolerate about 1.7dB UMTS uplink capacity loss, 2.4MHz carrier separation is needed (i.e. UMTS 900 carrier is allocated 4.6MHz). In uncoordinated deployment, 2.6 MHz frequency offset satisfied the capacity and coverage requirements.

The paper actually considered the major steps required to address the issue of transmitter noise interference by first conducting a laboratory measurement to evaluate the levels of the received signal strength degradation with respect to the corresponding rise in interfering power, but failed to analyze the various levels of capacity degradation and noise rise as the interfering power increases. This research is an improvement because it identified the levels of the capacity degradations and percentage loss as the interfering power increases with rise in noise floor level. This is very important because it gives the network optimization engineer the steps to monitor and evaluate the degree of connectivity by the mobile subscribers within the assigned channel during peak and off peak periods and strategize ways to improve the system performance.

In the works of [52], a new frequency planning strategy to optimize the quality of service (QoS) of 3G wireless system was developed. From their work

captioned “the Impact of Intermodulation Interference in Superimposed 2G and 3G wireless networks”, investigated the critical parameters that affected the overall operation of the system belonging to different competing wireless communication consortia. It was anticipated that the consortia would operate separate wireless systems (2G and 3G) in the same geographical areas where block allocations of channels were made. In their analysis, the overlapping of 2G and 3G were examined; more specifically the interaction between the already installed GSM with the new WCDMA technology of UMTS was showcased. A frequency planning algorithm for 2G systems were considered for the tradeoff between adjacent channel and intermodulation interference. A new frequency planning logic that optimizes the performance of both GSM and UMTS systems when they coexist in a geographical area was proposed. 2G-3G superposition issues were presented and a theoretical background of intermodulation interference was also developed. An estimation of interference power level was calculated which involved measuring the path of IMI and extract the valuable information directly. COST 231 Hata model and Simple $d^{-\gamma}$ models were used. Evaluation of the results was given in equation 2.8.

$$L_P = 69.55 + 26.16\log f_i - 13.82\log h_l - a(h_m) + (44.9 - 6.55\log h_1)\log d \qquad (2.8)$$

where f_i is the frequency of IM products, h_1 is the effective height of the base station antenna (30-200m), h_m is the height of the receiver antenna (1-10m), d is the distance between two points, $a(h_m)$ is given as;

$$a(h_m) = (1.1\log f_i - 0.7)h_m - (1.56\log f_i - 0.8) \quad (2.9)$$

The impact of WCDMA capacity was explained. First UMTS features like Signal to Interference Ratio (SIR) and capacity were analyzed, in order to maintain the desirable Quality of Service (QoS), probability of error was kept constant and below the threshold given in the range of 5-9dB. It was concluded that from the deduced mathematical analysis applied on this study, when the IMI rises, the capacity of the system has to be reduced in order to maintain the required SIR. This study finally demonstrated the existence of this tradeoff and some general rules for the optimization of the system's co-existence and its application in 3G and 4G wireless systems.

The reviewed work primarily considered developing a new frequency strategy to optimize the quality of service. Take for instance, a country like Nigeria where frequency assignment for circuit switched networks for 1G, 2G and 3G is saturated, planning a new frequency strategy is not the best option because it may affect the entire licensed frequencies and may interfere with the unlicensed frequency bands. The weakness in this reviewed work lies to the fact that the authors could not proffer technical measures to improve the quality of service in the co-existence network. It was significantly achieved in this research through the application of Band Pass Filter (BPF). An improvement to the limitations of BPF was also achieved using the research proposed Adaptive Noise Cancellation Technique. This technique is adequate

for perfect noise cancellation in all co-located networks in spite of the frequency of operation.

The authors of [53], in their work investigated on the effect of adjacent channel interference generated by CDMA2000 on the WCDMA system uplink and downlink scheme in Indonesia. They deployed several scenarios and calculation models to evaluate the impact on the uplink and downlink scheme. The work emphasized on the calculations and simulation performance in one cell scenario, where one WCDMA base station, referred to 3G Node B and serving greater number of WCDMA mobile stations(Ms). Two calculations were made on the uplink by varying the distance, guard band frequency and number of CDMA 2000 MS. It was designed by setting CDMA2000 MS as source of interfere. The first calculation was to obtain the minimum allowed received power at WCDMA BS while the second calculation provided the capacity degradation. In the downlink scenario, measurements were conducted to obtain the capacity degradation of WCDMA MS due to the presence of CDMA 2000 BS. Simulation analysis was developed in one cell scenario where one WCDMA BS served numbers of its user's i.e WCDMA MS. The WCDMA downlink simulation was actualized through the following procedure: distributing the number of WCDMA MS randomly in one cell, defining the position of one CDMA 2000 BS and its distance to the WCDMA BS and calculating the pathloss value for each WCDMA MS towards

WCDMA BS and CDMA2000 BS. Others include: calculating the total transmission power of WCDMA BS, calculating the allocated transmission power for every WCDMA MS before the presence of the CDMA2000 BS and calculating the interference power generated by CDMA2000 BS for each pathloss value and the Signal to Interference Ratio (SIR) value for every WCDMA MS after the presence of CDMA 2000 BS.

Graphs were generated to show the minimum allowed received power at WCDMA BS for different number of users. The values obtained before and after the presence of interference from CDMA 2000 MS was used for comparative evaluation. Distance of WCDMA BS and CDMA2000 MS was set to be 100m, using guard bands of 5MHz and 10MHz consecutively. The result obtained show that the minimum allowed received power at WCDMA BS was decreased by the interference from CDMA2000 MS which decreases the number of served user. Calculation results when the distance between WCDMA BS and CDMA 2000 MS was reduced to 500m, showed that minimum allowed received power at WCDMA BS was larger compare to 1000m. This implies that the distance factor between CDMA2000 MS and WCDMA BS is significant. The smaller the distance, the larger the interference power, hence reducing the active number of subscribers. It was also observed that at 1000m distance and 10MHz guard band interference from sampled 100 CDMA 2000 MS gave a -110dBm, WCDMA BS can only serve

110 users. Also within 500m distance, it can only serve 65 users which results in significant reduction. The capacity loss of WCDMA system was also obtained, the distance reduction between WCDMA BS and CDMA 2000 MS causes larger capacity loss. For only 10 users of CDMA2000 MS, the 50m distance resulted in the WCDMA capacity loss to be 2.1%, when the number of CDMA 2000 was increased to be 100 users, capacity loss of WCDMA system was increased to 20%. It was concluded that the presence of CDMA 2000 system influenced WCDMA performance. Interference generated by CDMA2000 MS increased the minimum allowed received power at WCDMA BS, leading to reduction of WCDMA coverage and cause a significant capacity loss. In the downlink scheme, interference due to CDMA 2000 BS influenced the performance of WCDMA communication system which gave a significant reduction of SIR value. Also it was deduced by the authors that the effect of interference depends on several factors including distance between WCDMA and CDMA 2000 terminals (BS and MS), number of CDMA2000 MS, interference power and guard band frequency. Hence the higher the guard band, the lesser the interference.

The scenario of [53], demonstrated the co-existence performance effect of CDMA2000 and WCDMA network. The work emphasized on the adjacent channel interference of CDMA2000 MS on the WCDMA BS and CDMA BS on WCDMA MS. The authors were able to establish the significant reduction effects on the SIR and capacity loss of the WCDMA network due to the

interference from CDMA 2000 BS which reduces the number of user equipment. The authors developed a comprehensive and adequate analysis but principally accentuated on the significant effects of interference on the networks of interest. On the other hand, no further work or proposal was put in place on the need towards developing adequate mitigation technique(s) to reduce the interference issue rather they considered increasing the distance and guard band frequencies which may have significant effect especially on coverage radius and bandwidth wastage (owing to its scarce resource). The research study tends to bridge the gap through extensive measurements conducted to ascertain the levels of interference power effects, though in a co-located network. This was used as a platform to develop mitigation techniques. Mitigation priority was also emphasized for signals operating in a dynamic environment.

Also in the work titled “Proposal Solution for Interference Inter-Operators” [54], developed an interference reduction mechanism based on a physical optimization of antenna system that could be understood as a physical symmetry rotation in the space of parameters such as tilt and azimuth control system. The main objective of the work was to develop a mitigation technique for local interference problems caused by CDMA800 and GSM900 MHz without the need to supplement cost. They studied the mutual interference between CDMA 800 operating at downlink 869-894MHz and GSM 900 uplink 890-915MHz. However, the two CDMA and GSM technologies operating in

adjacent frequency bands was the main source of interference leading to a significant degradation of quality of service.

The approaches adopted were based on physical optimization of antenna systems. The method acts only on some parameters of the system such as tilt and Azimuth. This gave a solution to independently reduce the interference effects on the distance between the base stations. The method improved client service without using hard installation and it can be considered as inexpensive technology.

One advantage of this physical approach is that it is simple and easy to implement but pose some limitations. One of the limitations is that only physical optimization of antenna isolation is not adequate for proper attenuation or cancellation of transmitter interference (sideband interference). Additional mitigation techniques are necessary to be introduced in order to achieve high performance network systems. The study introduced adequate mitigation techniques viz the applications of fixed filter and adaptive cancellation techniques respectively.

In another development, [55] proposed a “brute-force solution for a military frequency hopping communication system” to enhance the system capacity. As seen in Figure 2.15, it involves the placement of frequency agile band pass filters in front of receiver Low Noise Amplifiers (LNAs) and after the transmitter Power Amplifiers (PAs). The receiver pre-filtering stops large

jamming signals and admits only the desired signal into the LNA. Likewise, transmitter post-filtering rejects any reverse signal from entering the PAs and stops IM products produced from being transmitted. However, expensive high-*Q* cavity filters with low insertion loss would be required to sufficiently attenuate the large transmitter signals, which, in some cases, have output powers of +47dBm (50W) [56].

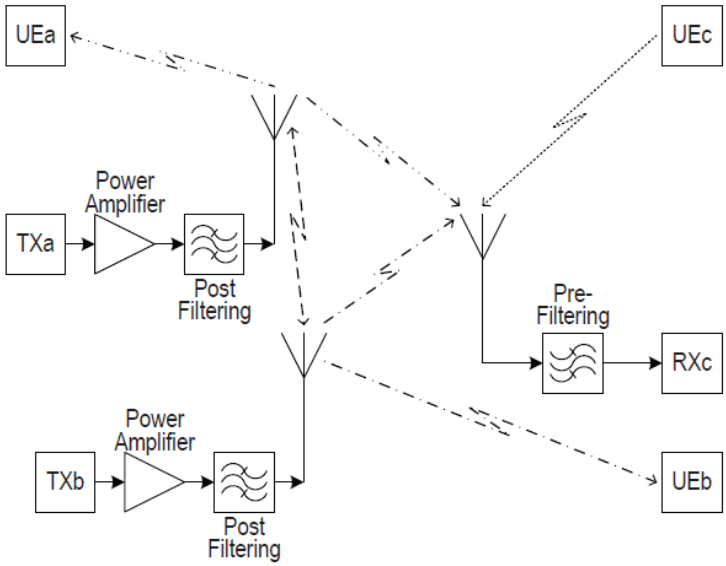

Figure 2.15: Passive pre and post filtering to mitigate co-located interference issues [55].

In addition, frequency agility adds another dimension of complexity and cost which is the key drawback of the work. For this reason, the technique is commercially unfeasible proposition for wireless service providers.

[57] and [58] in their own mechanisms proposed a "single-loop adaptive cancellation system for co-locating a global positioning system (GPS) receiver unit within a mobile communication UE". As seen in Figure 2.16, the cancellation system couples out a sample of the interfering mobile

communication transmit signal. The compensation path signal is then adaptively gain-phase adjusted such that it is equal in magnitude and 180^0 out of phase to the interference path signal when coupled back in the receive path of the GPS unit. This mitigates the interfering mobile communication transmit signal before it reaches the GPS receiver. A variable attenuator and a phase shifter can only cancel narrow-band noise signals.

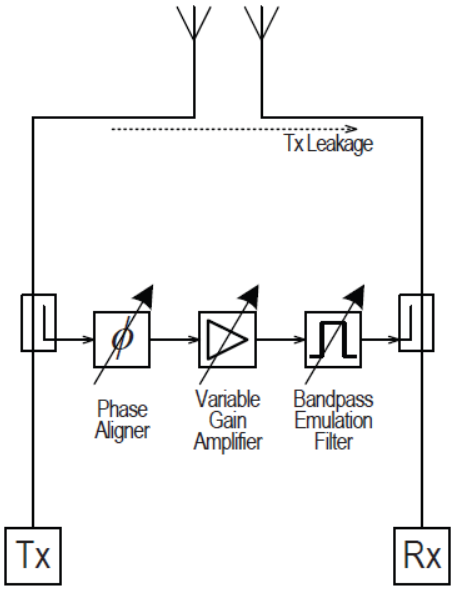

Figure 2.16: Interference cancellation unit for co-located radios [57].

The inherent flaw in the reviewed work was that wideband signal cancellation will require an accurate delay match of the compensation path to the interference path. Also, a variable attenuator and a phase shifter can only cancel narrow-band noise signals. To optimize this technique in the research study, an Adaptive Noise Cancellation System comprising of a gain-phase adjuster (vector modulator) and a controlled algorithm was developed which can drive the weight variables into perfect cancellation. This technique has the

potentials to achieve real-time correlated broadband noise cancellation performance, thereby achieving optimal desired signal at the receiving end. It can also perform for both-narrow band and wide-band noise signal cancellation.

The Application of passive Surface Acoustic Wave (SAW) duplexing band pass filters" as proposed by [59], showed how the transmit chain band pass filter stops the radiation of transmitter noise into the receiver's desired channel. The receiver path band pass filter stops the transmitter signal from overloading the receiver (desensitization). But these band pass filters do not have sufficient power handling capability when used in base station environments and are not frequency agile. An alternative approach taken by the authors of [60] proposed an adaptive duplexing circuit for multi-band operation. As seen in Figure 2.17, the adaptive duplexer uses a circulator to direct the transmit signal into the antenna port and to direct the desired signal into the receive path. However, the limited reverse isolation of the circulator allows leakage of the transmit signal and noise into the receive path. The authors use a direct feed from the transmitter in an adaptive double-loop cancellation path to create two nulls, as seen in Figure 2.16(b), effectively removing the interfering transmit signal and transmitter noise from the receiver. Further, delay lines were used to ensure the required matching between the interference path and the cancellation path such that a 5MHz

(WCDMA) wideband cancellation was achieved at the nulls. The loops achieved a higher cancellation of the transmit signal and a reduced transmitter noise at the receiver.

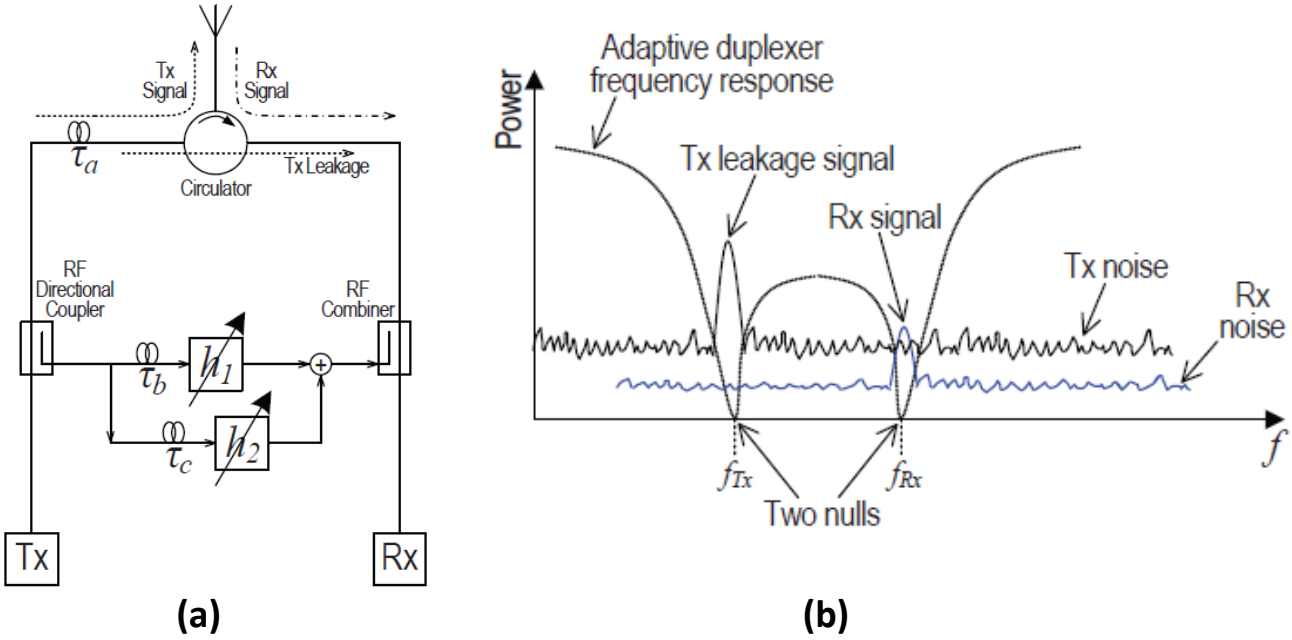

Figure 2.17(a): Adaptive Duplexer Architecture (b) Adaptive duplexer provides two nulls at the transmitted frequency and the desired receive frequency [60].

However, in a co-located base station scenario, each of the transceivers are independent and a direct feed from co-located aggressor transmitters. Further, both papers of [59] and [60] published good cancellation performance, but neither of them considered deploying strategies to reduce the noise generated by the cancelling loops themselves.

The research work considered using a coupler of lower values (-10dB and -20dB). These couplers generate negligible insertion loss, which may not have

significant impact on the canceling signals at the primary and reference paths. On the other hand, the insertion loss generated by the vector modulator was compensated by introducing an amplifier to boost the noise signal at the reference path in order to obtain the actual magnitude required for cancellation with reference to the correlated noise amplitude signal at the primary path.

The application of active cancellation technique for Tx/Rx feed through in an auxiliary transmitters as developed by [61], showed how a flexible multiband front end involving an additional multi-band transmitter chain was used to cancel the transmitter interference signal. The cancellation signal was computed over the Tx channel bandwidth in the baseband and then transformed up to RF via an auxiliary transmitter Ax as shown in Figure 2.18

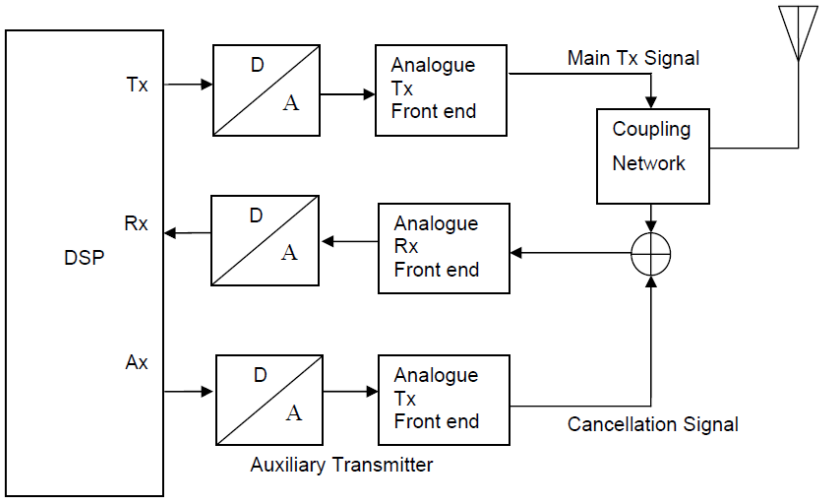

Figure 2.18: Active cancellation concept of the Tx/Rx feedthrough applying an auxiliary transmitter

Based on the understanding of the architecture, the design does not cancel the transmitter noise in the receiver band because the transmitter noise and the auxiliary transmitter noise introduced are not correlated, instead of cancelling

the transmitter noise, the technique introduces additional noise components, effectively doubling the additional thermal noise flow to the receiver. This further could degrade the receiver noise figure. The introduction of auxiliary transmitter adds more cost to the design. The strategy adopted in this research proffered an improvement to the design of [61] both in cost of implementation and in noise cancellation performance. The noise signal at the reference path is correlated with the noise signal at the primary path, providing the necessary condition to achieve good noise cancellation.

CHAPTER THREE

RESEARCH METHODOLOGY AND IMPLEMENTATION

3.1 Proposed Techniques

The communication channel considered in this study was the RF path present from the transmit power amplifier to the receive antenna of a wireless base station. The thesis proposed a mitigation technique that comprised two different design methods; Band Pass Filter (BPF) and Adaptive Noise Cancellation (ANC) Techniques. The BPF technique required the application of digital band pass filter which eliminates substantially the sideband noise generated by the transmitter. However, the sideband noise leakages at the output of the filter might affect the desired signal due to the lack of perfect isolation by the fixed filter. Meanwhile, the dynamic nature of the noise characteristics could also enhance more leakages since the filter is of fixed category. On the other hand, the later technique was introduced to demonstrate an improved feature over the BPF technique, especially in a time-varying environment and its attributes to achieve perfect noise cancellation.

The application of band pass filtering technique requires a priori knowledge of both the signal and noise characteristics. The method is based on knowing the interference properties and knowing the parameters of the radio devices, which requires evaluating the interfering signal power level of the offending transmitter on the victim receiver. This technique is typified by its accessibility

issues, characterized by huge capital requirements. The digital filter was considered for this research in lieu the analog counterpart owing to the fact that any amount of information can be managed to any level appropriate for each application. A set of configuration adjustments and the application of the filter device could be relevant to mitigate the sideband noise. The ANC technique requires little or no prior knowledge of the signal and noise characteristics, it requires a signal that is correlated in some sense to the signal to be estimated. The ANC technique possesses enhanced feature over the BPF technique with the capability to adaptively track signals under non-stationary conditions towards achieving perfect cancellation.

This technique entails deploying a reference antenna to pick the noise or jamming signals, apply the necessary gain-phase adjustment towards removing the noise signals from the primary input [47]. Mitigating the noise signals before arriving at the Low Noise Amplifier (LNA), would stop it from generating distortions within the receiver [46]. The theoretical feasibility of the technique was characterized and simulated using existing models by studying the effects of the cancellation loop on the receiver's dynamic range. Meanwhile, the application of band pass filter are suitable and conventionally used but pose major limitations especially for efficient power handling capability and unstable performance in a time-varying environment.

3.2 Characterization of the System and Analysis for the BPF Design

The performance effects of interference emission on the victim receiver front ends in a co-located network and the isolation requirements (dB) were evaluated first. The approach was considered using two scenarios. The first scenario involved an unco-located WCDMA network while the second scenario involved a co-located network comprising of CDMA 2000 and WCDMA. The technique constituted the application of empirical analysis.

3.2.1 Empirical and Mathematical Techniques

The term “noise” as used in the context of this work refers to any undesired spectral components above the thermal noise floor which fall within the receive band of a communication receiver [19]. When RF signal is power amplified to form the transmit signal, a significant amount of emissions are generated outside the transmit band referred to as sideband noise emission [62]. The emission occurs due to the non-linearity and noise generated inside the power amplifier. This emission or undesired noise components which mostly operate above and below the operating frequency bands could fall within the pass bands of a nearby or co-located receiver, degrading the received signal strength and increasing the noise floor level. This system distortion usually occurs when the transmitter and the receiver, operating within close frequency bands are in proximity.

The undesired fundamental component considered in this research was the side band noise generated from the co-located transmitter. This primarily contributes to reducing the Carrier to Interference ratio (C/I) in the receiver channel of a communication system. Therefore, the undesired spectral component is required to be mitigated or reduced to avoid the introduction of excessive noise in the receiver channel.

Scenario One involved the measurements of the reference received signal strength and evaluation of the system noise floor level, system capacity and the carrier to interference ratio for the unco-located networks.

Scenario Two considered the measurements of the received signal power, Effective Radiated Power (ERP) and the evaluation of the interfering signal power. Others include calculating the noise floor level, vertical antenna-to-antenna isolation in dB, Carrier to Interference (C/I) ratio, system capacity and percentage C/I degradation respectively for the co-located networks.

Scenario One

- **Empirical Procedure**

Measurements were carried out on the WCDMA stand-alone site to obtain the average received signal power using a *Huawei software M2000 service maintenance system CBSS* installed in a laptop. The measurements were conducted in two seasonal periods (dry and rainy season), primarily aimed to

obtain the best possible average received signal power and effective radiated power for a better system evaluation and design.

- **Mathematical Procedure**

The following parameters were calculated:

a. **The Noise Figure (NF):** NF is mostly used to describe the way in which a device adds noise to a signal. The basic approach applied to estimate the noise figure for WCDMA systems was the Minimum Detectable Signal (MDS). The knowledge of the MDS is also necessary when calculating the dynamic range or signal to noise ratio for a particular receiver configuration. The MDS by standard measurement is given as -102dBm for WCDMA network [63]. The mathematical model used for the noise figure estimation is given in equation (3.1) as in NF(dB) [63].

$$NF(dB) = MDS(dBm) - (-174(dBm) - 10\log B(dB) \quad (3.1)$$

Where, B is the channel bandwidth for the WCDMA given as 5MHz [39], -174dBm is the thermal noise power = kT_0B, where k is the Boltzmann's constant given as $1.38x10^{-23}\,J/k$, T_0 is the absolute temperature in Kelvin given as $290k$, that is $K = 273 + {}^0C$, where ${}^0C$ is given as $16.85\,{}^0C$, approximately $17\,{}^0C$, which is the ambient temperature for Noise Figure (NF) measurement as defined by the IEEE standard [64,65], B is the measurement bandwidth.

For comparison of receivers working at different impedance levels, the use of equivalent noise resistance is usually misleading; hence, the noise figure is mostly used. The noise factor (F) is defined in equation (3.2) as the ratio of the signal-to-noise power supplied to the input terminals of a receiver (ideal receiver) to the signal-to-noise power supplied to the output (practical receiver) [65].

$$F = \frac{S/N\,(ideal.reciever)}{S/N\,(practical.receiver)} = \frac{S_i/N_i}{S_o/N_o} \tag{3.2}$$

Where,

S_i = Available signal input power model, N_i = Available noise input power, S_o = Available signal output power, N_o = Available noise output power.

Using the definition from equation 3.2, it can be seen that an ideal receiver adds no noise to a signal. Hence, its output signal-to-noise ratio is same as that at the input and therefore, the noise factor is 1. On the other hand, this research involved a practical receiver (sensible receiver) other than an ideal receiver. Hence, noise emission results to the Signal-to-Noise (S/N) ratio deterioration as the signals move towards the output. This shows that output S/N ratio may be lower than the input value and so the noise figure will exceed the ideal state. The NF was deduced as noise factor expressed in Db as given in equation (3.3) [64].

$$NF = 10\log F(dB) \tag{3.3}$$

b. **The Noise Floor Level**: It requires the knowledge of the noise figure in other to evaluate the system carrier to interference ratio (C/I) ratio. Table 2.4 showed the standard noise figure for WCDMA given by 3GPP as 5dB [39, 66]. Increase in noise floor level decreases the channel capacity and degrades the receiver sensitivity. The mathematical model used in this study to evaluate the noise floor level is given as N_{floor} and as stated in equation (3.4) [67].

$$N_{floor} = 10\frac{KT_0B + NF}{10}mw \tag{3.4}$$

$$N_{floor} = KT_0B + NF = -174dBm/Hz + 10\log(3.84x10^6) + NF$$

where B is the signal bandwidth of WCDMA = 3.84MHz [39].

Based on the results obtained using equation (3.4), the C/I ratio for the unco-located network was obtained using equation (3.5) [67].

$$\left(\frac{C}{I}\right)_m = S_{0u} - N_{floor} \tag{3.5}$$

Where, S_{0u} is the average received signal strength for unco-located network.

The C/I ratio in a communication channel characterizes the quality with which information is transferred through the channel. It also sets a limit on the minimum required information carrying characteristics of the signal such that the information can be properly detected and recovered.

In digital communication systems, the performance is mostly characterized using the bit error rate (BER) performance criteria. The primary requirement of the communication system is to achieve and maintain a low BER performance by attaining a very high C/I.

Scenario Two

- **Empirical Procedure**

The following parameters were obtained through measurement:

a. The average transmitted signal power for CDMA-2000 network and
b. The average received signal power for the WCDMA network.

Data was obtained for two distinct seasons. The first was conducted during the dry season, while the second took place during the rainy period.

- **Mathematical Procedure**

The following parameters were obtained through computation:

a. The vertical collinear antenna-to-antenna isolation (dB). As explained previously, antenna-to-antenna isolation specification (dB) is given and standardized by NCC for all PCS and DCS co-located sites as 50dB was adopted in this study [23]

b. **The Noise Floor Level**: The difference in the received signal level for co-located and unco-located networks gave the degraded receiver sensitivity, denoted by eta symbol (ηdB). If the received signal strength is degraded by η, then the interference plus noise power is given by equation (3.6) [67].

$$N_{FT} = N_{floor} + \eta = 10\frac{KT_0B + NF}{10}10\frac{\eta}{10}mw$$

or

$$N_{FT}(dBm) = (N_{floor} + \eta)dBm = KT_0B + NF + \eta(dBm) \quad (3.6)$$

If the interference level is equal to the equivalent noise level of the original signal, the signal sensitivity will be degraded by 3dB [39]. Therefore, the noise level of the original signal is expected to always be 3dB above the interference noise level in other to maintain victim's percentage ratio (i.e an acceptable desired signal level).

c. **The Interfering Signal Power:** In the process of proffering solution to the prevailing interference, one of the fundamental considerations is to evaluate and quantify the intensity and effects of the interfering power (sideband noise) on the overall system performance. The performance effects of the interfering powers affect basically-the received signal strength, the system noise floor level and the C/I ratio. The interfering power at the receiver input, represented by a gamma symbol (γ) in dBm is computed using equation (3.7) [67].

$$\gamma = 10\log_{10}\left\{10\frac{KTB + NF + \eta}{10} - 10\frac{KTB + NF}{10}\right\}dBm$$

or

$$\gamma = (KTB + NF) + 10\log_{10}\left\{10\frac{\eta}{10} - 1\right\}dBm \quad (3.7)$$

It is important to note that a degradation of received signal strength (dB) is equal to the increase in the total noise plus interference [39]. This further

explains that if the noise floor level of a receiver increases by 1dB, the received signal strength will also decrease by 1dB.

d. **The Carrier-to-Interference (C/I) Ratio**: This parameter was considered a vital tool to evaluate the system capacity and its percentage degradation. Having obtained the average values for the received signal power, both in a co-located and unco-located networks, also evaluated the noise floor levels for both networks in different scenarios. The model to obtain the minimum carrier-to-interference ratio (dB) for the co-located network is given by equation (3.8) [67].

$$\left(\frac{C}{I}\right)_m = S_{0c} - (N_{floor} + \eta) \quad (3.8)$$

Where S_{0c} is the average received signal strength for co-located network

3.3 Measurement Test-Bed and Environment

The purpose of the measurement was to examine the interference leakage of CDMA-2000 Tx on WCDMA Rx signals. The test network set-up was in Enugu State, involving a co-located and unco-located site respectively. The co-located site comprised a CDMA-2000 network; owned by Visaphone network operator and a WCDMA network; owned by MTN network operator. The co-located networks consist of distinct antennas placed vertically collinear to each other, situated at Plot 5 peace Close Federal Housing Estate Trans Ekulu Enugu, Enugu State with the following characteristics: Visa ID: ENU005, IHS ID: IHS_ENG_007, Network operators: MTN-Starcomms-Visaphone, BTS or

Local cell ID: 2155, sector ID: 0, Carrier ID: 18. This network is managed by the IHS vendors. The unco-located site involved a standalone WCDMA Network, owned by MTN network provider situated at Independent Layout, opposite Brown and Brown hotel new Haven, Enugu, characterized by the following: Site ID: HENB549, Cell ID:EN0099C, longitude and latitude of 7.5286945 and 6.44658 respectively. The standalone network is managed by Huawei technology. The co-located and the unco-located sites were situated in urban and free space environments. Figure 3.1 (a) and (b) show the unco-located and co-located sites respectively while Figures. 3.2 and 3.3 show the measurement environment configured using goggle earth device and the flowchart representing the steps to obtain the filter magnitude respectively

(a) (b)

Fig 3.1: (a) Unco-located WCDMA site (b) Co-located Site (WCDMA & CDMA-2000)

Fig 3.2: Environment measurement site

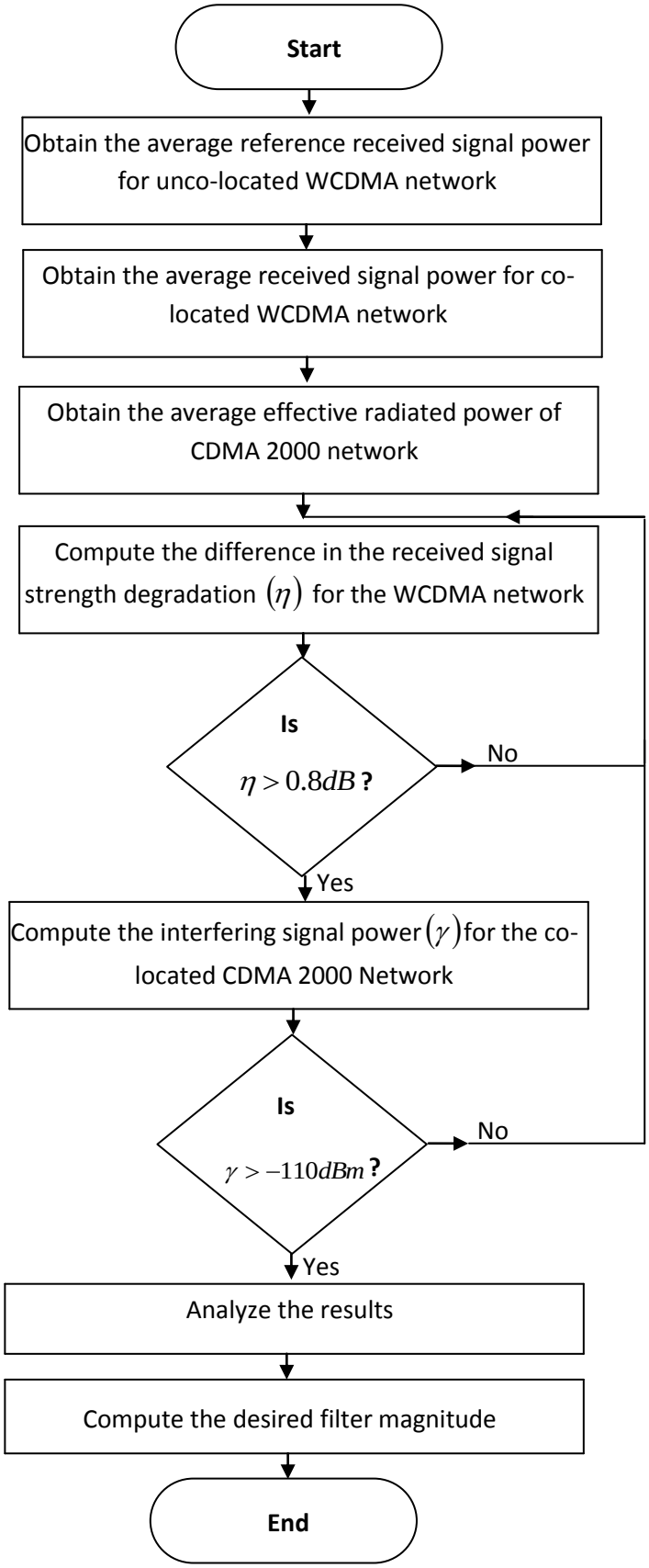

Figure 3.3: Steps to Obtain the Desired Filter Magnitude

3.4 Proposed Adaptive Noise Cancellation Architecture

The co-located scenario required a single system that will adaptively filter all co-located high power transmit jammers and allow only the desired received signal at the receiver. The Proposed Adaptive Noise Cancellation Technique (ANCT) generally comes into play in this thesis as a measure to improve on the limitations of the Band Pass Filter (BPF) especially when operating in a dynamic environment and its potentials to achieve perfect cancellation with optimal SIR performance at the victim receiver. In the electromagnetic spectrum, signals commonly carry information in terms of Amplitude, Phase and Frequency [23]. The proposed ANCT requires developing an expression for the SNR performance at the primary path using a reference path as the sampler. The SIR in a communication channel characterizes the quality with which information is transferred through the channel i.e., it sets a limit on the minimum required information carrying characteristics of the signal such that the information can be properly detected and recovered.

ANCT operates on the principles of destructive interference between a primary path and the reference path correlated noise signals [46]. In order to cancel the correlated noise signal at the point of cancellation by vector addition, a sample of the input noise signal must be synthesized, phase-inverted by the gain-phase adjuster, a sample of the error signals obtained is fedback via the coupler, and the error signal is adjusted by the signal controller [46]. For the purpose of this

research, primary path was used interchangeable to main path, as well reference path to cancellation path.

3.4.1Theoretical Concept of the Proposed ANCT

It is necessary to discuss some key mechanisms that determine the cancelation level of the proposed ANCT. This includes the system methodology. The ANCT architecture shown in Figure 3.4 was used to derive fundamental theory applied in the cancellation mechanism, which also functions as the system architecture for the simulation analysis. In the theoretical perspective, ANCT was applied as a technique to sample the undesired spectral components that interfere with the receiver front end. The primary antenna picks up the desired signal $S_{\Pr i}$, with the jamming signals $X_{\Pr i}$. The reference antenna is directed to pick only the jamming signal $X_{\mathrm{Re}f}$ (or more practically have much larger interference to signal ratio than the primary).

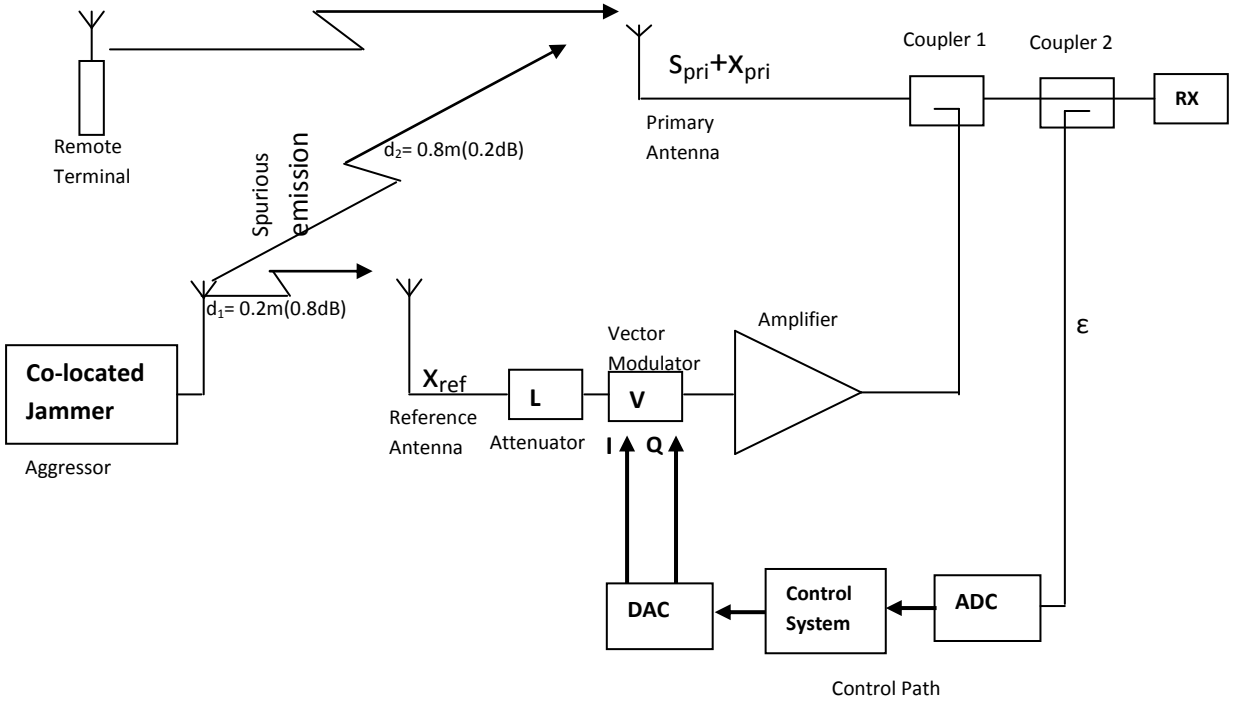

Figure 3.4: Proposed Adaptive Cancellation System for a co-located network

The interfering signal was sampled using a reference antenna oriented in the direction of arrival of the interfering signal or directly from the source such as the output of the power transmitter. The sampled signal was then used to cancel by vector addition the interference present in the primary antenna path of the affected receiver before the interference enters the receiver channel or degrades the sensitivity of the receiver operating at close frequency bands. The proposed technique can theoretically provide perfect cancellation for all distorted signals. It possesses the following important characteristics [47]:

- Requires no prior knowledge of the environment
- Stable in a dynamic environment
- Capable of adaptively tracking the signal under non-stationary conditions
- Possesses better power handling capabilities
- Achieves higher frequency agility response
- Its application is also well suited for dynamic channel allocation such as in a cellular system and can operate over a wider bandwidth.
- Can also be integrated in RF communication systems without any major overhaul.

The ANCT signal controller consists of two components at the cancellation path. The vector modulator and amplifier components. The vector modulator is necessary to modify the noise signal such that it matches its complement in the primary path. An attenuator in the vector modulator is required when the amplitude of the noise signals picked on the reference antenna are sufficiently

larger than that on the primary. The amplifier is necessary to compensate for the insertion loss generated by the vector modulator; the In-phase (I) and the Quadrature phase (Q), which reduces signal amplitude; provide the amplification needed to cancel the noise correlated signals in the primary path. The vector modulator works by adjusting the I and Q components of the noise signal, resulting in simultaneous amplitude balance and minimum phase error between the primary signal and the cancellation signal through the adaptive adjustment of I and Q signal amplitude levels. I and Q modulators acts as an actuator used to adjust the cancellation signal in the cancellation signal path. Furthermore, the I and Q control inputs and vector modulator can be considered as the weight variables of the adaptive systems.

The weight variables are the parameters that must be optimized to achieve perfect cancellation. The reference path and the primary path have different delay characteristics. The primary reason why the two paths have different delay characteristics is because each path uses different components. The primary path consists of two directional couplers and a delay line, exhibit fairly active component characteristics with extremely low insertion loss while the reference path contains both passive and active RF components, namely: I and Q (vector modulator), amplifiers and transmission lines. It is important to realize that any signal component from the primary path leaking into the reference path will be suppressed at the point of cancellation. This is because the system was designed such that the signal to interference ratio on the

primary antenna will be more sufficient than the signal to interference ratio on the reference antenna, which encapsulates to a high interference to signal ratio (ISR) at the reference antenna. Only the undesired signal components (i.e. the correlated noise) will be sampled for cancellation to obtain the desired signal components.

Directional couplers are commonly used to both combine and divide signals; its basic function is to operate on an input so that two output signals are available. It separates signals based on the direction of signal propagation and usually generates low insertion loss [68]. Coupler 1 as shown in Fig. 3.4 was the center point for cancellation of the correlated undesired signals, while coupler 2 extracts the feedback signal for the convergence algorithm. The primary contributor to the minimal insertion loss at the primary path was the directional couplers. Reducing the coupling value of the directional coupler would give a negligible insertion loss in the primary path while maintaining a large enough correction signal for the cancellation. In the most practical applications, the coupler is an off-the-shelf item and only certain values are available namely -3dB, -6dB, -10dB, -20dB [69]. For the purpose of the research, a -10dB and -20dB couplers were proposed for coupler 1 and coupler 2. This was because, they generate negligible insertion loss. Also for hardware design applications, it is recommended to consider devices with low insertion losses, to avoid forward coverage reduction.

Another contributor of a negligible insertion loss in the primary path was the delay line length. The cancellation signal was ultimately delayed by propagating through the different stages of the signal processor or gain-phase adjuster. The signal processing delay can be expressed as the electrical time delay through the cancellation path from the point where the signal is sampled to the point of cancellation. It is necessary to compensate the reference path with a delay element τ_{pri} introduced at the primary path. A successful and perfect cancellation reduces the spectral components to zero or acceptable level while maintaining the integrity of the desired signal [69].

The reference antenna and primary antenna in practice were designed to be directional. In the research, the SNR on the reference antenna was reduced by placing the reference antenna closed to offending transmitter in the ratio of 0.2:0.8, considering a maximum distance of one meter (1m) between the co-located antennas. Hence, d_1 which is the distance between the jammer and the reference antenna slated as 0.2m while d_2, the distance between the jammer and the primary antenna given as 0.8m. Meanwhile, the amplitudes of the noise signals in the reference and primary antenna paths are divided in the ratio of 0.8:0.2. See Figure 3.4.

The proposed technique was considered to be adaptive because it has the potential to adjust to any dynamic environmental changes. Also it has the capability to adapt to new operating conditions and tracks the optimal

cancellation levels. The ANCT most popular approach for the control system generates error signals from the residual cancellation vector present at the output of the summing junction at coupler 2. The information extracted from the error signal requires developing an algorithm to ensure fast convergence for perfect cancellation. The control system is adaptive in the sense that the error signal (feedback error) contains the necessary information to drive the weight variables towards perfect cancelation. The control system takes the feedback error ε from the cancellation output to provide the necessary adjustments to the vector modulator. In order words, the algorithm is designed to perform iteratively, realized by using a control system in an attempt to actualize the cancellation residual power level.

To further analyze the circuit with respect to coupler 1, the conceptual system of Figure 3.4 was redrawn with coupler 1 and coupler 2, restructured as shown in Figure 3.5.

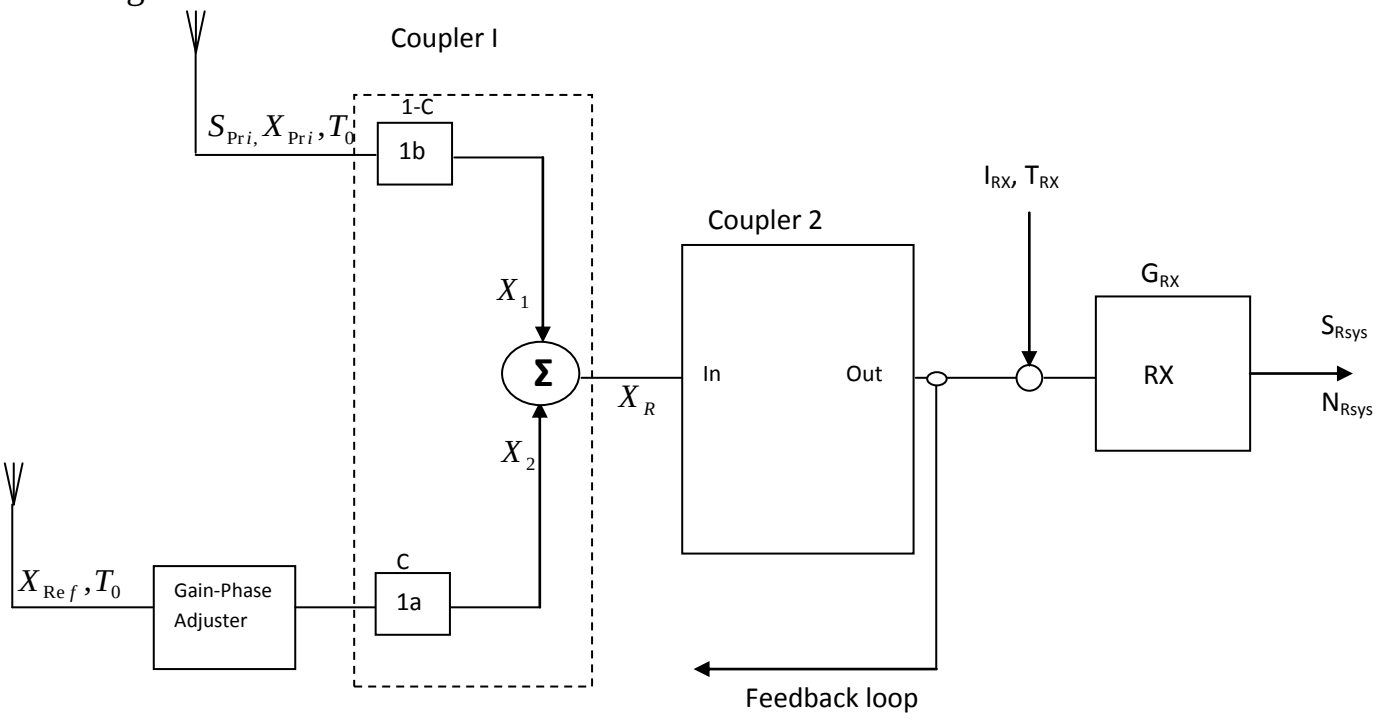

Figure 3.5: Signal to Noise ratio Analysis

At the cancellation point, the cancellation signal X_2 is subtracted from the correlated signal at the primary path X_1 to give the resultant signal $X_R = X_2 - X_1$. From the study, it was considered that the cancellation system had converged and obtain a perfect cancellation at the cancellation point, i.e. $X_a = X_b$, hence $X_R = 0$. Therefore, the GPA effective gain (Ge) was obtained in equation [3.9]:

$$G_e = \frac{1-C}{C} \tag{3.9}$$

where C is the coupling gain.

The resultant of the power signal X_R was fedback through coupler 2 for proper adjustment to achieve a perfect cancellation. From Figure 3.6, let the coupling gain at the cancellation coupler 1 be C and the through path gain as 1-C. It was assumed that the domain of C is limited to 0<C<1. The primary and reference antenna noises are uncorrelated to one another, they are white noise and have a noise temperature of T_0 (standard temperature 290k), where T_e is the GPA effective temperature, G_{Rx} is the receiver gain, I_{Rx} is the receiver input and T_{Rx} is the receiver input noise temperature. It deemed necessary to model the signal to noise ratio performance at the receiver using the valued parameters. It is obvious that the active system components generate inherent noise known as thermal noise or white noise. Therefore, the total generated noise by the system components at the receiver output is given as N_{Rsys} see equation (3.10) [69].

$$N_{Rsys} = K_B B_W G_{Rx}(T_0 + T_e C + T_{Rx}) \tag{3.10}$$

where K_B is the Boltzmann's constant $1.38x10^{-23} J/K$, B_W is the noise bandwidth (Hz). The desired signal level at the receiver output after cancellation was modeled as [69]:

$$S_{Rsys} = S(1-C)G_{Rx} \tag{3.11}$$

It is assumed that the interference (distortion) signal level had been cancelled out at the cancellation point with a minimal resolution value. Therefore the signal to noise ratio (SNR) performance at the receiver was modeled as [69]:

$$SNR = \frac{S(1-C)G_{Rx}}{K_B B_W G_{Rx}(T_0 + T_e C + T_{Rx})} = \frac{S(1-C)}{K_B B_W (T_0 + T_e C + T_{Rx})} \tag{3.12}$$

As C increases, the SNR at the output also increases.

For the purpose of this research, insertion loss effects at the primary path are considered negligible and contribute to no loss to the signal. The amplitude imbalance, phase error and delay mismatch was modeled and simulated. A self-developed algorithm was considered as a control mechanism to achieve the desired cancelation.

CHAPTER FOUR

DATA PRESENTATION AND RESULT ANALYSIS

4.1 Measuring Equipment and Configuration

A detailed experiment was carried out to measure the interference leakage using a *Huawei software M2000 service maintenance system CBSS* installed in a laptop. The software provided the window where the site to be measured was selected within the sector and the carrier. The M2000 software provided a centralized network management and an integrated topology window, through which users can create and manage the topology view of the entire network. The topology view displayed the networking status, geographical locations of devices, alarms generated during device operation, link status between devices, and connection status between devices and the M2000. This helps users to monitor the running status of the entire network.

M2000 system worked with a database server to support the daily operation and maintenance of wireless networks. It provided the remote and centralized configuration adjustment function for network troubleshooting and optimization. The physical structure of M2000 system consists of M2000 servers, M2000 clients, alarm boxes, and some networking devices. Figure 4-1 showed the hardware structure of the M2000 single-server system.

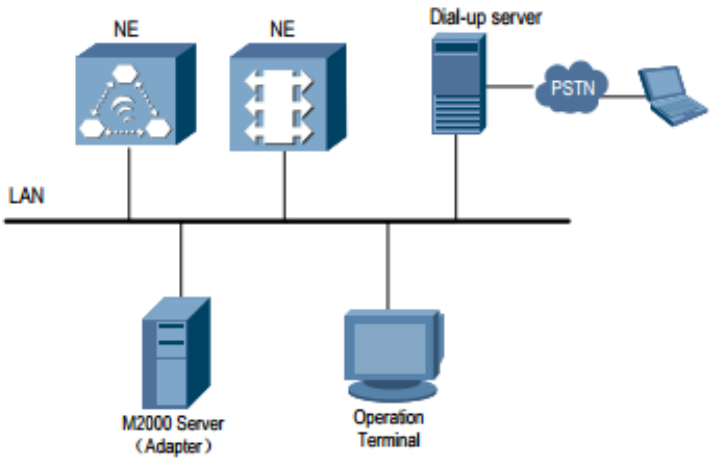

Fig 4.1 Schematic Physical Structure of M2000 System

Source: IHS Nigeria Plc 2013

The M2000 server was configured in single-server mode. The server was used for the file transfer between M2000 and the Network Elements (NEs). The server deployed was IBM PC Server which supports the Linux operating system and uses the Oracle database. The M2000 client was installed on a PC. The client configuration requirements are the CPU, E5300, memory 2GB; Hard disk 160GB, Accessories: DVDRW-integrated, Ethernet, adapter integrated audio, adapter-built-in sound, box 19LCD. The software is adaptable with Widows XP (32-bit) and other higher version Windows

The server software consists of the main version software and mediation software. The main version software was used to implement the system functions while the mediation software was used for the adaptation of different NE interfaces. Figure 4.2 illustrated the software structure of the M2000 system.

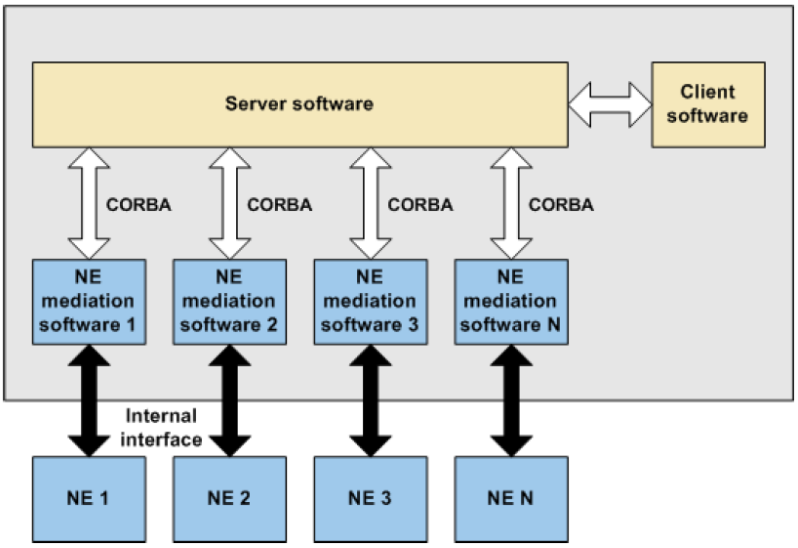

Figure 4.2 Software structure of the M2000 system

Source: IHS Nigeria Plc 2013

All the measurements obtained were conducted and facilitated by the IHS vendors and Helios towers on the reference sites based on the fundamental parameters and information provided for the study. The BTS received signal power measurements for the standalone unco-located and co-located networks, the transmitter power (effective radiated power) for the co-located CDMA 2000 networks were conducted for two major climatic seasons; the dry and rainy seasons. The measurements were spanned within six months interval (in February and in July 2013), primarily aimed towards obtaining an optimal data for the system analysis, design and evaluation. Refer to appendix A.

The received signal power measurements were conducted from Huawei site for the unco-located network and IHS site for the co-located network respectively. Average received signal power and transmitter power at the sectors were obtained.

4.2 Average Measured Data Obtained from the two Scenarios

The average received signal power for both the co-located WCDMA and the unco-located WCDMA networks were obtained, as shown in Table 4.1. The average received signal strength degradation (η) for the two scenarios and the average transmitted power (Effective Radiated Power) from CDMA-2000 network are also shown in Table 4.1. The received signal strength degradation (η) was obtained by the difference between the unco-located WCDMA average reference sensitivity and the co-located WCDMA average receiver sensitivity. However, since the insertion losses generated by the power amplifiers in transmit path reduces the output transmitted power; the Effective Radiated Power (ERP) obtained using the M2000 Service Maintenance System CBSS software was averaged as 38.6dBm. Though, 38.6dBm was certainly not the actual transmitted power if measured from the source.

Table 4.1: Summary of the Measured Data

1	Average received signal power for the unco-located network (WCDMA)	-109.69dBm
2	Average received signal power for the co-located network (WCDMA)	-110.70dBm
3	Average transmitted power (CDMA-2000)	38.6dBm
4	Recieved signal strength degradation (η)	1.01dBm

4.3 Computed Results Obtained from the Unco-located Scenario

Using equation 3.1, the noise figure for the unco-located network was obtained as 5dB. The system reference noise floor was calculated as -103dBm using

equation 3.4. The minimum demodulation carrier to interference ratio C/I was obtained as -6.69 using equation 3.5. The summary of the results obtained are shown in Table 4.2.

4.4 Computed Results Obtained from the Co-located Scenario

Using equation 3.6, the noise floor level was obtained as -101.99dBm. Using equation 3.7, the interfering signal power (side-band noise) was obtained as -108.80dBm. The minimum demodulation C/I ratio was evaluated as -8.70 using equation 3.9, which gave about 30% C/I ratio degradation. The summary of the results obtained are shown in Table 4.2. Refer to appendix B for the computation procedure for both the co-located and unco-located scenario.

Table 4.2: Summary of the Obtained Results

Noise floor for the unco-located site	**Noise floor for the co-located site**	**Interfering power level dBm**	**Minimum demodulation C/I (dB) for unco-located site**	**Minimum demodulation C/I (dB) for co-located site**	**C/I degradation**	**% C/I degradation**
-103	-101.99	-108.80	-6.69	-8.71	2.02	30

Table 4.2, showed that the interfering power of -108.8dBm from the CDMA 2000 co-located antenna degraded the received signal strength of the co-located WCDMA receiver antenna by 1.01dBm, given rise to the increase in the total noise floor level by 1.01dBm. This analogy was also validated from equation 3.6. This literally means that as the received signal strength degrades by a value, the total noise floor increases by the same value. Extensive results developed from the research study are shown in Table 4.3.

Table: 4.3 Average Ranges of the Generated Values

Recieved signal strength degradation (dB)	**Rise in total noise level after the system is interfered (dBm)**	**Interfering power level dBm**	**Decrease in interfering level compare to the original noise level (dB)**	**Noise figure (NF) dB**	**Minimum Demodulation C/I ratio**	**C/I ratio degradation**	**% C/I ratio degradation**
0.01	0.01	-129.37	26.37	5	-6.71	0.02	0.3%
0.10	0.10	-119.32	16.32	5	-6.89	0.20	3%
0.19	0.19	-116.39	13.49	5	-7.07	0.38	6%
0.28	0.28	-114.76	11.76	5	-7.25	0.56	8.4%
0.37	0.37	-113.50	10.50	5	-7.43	0.74	11%
0.46	0.46	-112.52	9.52	5	-7.61	0.92	14%
0.55	0.55	-111.70	8.70	5	-7.79	1.1	16.4%
0.64	0.64	-110.99	7.99	5	-7.97	1.28	19%
0.73	0.73	-110.40	7.37	5	-8.15	1.46	22%
0.82	0.82	-109.82	6.82	5	-8.33	1.64	25%
0.91	0.91	-109.32	6.32	5	-8.51	1.82	27%
1.00	1.00	-108.87	5.87	5	-8.69	2.0	30%
1.01	**1.01**	**-108.80**	**5.80**	**5**	**-8.71**	**2.02**	**30%**
1.09	1.09	-108.45	5.45	5	-8.78	2.09	31%
1.18	1.18	-108.06	5.06	5	-8.96	2.27	34%
1.27	1.27	-107.69	4.69	5	-9.14	2.45	37%
1.36	1.36	-107.34	4.34	5	-9.32	2.63	39%
1.45	1.45	-107.02	4.02	5	-9.5	2.81	42%
1.54	1.54	-106.70	3.71	5	-9.68	2.99	45%
1.63	1.63	-106.40	3.42	5	-9.86	3.17	47%
1.72	1.72	-106.13	3.13	5	-10.04	3.35	50%
1.81	1.81	-105.86	2.86	5	-10.22	3.53	53%
1.90	1.90	-105.61	2.61	5	-10.4	3.71	56%
1.99	1.99	-105.36	2.36	5	-10.58	3.89	58%
2.08	2.08	-105.12	2.12	5	-10.76	4.07	61%
2.17	2.17	-104.88	1.88	5	-10.94	4.25	64%
2.26	2.26	-104.66	1.66	5	-11.12	4.43	66%
2.35	2.35	-104.44	1.44	5	-11.3	4.61	69%
2.44	2.44	-104.23	1.23	5	-11.48	4.79	72%
2.53	2.53	-104.02	1.02	5	-11.66	4.97	74%
2.62	2.62	-103.82	0.82	5	-11.84	5.15	77%
2.71	2.71	-103.62	0.62	5	-12.02	5.33	80%
2.80	2.80	-103.43	0.43	5	-12.2	5.51	82%
2.89	2.89	-103.24	0.24	5	-12.38	5.69	85%
2.98	2.98	-103.10	0.10	5	-12.56	5.87	88%
3.00	3.00	-103.02	0.02	5	-12.60	5.91	88.3%
3.07	3.07	-102.88	-0.12	5	-12.74	6.05	90%

Tables are often used to show numerical results more accurately for comparison. Table 4.3 shows detailed generated values obtained from the analysis. The received signal strength degradation was considered in the range of 0.01 to 3.07 dB, using 0.09 as the increment. The first and the second column show the range of degradation in the received signal strength and the corresponding rise in total noise level after the system is interfered (refer to equation 3.6). The third column was obtained using equation 3.7, while the fourth column shows the decrease in interfering level compared to the original noise level of the WCDMA. The original noise level was obtained as -103dBm using equation 3.4. The fifth and sixth columns were obtained using equations 3.1 and 3.9 respectively. On the other hand, column four, row one and row two show that the noise floor level of the system is 26.37dB and 16.32dB higher than the interfering power level. This explained that the noise floor levels are within an acceptable range. If the interfering noise level is equivalent to the original noise level as shown in row thirty-six, column three and column four, where the interfering noise level was -103.02dB and the original noise level was -103dB, the entire desired received signal at that point will be completely corrupted. Hence, the received signal strength at that instance was degraded by 3dB, given rise to 88.3% degradation of the carrier to interference ratio. Therefore, it is always important to ensure that the noise floor level of the original signal is 3dB above the interference noise level to

maintain victim's percentage ratio [39]. The condition of such illustrated scenario can be improved by adding 3dB to the original noise floor level.

Columns six and eight show the minimum demodulation and percentage degradation of carrier to interference ratio when the received signal strength degrades by a value with the corresponding noise rise of the same value. The C/I ratio degradation in column seven was obtained by the difference in C/I ratio for unco-located and co-located networks. The graphical representations of Table 4.3 are illustrated in Figures 4.1-4.11 and the generated Matlab codes are shown in appendix C1-C11.

The results from Table 4.3 provided the following findings:

i. Increase in interfering power reduces the received signal strength of the WCDMA system. For this reason, the coverage radius was reduced resulting to high call drop rate thereby restraining subscribers from enjoying consistent and high quality services in a WCDMA cell.
ii. Increase in interfering power increase the noise level, hence fewer subscribers would only be accommodated.
iii. Under worst condition, only about 70% calls on WCDMA can be made. This explains that a highly interfered cell has less capacity; hence can support less user equipment simultaneously
iv. 1.01 dB degradation gave rise to 1.01dB noise floor and interfering power of 108.80dBm.

4.5 Comparisons of the Results Obtained with Existing Standards

Ericsson recommended 0.11dB as the maximum degradation required to maintain quality network performance with the allowable interfering power of -120dBm/3.84MHz [70]. The results obtained in the research work are in consonance with the recommendations by Ericsson. From Table 4.3, at maximum degradation of 0.11dB gave an allowable interfering power of -119.7dBm/3.84MHz).

3GPP specified a tolerable level of interference from the offending transmitter to the victim receiver as -110 dBm/3.84 MHz [71]. A spurious signal would be 7dB below the original noise floor value and its presence would cause a received signal strength degradation of 0.8 dB. The 3GPP standard agrees with the tabulated results obtained on the research as shown in Table 4.3. At 0.8 received signal strength degradation, gave interfering power of -109.9dBm/3.84MHz, a spurious signal is 6.97dB below the original noise floor value.

With reference to the results obtained as shown in table 4.3, the interfering power level from the offending transmitter to the victim receiver, evaluated as -108.80dBm/3.84MHz was beyond the specified tolerable level by the 3GPP given as -110 dBm/3.84 MHz. On that note, the result validated the proof of existence of interference in the co-located network of interest and therefore requires a mitigation technique for optimal network performance.

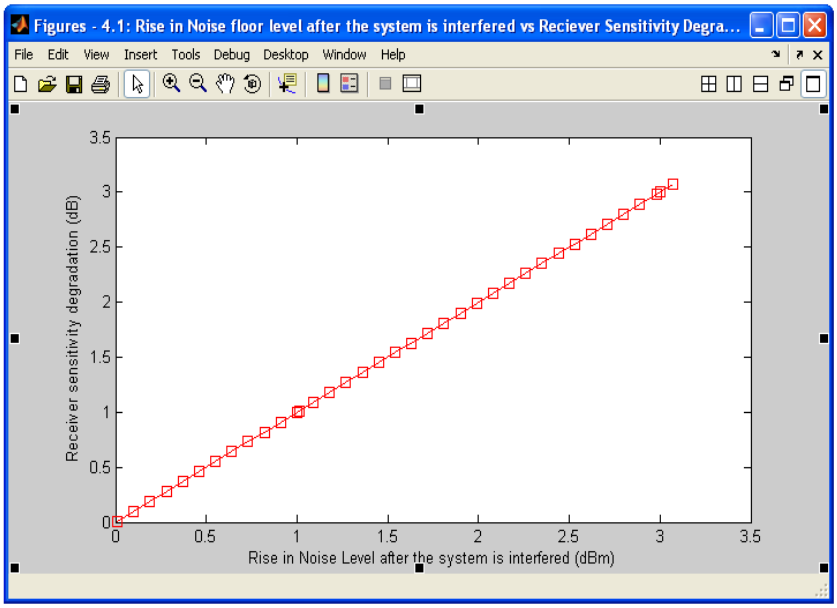

Figure 4.3: Rise in Noise floor level vs Received signal strength degradation

A linear graph as shown in Figure 4.3 showed the level of increase in noise and the corresponding degradation in received signal strength caused by the interfering power from the offending transmitter. A degradation of received signal strength (dB) is equal to the increase in the total noise plus interference. Hence received signal strength degradation of 1.01dBm gave rise to increase in noise floor level by same value. The trend follows that decrease in the received signal power results to corresponding increase in the system noise floor level.

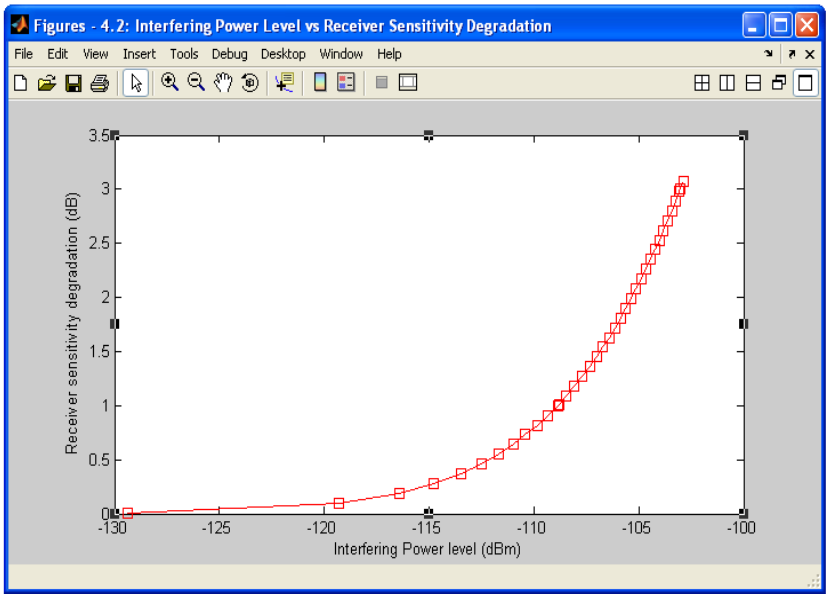

Figure 4.4: Interfering power level vs Received signal strength degradation

The exponential graph showed the performance effects of the interfering power from the co-located offending transmitter on the receiver sensitivity. Interfering power level of -108.80dBm degraded the sensitivity of the receiver by 1.01dBm. Refer to Table 4.3, as the interfering power from the offending transmitter increases, the received signal strength of the victim receiver degrades.

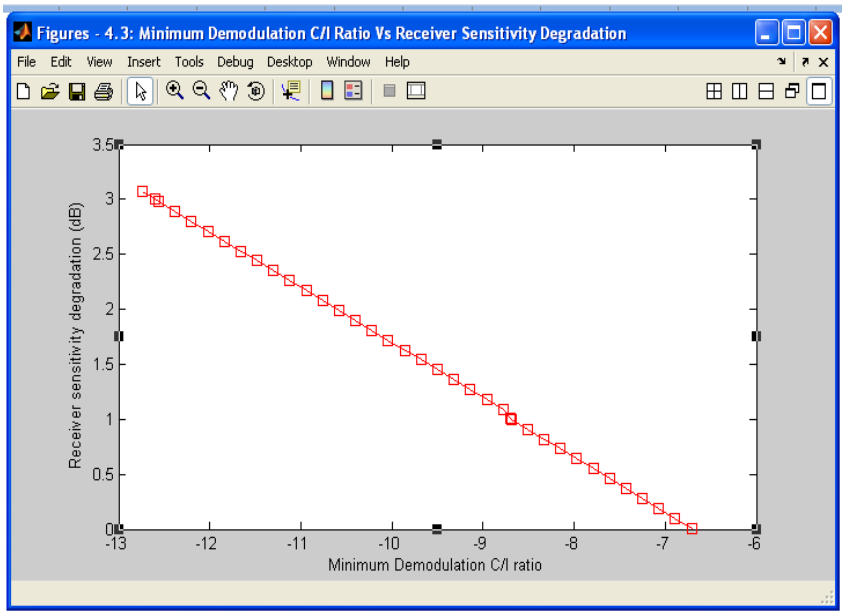

Figure 4.5: Minimum demodulation C/I ratio vs Recieved signal strength degradation

The negative slope in Figure 4.5 depicted the relationship between the received signal strength degradation from the victim receiver and the minimum demodulation Carrier-to-Interference (C/I) ratio. Decrease in the received signal strength resulted to decrease in minimum demodulation C/I ratio. This infers that as the interfering power of the co-located CDMA 2000 networks kept increasing, it inhibits the performance of the Received Signal Strength (RSS) of the WCDMA network. The reduction in the RSS gave rise to the

increase in the noise floor level of the system channel which directly reduces the C/I ratio performance of the system. Therefore, the higher the reduction in the RSS performance, the more the decrease in performance of the channel capacity. See Table 4.3.

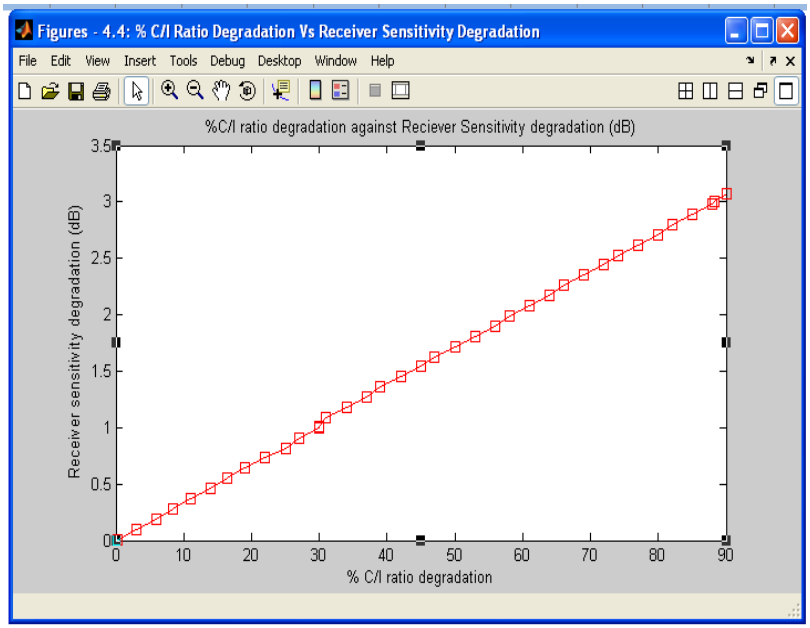

Figure 4.6: % C/I Ratio Degradation vs Received signal strength degradation

Figure 4.6 clearly demonstrated the linear response in percentage degradation performance of the C/I ratio as the received signal strength degrades. From the graph, 1.01dBm sensitivity degradation resulted to 30% C/I ratio reduction, also, at 3.0dBm received signal strength degradation gave rise to 88.3% C/I ratio degradation. At this point, the channel capacity was absolutely affected, only about 11.7% utilization. This effect generally impedes the overall performance of the system capacity. Hence, fewer subscribers will only be accommodated.

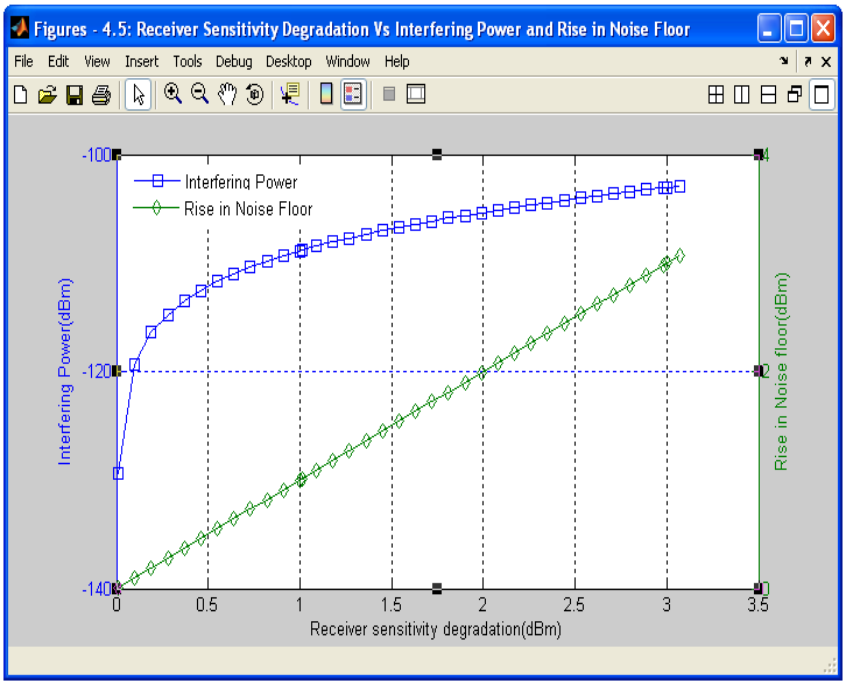

Figure 4.7: Received signal strength degradation vs Interfering Power and Rise in Noise floor

Figure 4.5 illustrated a combinatory graphical representation of the effects of increase in interfering power and noise floor on the system received signal strength performance in an interfering bound co-located network.

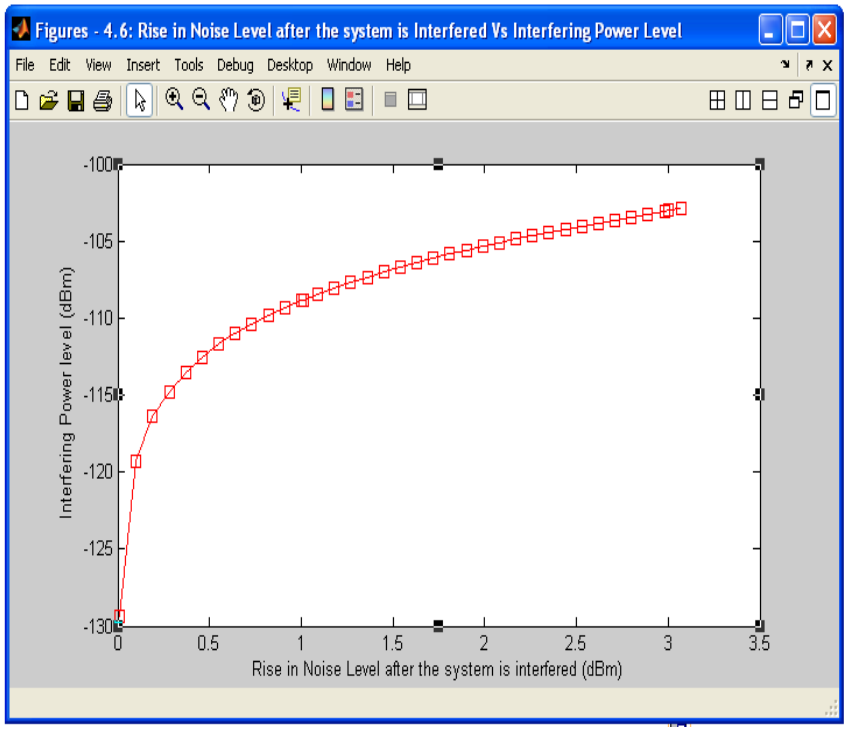

Figure 4.8: Rise in noise floor level after the system is interfered vs Interfering Power level

Figure 4.8, demonstrated the exponential performance characteristics of the increase in interfering power level and its effect on the system noise floor. From the graph, increase in interfering power of -108.80dBm, -106.13 dBm, and -103.43dBm gave rise to the corresponding noise floor levels of 1.01dBm, 1.72dBm and 2.80dBm respectively. Figure 4.8 further explained that the higher the interfering power from the co-located jammer (CDMA2000), the higher the increase in the noise floor level. Increase in noise floor level decreases the overall system capacity, hence could lead to an overall poor network performance.

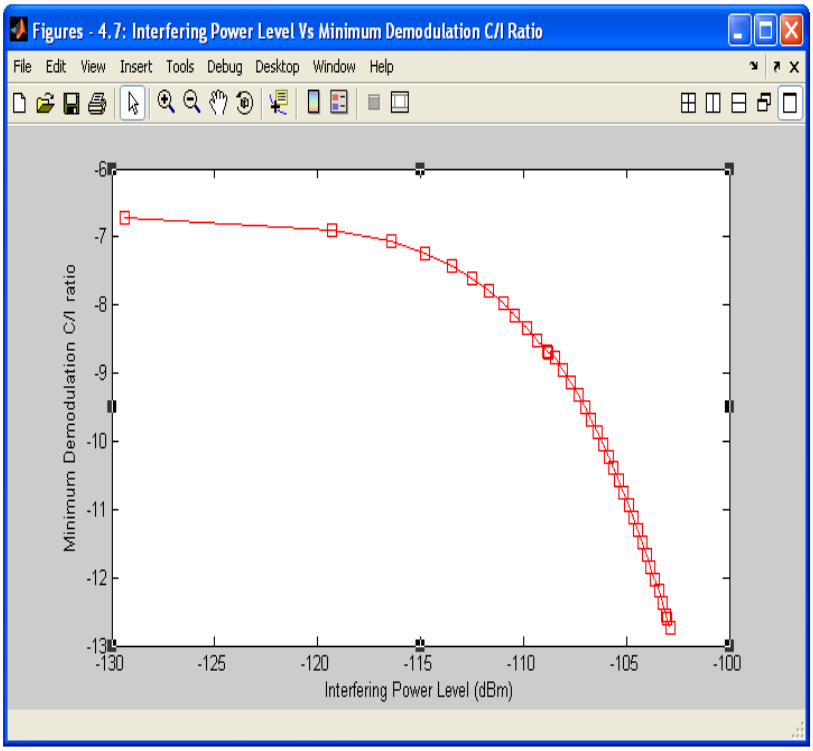

Figure 4.9: Interfering Power Level vs Minimum Demodulation C/I Ratio

The graph in Figure 4.9 explained the degradation response of the C/I ratio with corresponding increase in interfering power. From the figure, it infers that an interfering power of -108.80dBm, gave rise to a minimum

demodulation C/I ratio of -8.70. This generally explained how an increase in the interfering power (sideband noise) limits the network performance with respect to the C/I ratio performance.

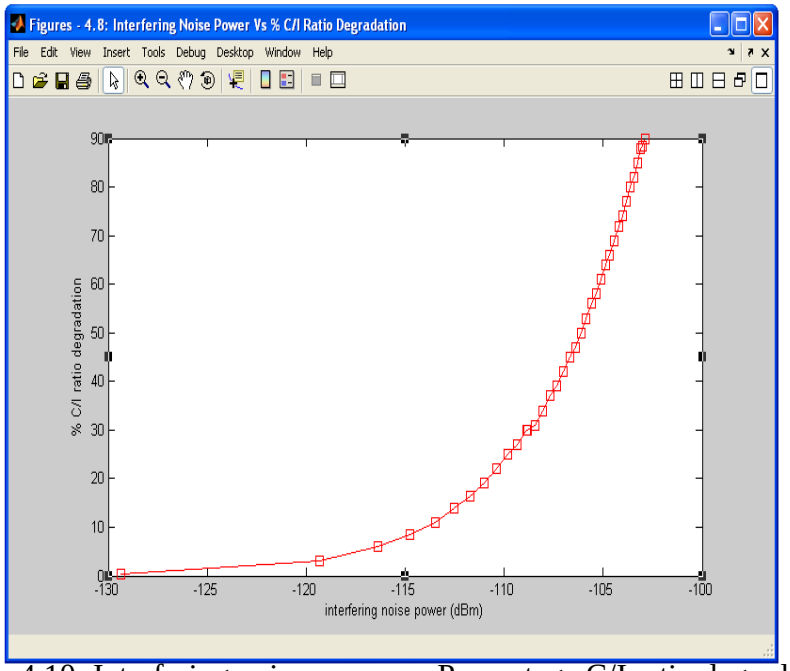

Figure 4.10: Interfering noise power vs Percentage C/I ratio degradation

The exponential relationship illustrated the performance effects of the interfering power on the percentage C/I ratio. The increase in the interfering power resulted to the decrease in C/I percentage ratio. Hence, from the graphical illustration, an increase in interfering power of -108.80dBm resulted to 30% degradation in C/I performance.

It is important to note that the interfering power of -108.8dBm, received signal strength degradation of 1.01dBm, rise in noise floor level of 1.01dBm, decrease in the interfering level compared to the original noise level of 5.80dBm, minimum demodulation C/I ratio of -8.70, C/I ratio degradation of 2.01 and percentage C/I ratio degradation of 30% are frequently exploited almost in all the graphical explanations. This is because the enumerated

parametric values are the primary results obtained in the research study involving the WCDMA and CDMA2000 co-located networks.

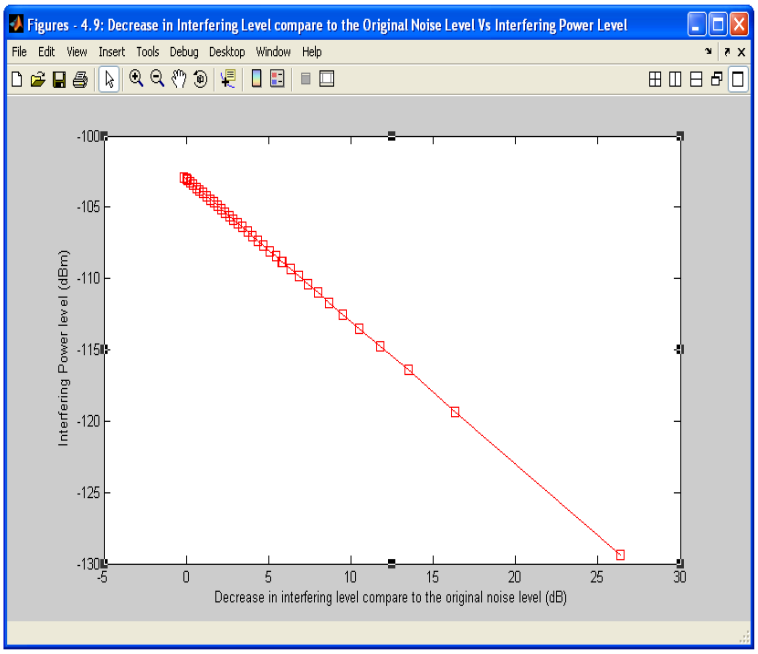

Figure 4.11: Decrease in interfering power level compared to the original noise level vs the interfering power

In order for the signal not to degrade, the original noise floor level supposed to be greater than the interfering level by +3dB. If the interference level is equal to the equivalent noise level of the original signal, the signal sensitivity will be degraded by 3dB and the system will be entirely corrupted. From Figure 4.11, it is shown that at-108.80dBm; the original noise floor level was still above the interfering level by 5.80dB. In this case, there is no need of +3dB addition. Furthermore, at -102.88dBm, the interfering level was above the original noise floor by 0.12dB, at that point the received signal strength level degraded by 3.07dBm, which gave rise to 90% C/I degradation ratio. Hence, the desired signal will be completely corrupted. Therefore a minimum of 6.07dBm is required to be added to maintain an acceptable SNR performance.

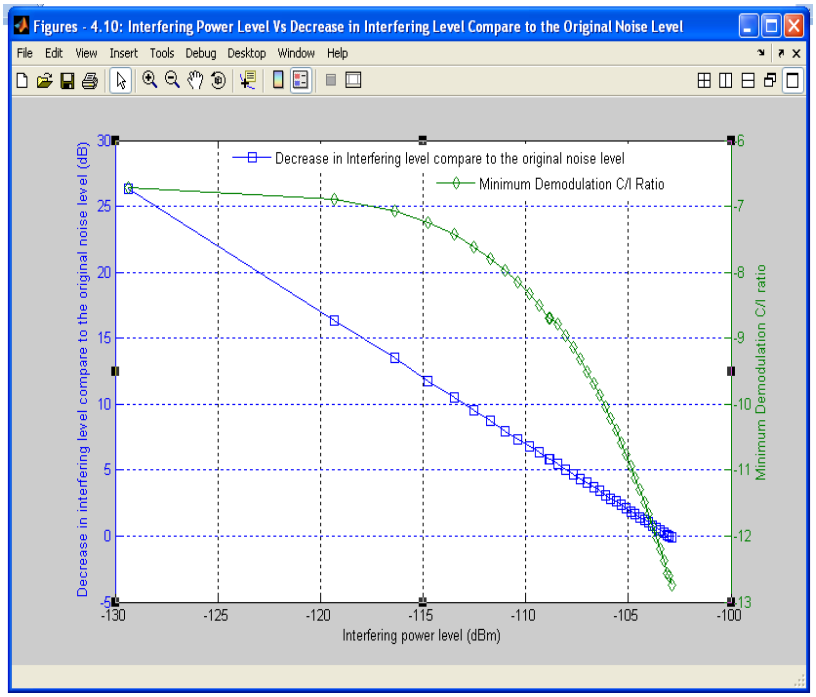

Figure 4.12: Interfering Power Level vs Decrease in Interfering Level Compare to the Original Noise Floor and the Minimum Demodulation C/I Ratio.

Figure 4.12, explained the system performance behavior relative to the minimum demodulation C/I ratio and decrease in interfering level compare to the original noise level when interfered.

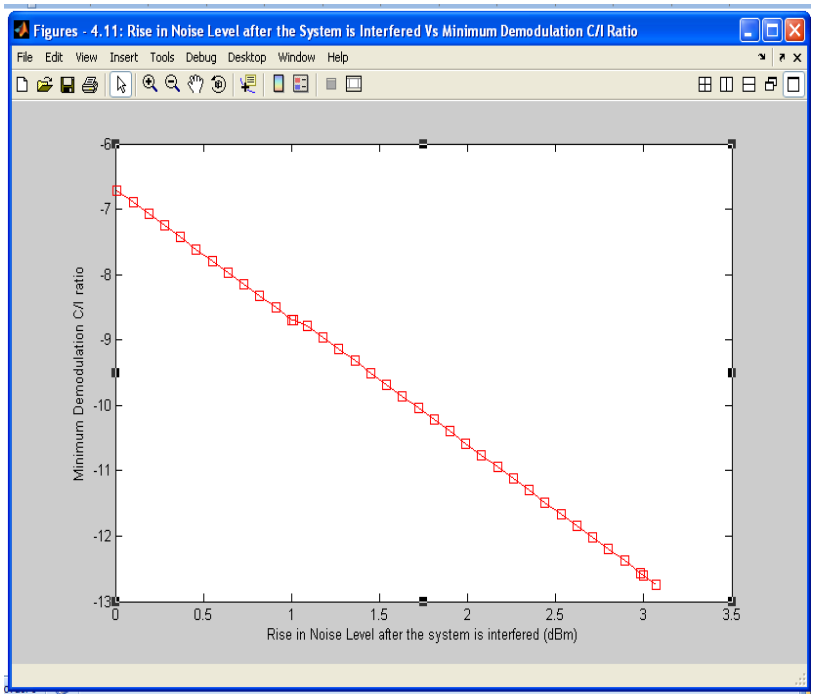

Figure 4.13: Rise in Noise level after the system is interfered vs minimum demodulation C/I Ratio

Figure 4.13 showed that as the noise floor level increases to 1.01dBm, the minimum demodulation C/I ratio decreases to -8.70. The scenario here implied that the higher the increase in the noise floor level, the lower the decrease in the minimum demodulation C/I ratio.

4.6 Filter Design Requirements and Specifications

Choosing the correct filter for a particular application requires defining the properties of the signal that the filter must attenuate or remove, as well as the properties that it must retain or allow to pass through. For the purpose of this research, Infinite Impulse Response (IIR) filter application was considered more suitable when compared to the counterpart Finite Impulse Response (FIR) filters due to the following considerations:

a. They typically meet a given set of specifications with a much lower filter order than a corresponding FIR filter. This has the obvious cost implementation advantage. This means that it can achieve given desired response with less computation than FIR.
b. They possess much better frequency response than FIR filters of the same order and a closed form design technique that does not require iteration
c. They exhibit Small group delay when compared to FIR of the same order.

A Butterworth filter is one of digital filters that belong to the group of the Infinite Impulse Response (IIR) filters. Butterworth Band Pass Filter (BBPF) design was primarily considered in the research among other classical IIR

filters which include; Chebyshev I, Chebyshev II, Elliptic and Bessel filters, because of its attributes to the least amount of phase distortion. Other enhanced features include; the transfer function of the filter offers maximally-flat response at the pass band and stop band, signifying that its frequency response decreases monotonically (smoothly), exhibiting no ripples at the pass band and stop band frequencies. This unique characteristic performance shows that the phase linearity of Butterworth filter is better than other IIR filters. It is important to note that the amount of ripples is related to the amount of distortion. In other words, Butterworth filter also provides infinite attenuation with respect to frequency.

From Table 2.1, the limits of spurious emission level by the ITU and 3GPP2 for CDMA far offset from carrier is given as -13dBm/1MHz (1GHz<f<5GHz)[24].

To ensure that the affected receiver's performance will not degrade, the isolation between the interfering transmitter and affected receiver should be:

$$-13dBm + 10\log 4 - (-108.80/3.84MHz) = 102dB$$

The total isolation required to maintain the received signal optimum performance in the co-located scenario is 102dB. Owing to the fact that the standard antenna-to-antenna isolation specification in dB by NCC for all PCS and DCS co-located sites is given as 50dB [23], a 52dB rejection is the required magnitude specification for the BBPF design. The output result

vividly interprets that any interfering signal (side-band noise) that comes out of the filter must be 52dB lower than its original input signal.

The goal of filtering is to perform frequency-dependent alteration of a signal. The design specifications using digital BBPF was primarily aimed at obtaining relevant array of design parameters to remove the sideband noise above a certain cutoff frequency. The filter design involves creating the filter coefficients to meet specific filtering requirements. The specifications which were in Hertz were converted to normalized frequencies (ω) in π radian/sample with specified intervals $0 \le f \le 1$ using equation 4.1[72].

$$\omega = \frac{2\pi f}{f_s} \tag{4.1}$$

where f is the absolute frequency in Hertz or cycles/second, f_s, the sampling frequency in samples/second and ω is the normalized frequency in π radian/sample.

In the study, the signal's magnitude after filtration is supposed to contain mostly the desired information. For this reason, the filter design was centered predominantly on the magnitude response regarding the phase response and others as secondary. Consequently, for such condition to be achieved requires sharp roll-off space for the filter. A guard band of 5MHz was considered relevant in the design because it will offer faster roll-off space for the BBPF taking into consideration the operating bandwidth of research interest, see Fig. 4.14. The higher the amount of guard band, the lesser the burdens on the filter

roll-off. It is also important to note that the stop band edge frequencies, which offers the guard band between the stop band and the pass band was basically selected by how fast it is desired for the signal response to roll off above and below the pass band. The roll-off space is described as the frequency at which the filter begins to filter out the harmonics [73].

To design this filter by simulation, three things were mostly considered:

1. The frequencies that need to be passed and those that need to be rejected
2. The signal amplitudes needed to be attenuated and
3. The Cut-off frequency (usually called 3-dB point), defined as the point at which the input signal power is attenuated by one-half or the frequency at which the magnitude response of the filter is $1/\sqrt{2}$ of its nominal value at the pass band.

It is necessary to note that for any practical design application, there is need to ensure low pass band insertion loss (less than 1dB) to avoid forward coverage degradation and high rejection band attenuation. Figure 4.15 illustrated the flowchart implementation of the proposed BBPF.

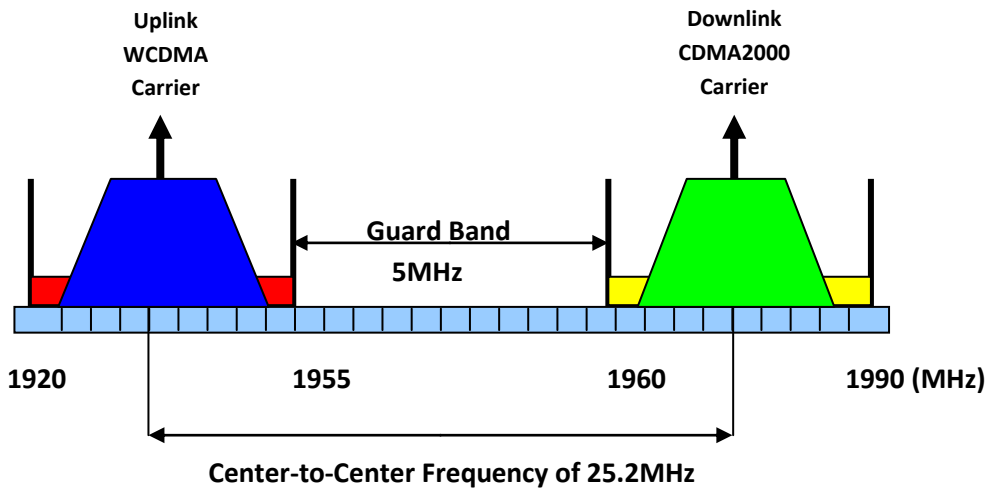

Figure 4.14: The Research Guard Band Allocation considered between DCS and PCS

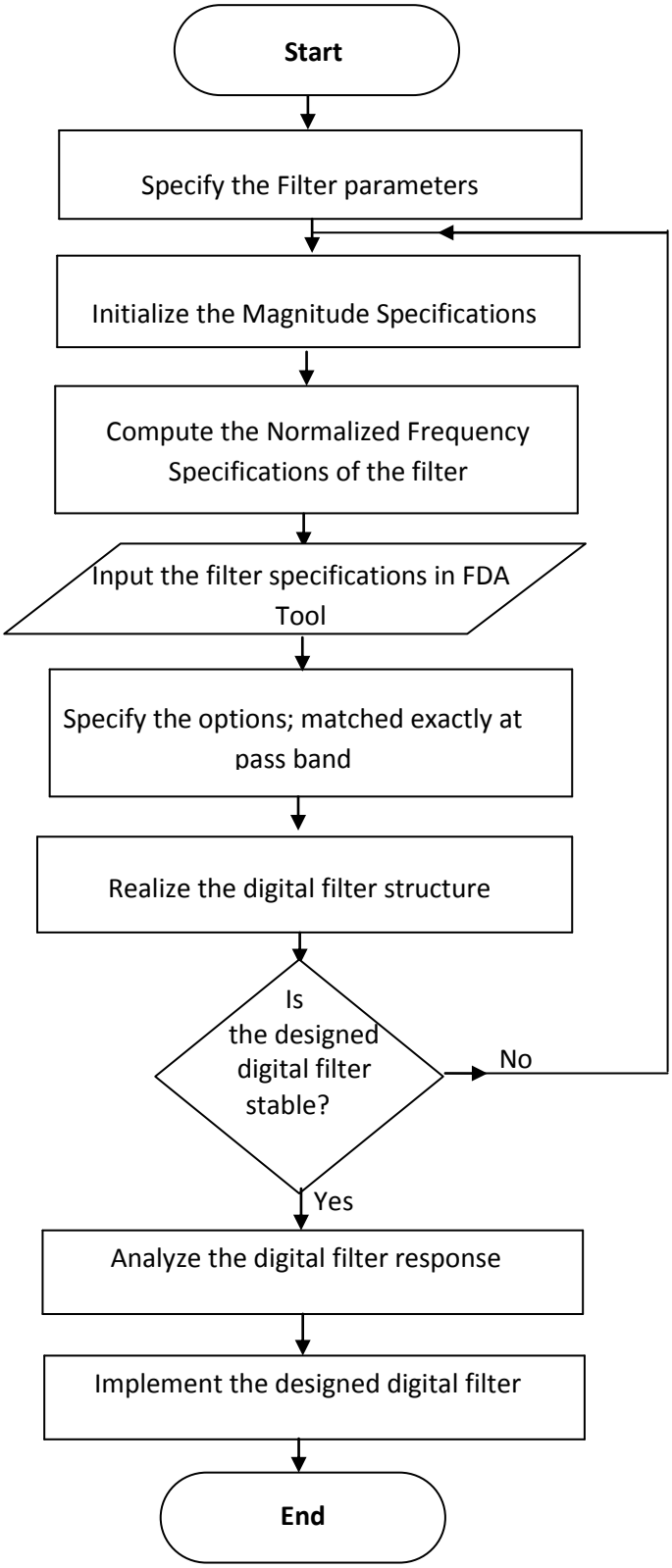

Figure 4.15.Flowchart Implementation of the Proposed BBPF

4.6.1 Procedure for Frequency conversion

Conversion from frequency specifications (KHz) to normalized frequency (π radian/sample) was obtained using equation 4.1. Sampling frequency of 7960,000 samples/second was considered for the BBPF design to achieve a higher sampling rate with low or minimal quantization error and processing time. This was obtained by sampling at four times the maximum frequency ($4xf_m$), where the maximum frequency was 1990000KHz. Obtained normalized frequencies (ω) (π radian/samples) for stop band 1 (ω_{stop1}), pass band 1 (ω_{pass1}), stop band 2 (ω_{stop2}) and pass band 2 (ω_{pass2}) and the frequency specifications(KHz) are shown in Table 4.4, while the magnitude specifications(dB) are shown in Table 4.5.

Table 4.4: Frequency and Normalized Frequency Specifications for the BPF

Filter parameters	**Frequency specifications(KHz)**	**Normalized frequency (ω) (π radian/samples)**
F_{stop1}	1955000	0.4912= ω_{Stop1}
F_{pass1}	1960000	0.4924= ω_{Pass1}
F_{pass2}	1990000	0.5000= ω_{Pass2}
F_{stop2}	1995000	0.5012= ω_{Stop2}
	Sampling frequency $f_s = 7960000$	

Table 4.5 Magnitude Specifications for the BPF

Filter parameters	**Magnitude specifications**
A_{stop1}	52dB
A_{pass}	0.1dB
A_{stop2}	52dB

where;

F_{pass1} : Frequency at the edge of the start of the pass band. Specified in normalized frequency units.

F_{pass2} : Frequency at the edge of the end of the pass band. Specified in normalized frequency units.

F_{stop1} : Frequency at the edge of the start of the first stop band, specified in normalized frequency units.

F_{stop2} : Frequency at the edge of the start of the second stop band, specified in normalized frequency.

A_{stop1}: Attenuation in the first stop band in dB.

A_{Pass}: Amount of ripple allowed in the pass band, known as the single pass band gain parameter.

A_{stop2}: Attenuation in the second stop band in dB.

The generated Matlab Codes for the BBPF design are shown in appendix C12.

4.7 BBPF Design Implementation

Filter design implementation basically involves choosing and applying a particular filter structure to those specifications earlier created to meet the filtering requirements. Filter Design and Analysis Tool (FDATool) was considered suitable in the research to facilitate quick design implementation for the digital BBPF, by setting the filter specifications using the values obtained in Tables 4.4 and 4.5 and importing the specified filter structure to the MATLAB workspace as illustrated in Figure 4.16, showing the filter magnitude response only. The graphs of magnitude response, phase response, group delay performance, impulse response and pole/zero plots are obtained and illustrated in Figures 4.17-4.21.

The IIR design is usually performed using second order sections by default [73]. The filter order is the number of stages used in the design of a filter. It is imperative to note that as the order of a filter increases, the response of filter is more close to the ideal response. High order IIR filters are best implemented in a cascaded form of second-order sections. The discrete-time IIR filter obtained in the design study is a stable direct-form II second order section characterized with a filter order of 58. The filter order was obtained in the design using FDATool and is implemented in a cascaded form of second-order 29 sections, refer to appendix B13. Figure 4.20 shows one section out of the 29 cascaded sections. It is imperative to note that the order of the filter obtained in the study was basically dependent on the edge frequency specifications used for the research.

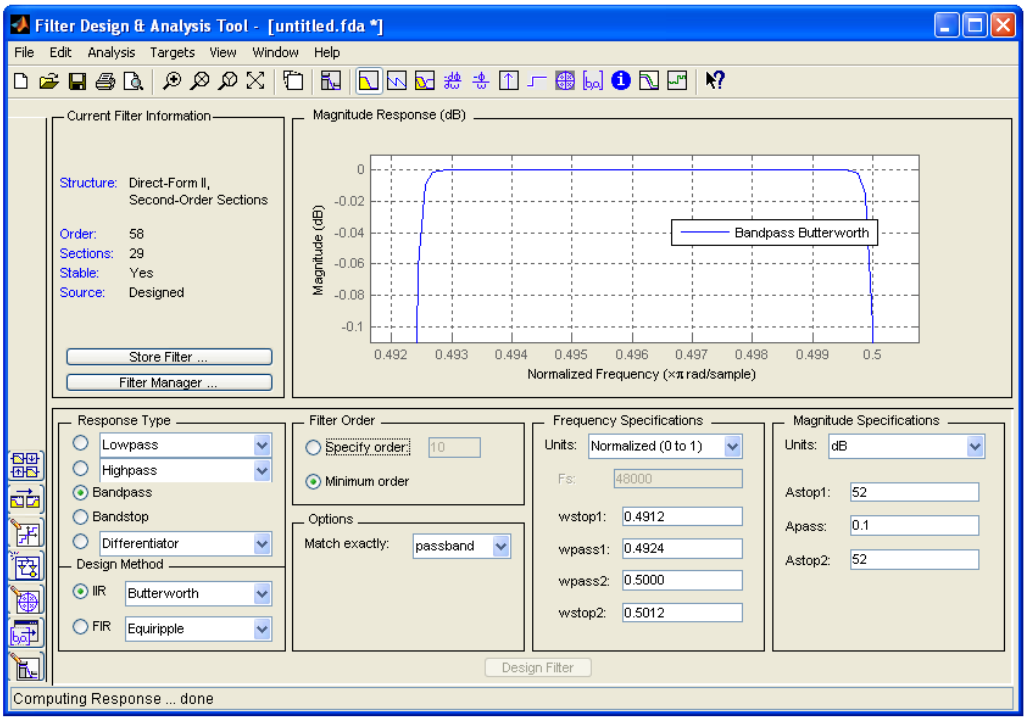

Fig 4.16: Filter Design and Analysis Specification Dialog Box for the BBPF showing the Magnitude Response only

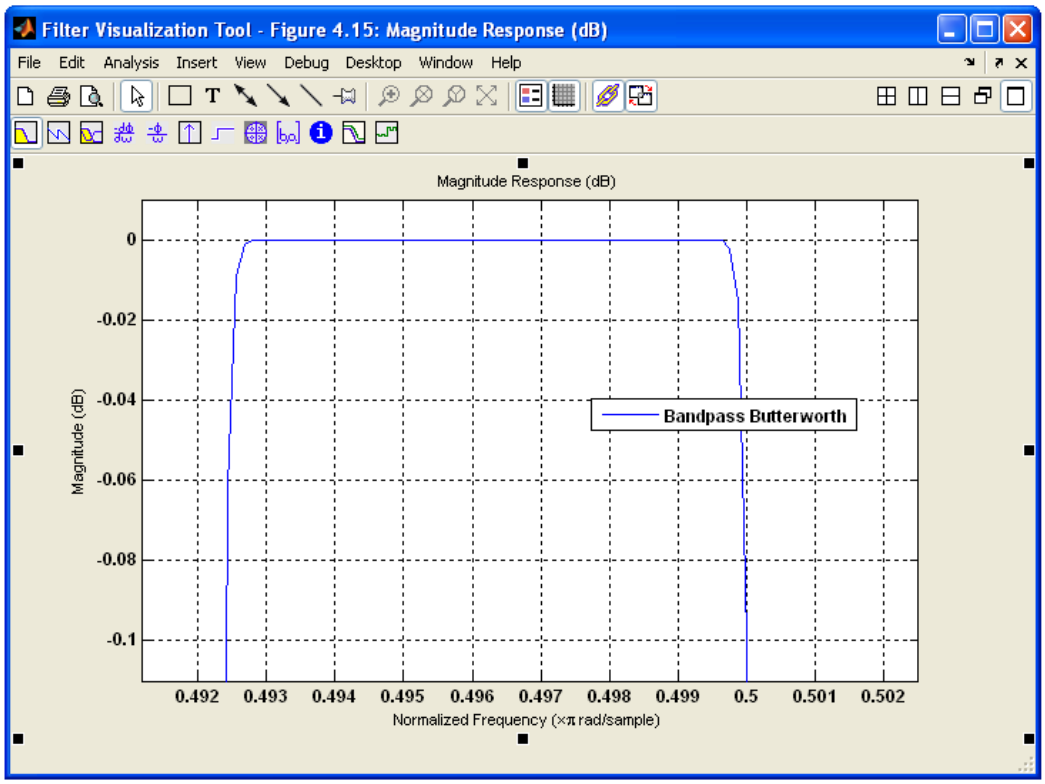

Figure 4.17: The Magnitude Response

The graph of Figure 4.17 showed a symmetrical magnitude response of digital Butterworth band pass filter. The graph demonstrated a maximally flat response at the pass bands and a smooth transition between the systems pass bands and the stop bands. Much importance was given to the magnitude response to show the cut-off frequencies and how selective the filter performs as it gets steeper. The first cut-off frequency (3-dB point) and the the second cut-off frequency were evaluated as 0.49215π rad/sample and 0.50025π rad/sample respectively. The geometric mean of the upper and lower 3-dB cut-off frequencies (i.e. the centre frequency) was also evaluated as 0.4962π rad/sample. It is significant to note that the filter achieves its maximum gain at 0.4962π rad/sample. The filter stop bands and the pass bands

were also illustrated in the figure, the pass band exists between the lower pass band normalized edge frequency (0.4924π rad/sample) and the upper pass band normalized edge frequency (0.5000π rad/sample). The lower stop band extends from zero to 0.4912π rad/sample, while the upper stop band extends from 0.5012π rad/sample towards infinity. Appendix C12 showed the Matlab generated results and the application codes while appendix C13 showed the function block parameters for the BBPF design.

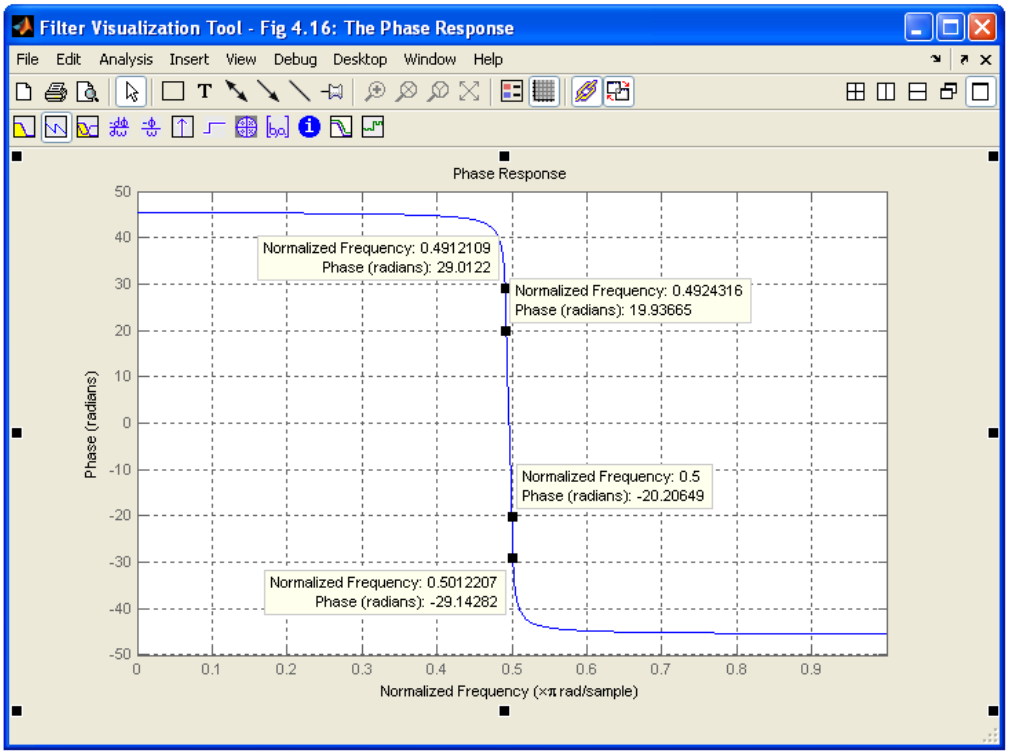

Figure 4.18: The Phase Response

Phase response is usually used to illustrate the phase shift (phase delay) of a system's output relative to its input. Figure 4.18 illustrated how the filter response decreases monotonically with no ripples both in the pass band and stop band edge frequencies, providing a sharp phase linear response with no distortion. It is essential to note that nonlinear phase response in audio systems

(e.g. cellular network), can cause noticeable phase distortion for the listener which of course cannot be tolerated. In data transmission systems also, nonlinear phase response produces group delays that are functions of frequency, which produces distortion in the pulses sent over the system and can distort the edge frequencies and the system performance to the point of causing errors in the received signal. Hence, it becomes imperative in the design of a system especially when dealing with audio (voice) conversation to ensure a linearised phase response by choosing appropriate application technique, given that phase characteristics of a filter is very crucial in selecting and designing projects. This was one of the motivations in the study for choosing the Butterworth filter because of its sharp linear response characteristics.

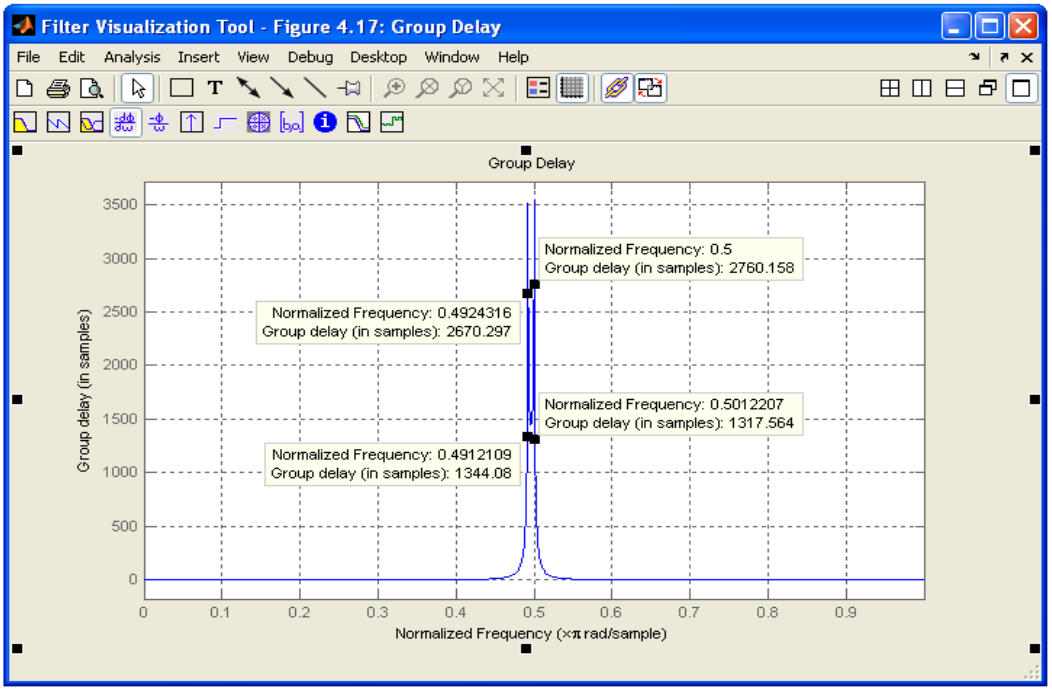

Figure 4.19: Group delay response

Group Delay (GD) of a filter (also called envelope delay), is the time taken for a narrow-band signal to pass from the input to the output of a device [74],

usually applied as a measure of the average delay time that a specified narrow range of frequencies experiences when passing through a circuit. Figure 4.19 shows relatively a Constant Group Delay (CGD) towards the mid pass-band frequency range, its response has a peak close to each pass band edge showing where the filter attenuation begins to increase rapidly. Also, the constant group delay towards the mid pass-band implies that the waveform distortion of the designed filter is low, given rise to the systems phase linearity response with the frequency. One of the important features of the constant group delay performance of the filter shown in the figure is that it preserves the transient waveform, keeping the disturbance at minimal level. This CGD response attributes to an outstanding performance especially for voice and data transmission.

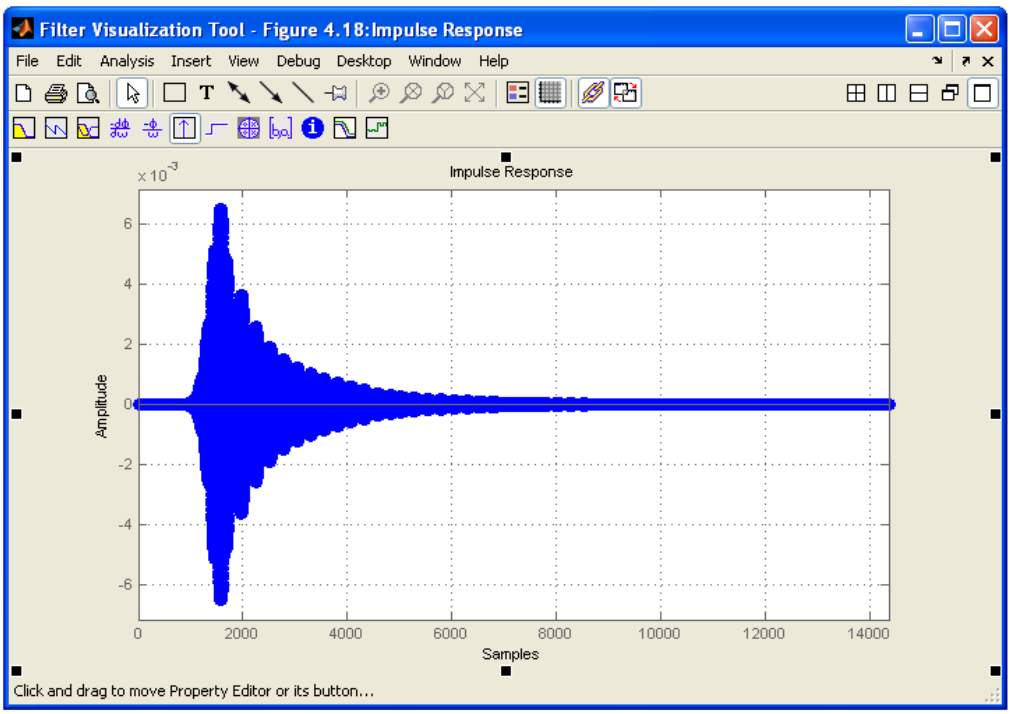

Figure 4.20: The Impulse Response

Impulse response in general is basically used to describe a system in its time domain. The Figure 4.20 shows a continuous and infinite impulse response of the filter.

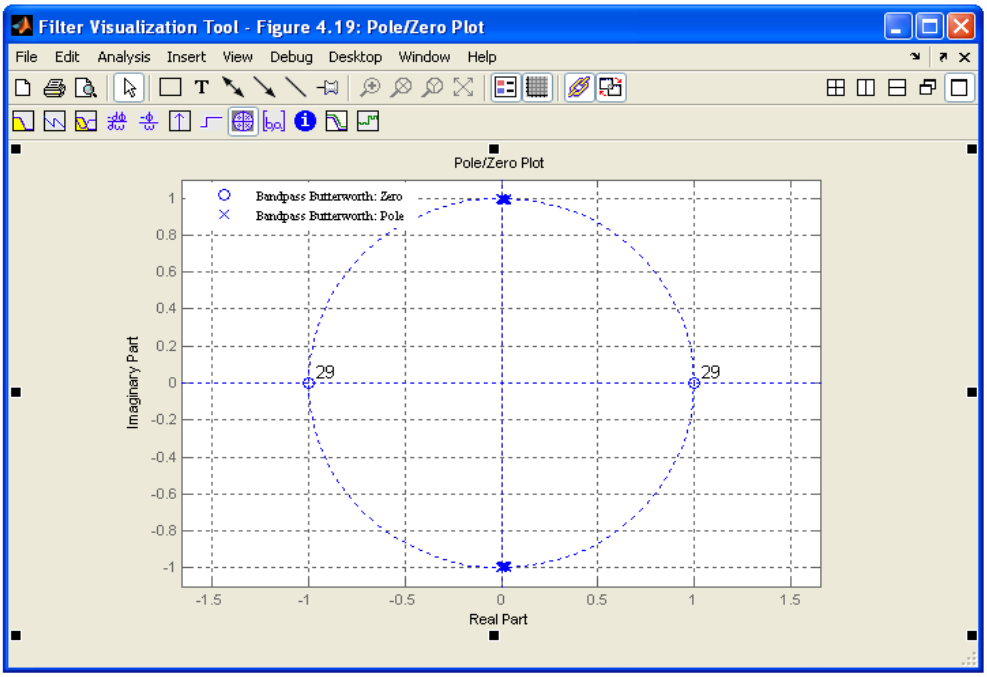

Figure 4.21: The Pole and Zero Plot

From Figure 4.21, it explained that the poles are symmetrical and did not fall outside the unit circle which signifies the stability of the system. One of the features that determine the stability of a filter is if the poles did not fall outside the unit circle. The distance of real poles and zeros to the imaginary axis determines the breadth of the frequency response. For the poles, the real parts from the axis are obtained as 0.006514464 and -0.0007802818 and the imaginary parts are 0.9884834 and -0.9993103. For the Zeros, the real parts are obtained as -1 and 1 while the imaginary parts are configured as 1exp-50 and 1exp-50 respectively. The values from the real and imaginery parts

discussed are not shown in the appendix, rather it was obtained by placing the cursor at the poles and at the zeros ends on the filter visualization tool environment.

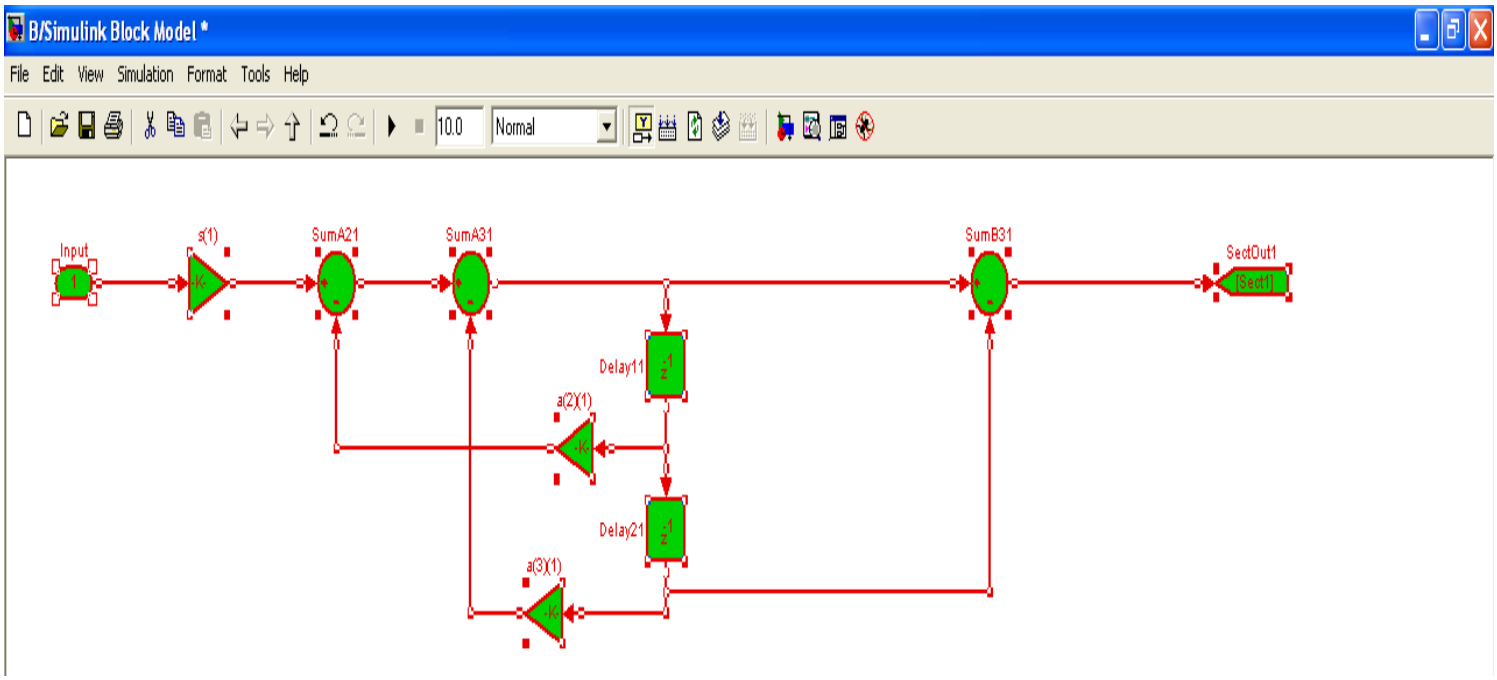

Figure 4.22: Simulink model for the Butterworth Band pass filter

Figure 4.22, showed the architecture model of the designed active BBPF in a simulink subsystem. The simulink model showed the function block parameters of the designed filter with the first section out of the cascaded 29 sections. The function block parameters represented the individual sums, gains and the positive delay samples. Implementation of this filter as a cascade of quadratic factors provides a better control stability for the designed filter.

4.8 Cancellation Performance of the Proposed ANCT

The major challenge requires achieving a perfect cancellation centers on three essential parameters that determine to a first order the level of cancellation that can be achieved at the point of cancellation. They are; the Amplitude balance, Phase (0^0), and Delay match between the reference and primary antenna signals. The cancellation performance of these essential parameters on the achievable ANCT system was introduced in the study. The research focused on achieving theoretical perfect cancellation. This could be realized by obtaining a signal amplitude balance, anti-phase of 180^0 and time delay match. The level of cancellation achieved was a measure of the ANCT performance. The amplitude imbalance is defined as the difference in voltage levels between the primary signal and the reference signal or the voltage amplitude difference between the reference signal and the primary signal in dB. Phase error is expressed as the phase deviation from perfect anti-phase (-180^0) between the reference signal and the primary signal expressed in degrees (^{0}). The delay mismatch between the primary path and the reference path is defined as the difference in arrival time between the two signals at the point of cancellation. Time delay is expressed in units of seconds; it does not depend on the frequency rather the traveling distance in a given propagation medium [47]. Figure 4.23 illustrated the proposed test-bed for the adaptive noise cancellation system

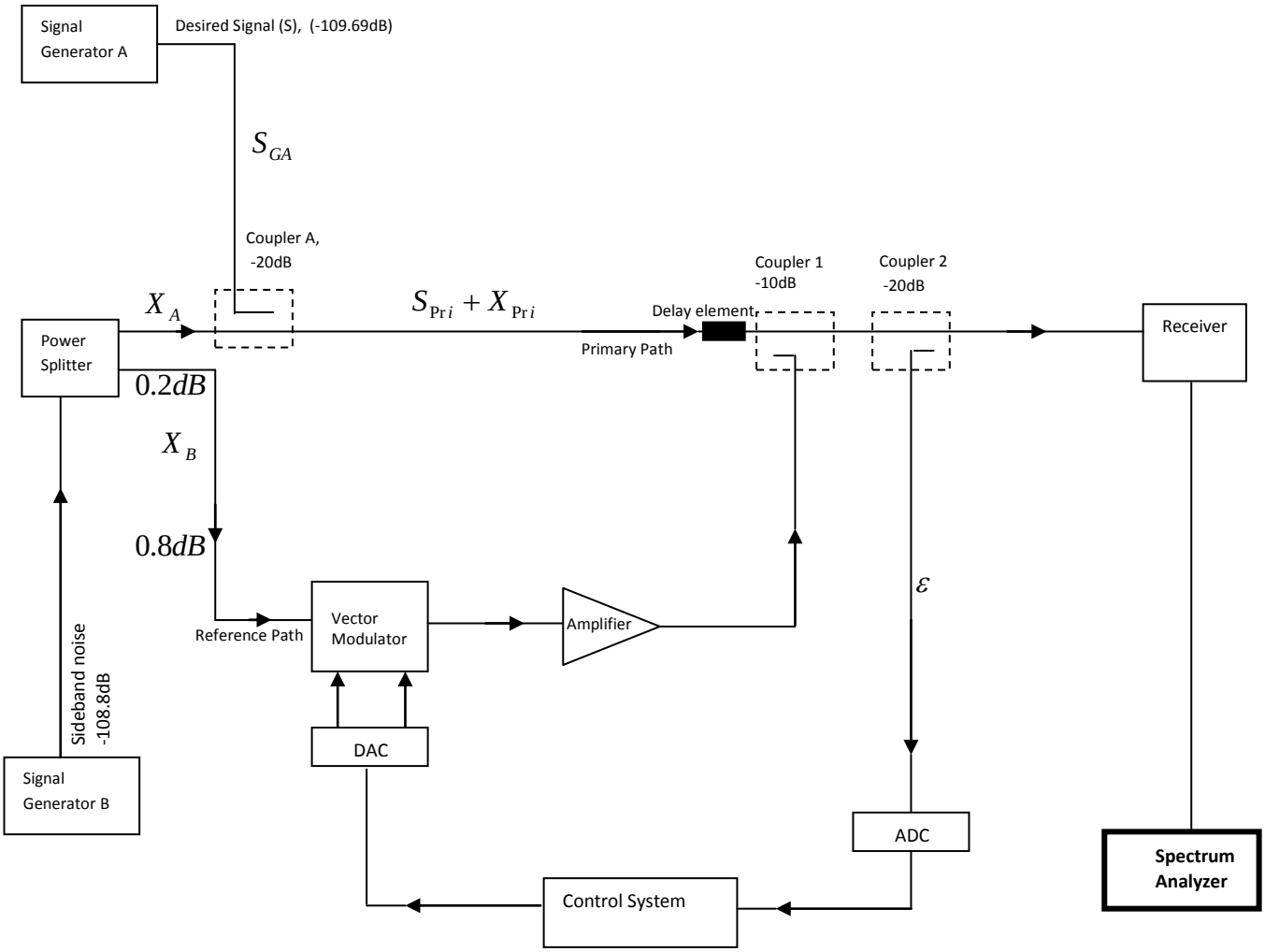

Figure 4.23: Implementation Test-Bed of the Proposed ANCT

4.9 Mathematical Representations of the ANCT Implementation Diagram

Let the signal generator A, generates the desired signal and represented as

$$S_{GA}(t) = V_{Spri} \sin(2\pi f_c t + \phi_{Spri}) \tag{4.15}$$

Where $S_{GA} = S_{pri} = -109.69dBm$

f_c is the instantaneous frequency, ϕ_{Spri} is the initial phase of the signal, V_{Spri} is the amplitude of the desired signal at the primary path. The signal power of

-109.69dBm considered, was the average desired signal obtained from the field measurement used for the band pass filter design.

Let the signal generator B generates the interfering signal and represented as

$$X_{GB} = V_{GB}\cos(2\pi f_c - \beta_c I_{GB} + \phi_{GB}) \tag{4.2}$$

$$X_{GB} = X_{ref} = -108.80dBm$$

-108.80dBm is the interfering signal power obtained for the band pass filter design analysis. Hence, a dBm-to-Amplitude converter was utilized for the conversion of the signal generator A and B, to facilitate a compromise for the Matlab-simulink design process.

V_{GB} is the amplitude of the undesired signal, generated by the signal generator B, β_c is the phase shift constant at f_c for a particular transmission line, I_{GB} is the length of the transmission path the signal passes before being input to the cancellation coupler, ϕ_{GB} is the initial phase of the signal. Since the cancelation signals are operating at the same frequency, therefore the reference signal and primary cancellation signal are represented to be a two single tone sinusoidal signal. Let the power splitter be represented as S_p, from the design, the amplitude of the power splitter is divided in the ratio of 0.2:0.8 at the primary and reference paths. This was prioritized due to the design placement of the antenna.

$$\therefore S_P = X_{GB}(t) = 0.2X_A(t) + 0.8X_B(t) \tag{4.3}$$

Where X_A represents the cancellation signal at the primary path and X_B, the interfering (jamming) signal at the reference path.

$$\therefore X_A(t) = X_{\Pr i}(t) = V_{X\Pr i}\cos(2\pi f_c t - \beta c I_{X\Pr i} + \phi_{X\Pr i}) \quad (4.4)$$

$$X_B(t) = X_{Rref}(t) = V_{X\mathrm{Re}f}\cos(2\pi f_c t - \beta c I_{X\mathrm{Re}f} + \phi_{X\mathrm{Re}f}) \quad (4.5)$$

Coupler A, represented as C_A is the summation point for the uncorrelated signals at the primary path.

$$\therefore C_A(t) = X_A(t) + S_{GA}(t) \text{ , where } X_A = X_{\Pr i} \text{ and } S_{GA} = S_{\Pr i} \quad (4.6)$$

$$C_A(t) = X_{\Pr i}(t) + S_{\Pr i}(t) = V_{X\Pr i}\cos(2\pi f_c t - \beta c I_{X\Pr i} + \phi_{X\Pr i}) + V_{S\Pr i}\sin(2\pi f_c t + \phi_{S\Pr i}) \quad (4.7)$$

At the input of the Vector Modulator (VM), the interfering signal is represented as:

$$X_{\mathrm{Re}f}(t) = V_{X\mathrm{Re}f}\cos(2\pi f_c t - \beta c I_{X\mathrm{Re}f} + \phi_{X\mathrm{Re}f}) \quad (4.8)$$

The basic function of a vector modulator is to ensure that the phase and amplitude is adjusted so that the phase difference of 180^0 (i.e. out of phase) is obtained in the reference path relative to the primary path with equal amplitude to actualize destructive cancellation. The expected output of the vector modulator is

$$X_{0\mathrm{Re}f}(t) = V_{X\mathrm{Re}f}(t)\cos\left\{2\pi f_c t - \beta c I_{X\mathrm{Re}f} + (\phi_{X\mathrm{Re}f} + 180^0)\right\} \quad (4.9)$$

$$\therefore \text{Transfer function for VM} = \frac{X_{0\mathrm{Re}f}(s)}{X_{\mathrm{Re}f}(s)} = \frac{V_{X\mathrm{Re}f}(s)\cos\left\{2\pi f_c t - \beta c I_{X\mathrm{Re}f} + (\phi_{X\mathrm{Re}f} + 180^0)\right\}}{V_{X\mathrm{Re}f}(s)\cos(2\pi f_c t - \beta c I_{X\mathrm{Re}f} + \phi_{X\mathrm{Re}f})} \quad (4.10)$$

At the Coupler 1, which is the summation point or cancellation point?

$$X_R = X_{\mathrm{Re}f} - X_{\mathrm{Pr}i} = e_{rr} \tag{4.11}$$

Where X_R is the residual noise signal .

Hence, it is important to note that the magnitude and phase characteristics of the error signal depends on the phase error, amplitude imbalance and delay mismatch between the primary signal path and reference signal path at the point of cancellation.

Let Δ_V represent the difference in amplitude imbalance

θ_{err} represent the phase error and

Δ_L represent the delay mismatch

$$\therefore \Delta_V = V_{X\,\mathrm{Re}f} - V_{X\,\mathrm{Pr}i}, \text{ hence } V_{X\,\mathrm{Re}f} = \Delta_V + V_{X\,\mathrm{Pr}i} \tag{4.12}$$

$$\theta_{err} = (\phi_{X\,\mathrm{Re}f} - \phi_{X\,\mathrm{Pr}i}) - 180^0, \text{ hence } \phi_{X\,\mathrm{Re}f} = \theta_{err} + \phi_{X\,\mathrm{Pr}i} + 180^0 \tag{4.13}$$

$$\Delta_L = I_{X\,\mathrm{Re}f} - I_{X\,\mathrm{Pr}i}, \text{ hence } I_{X\,\mathrm{Re}f} = \Delta_L + I_{X\,\mathrm{Pr}i} \tag{4.14}$$

Substituting equations 4.12, 4.13 and 4.14 into 4.8. Therefore,

$$X_{\mathrm{Re}f} = (\Delta_V + V_{X\,\mathrm{Pr}i})\cos(2\pi f_c - \beta c(\Delta_L + I_{X\,\mathrm{Pr}i}) + \theta_{err} + \phi_{X\,\mathrm{Pr}i} + 180^0 \tag{4.15}$$

Hence, ε_{rr} is the outcome of the vector addition of the primary signal and the reference signal at the cancellation point, which takes place at coupler 2.

$$\therefore \varepsilon_{rr} = \varepsilon_{Xref} + \varepsilon_{X\,\mathrm{Pr}i} \tag{4.16}$$

It is the feedback error that provided the necessary information required for adjustment by the vector modulator. A control algorithm was developed and implemented for the In-phase and Quadrature phase adjustment in a closed loop function to achieve the desired system performance, refer to appendix D for the codes.

For hardware design and implementation, it is recommended to consider using lower couplers as exemplified in Figure 4.23 to minimize the rate of insertion loss and to avoid further signal strength reduction. The implementation of the cancellation performance of the proposed ANCT was developed using a flow chart algorithm as shown Figure 4.24. Figures 4.25- 4.27 illustrated the Matlab-SimulinkTest-bed of the Adaptive Noise Cancellation System, the signal conditioning phase and the power splitter respectively.

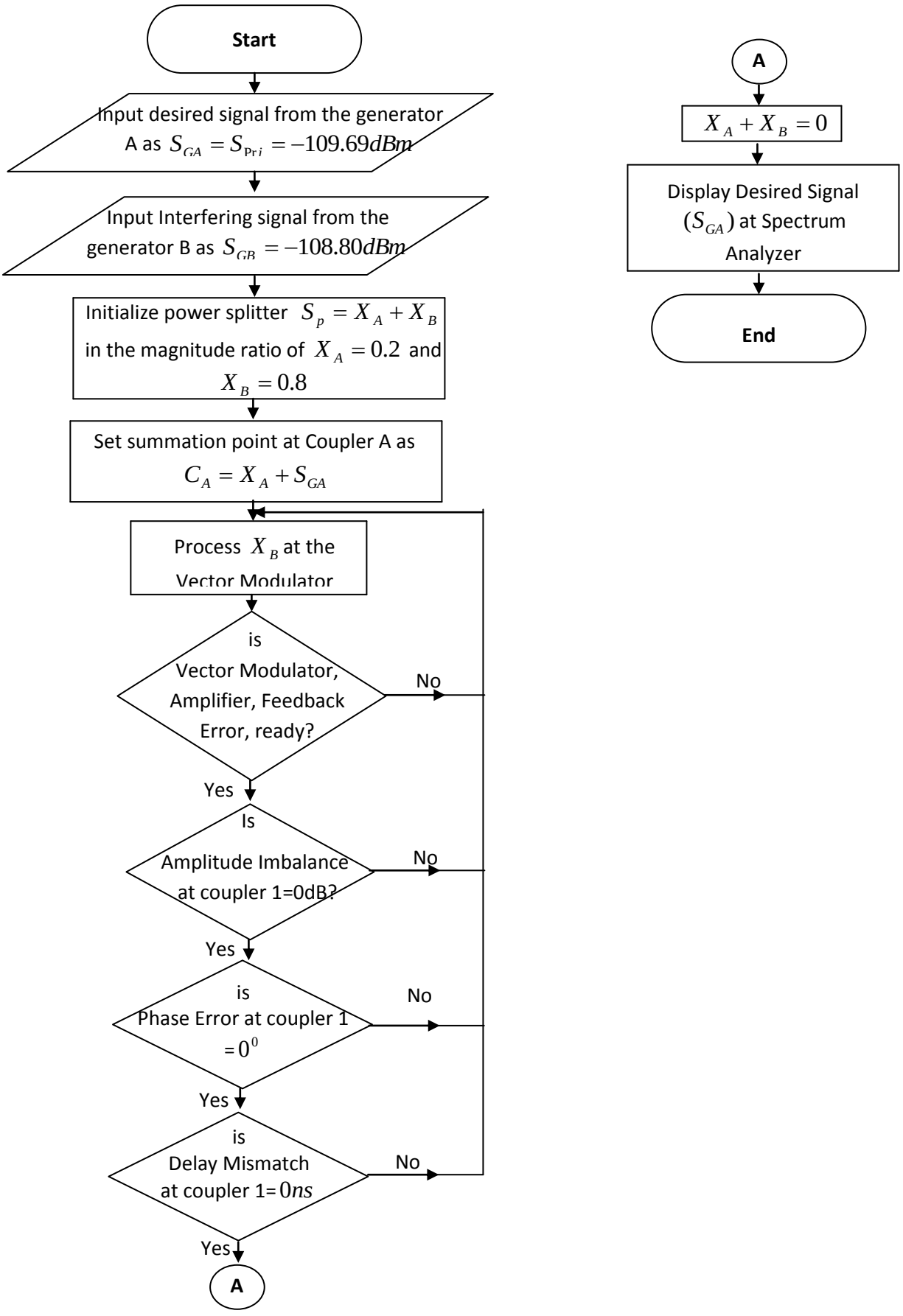

Figure 4.24: Steps for implementing the Proposed ANC system using a flow chart algorithm

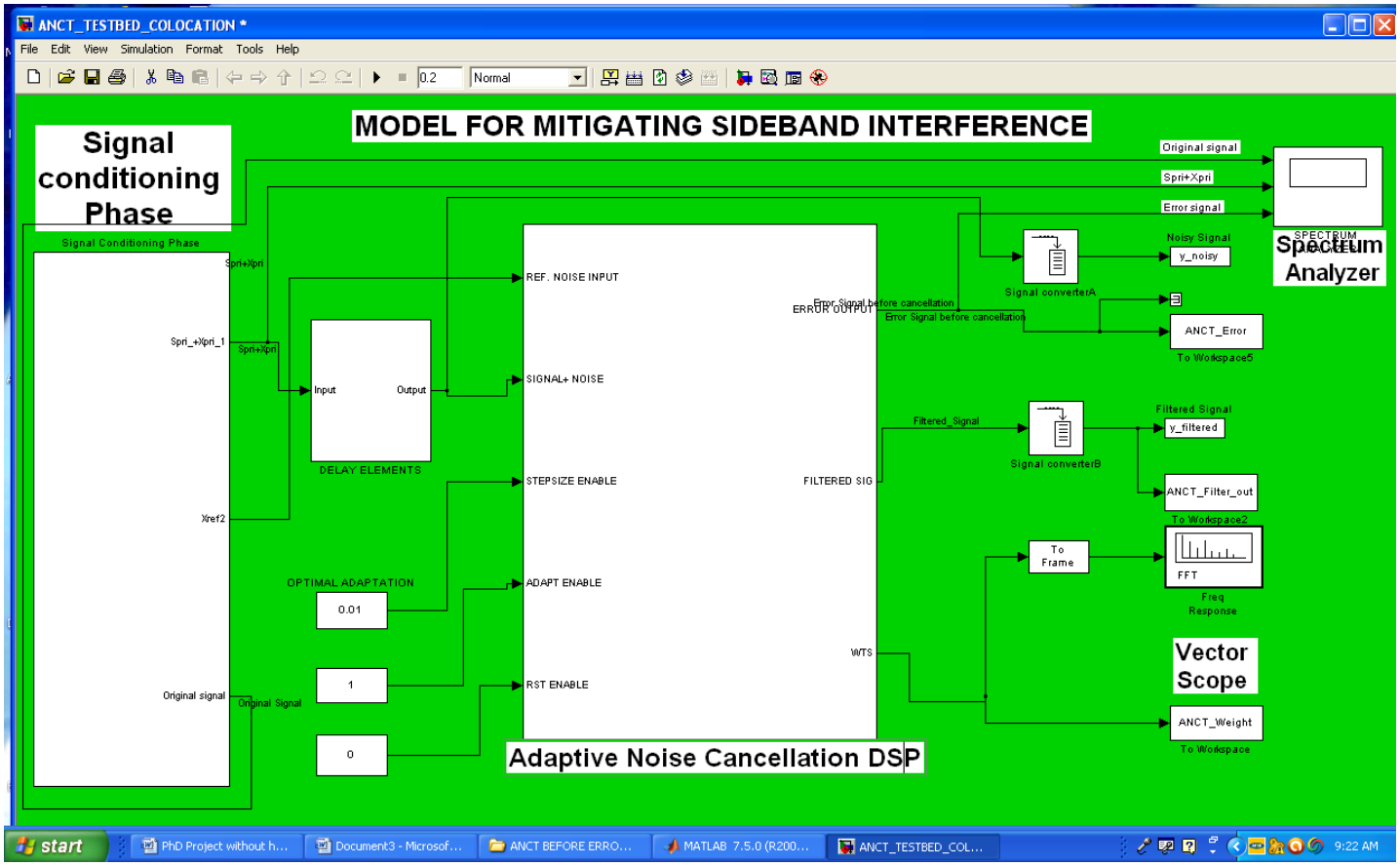

Figure 4.25 Matlab-SimulinkTest-bed of the Adaptive Noise Cancellation System

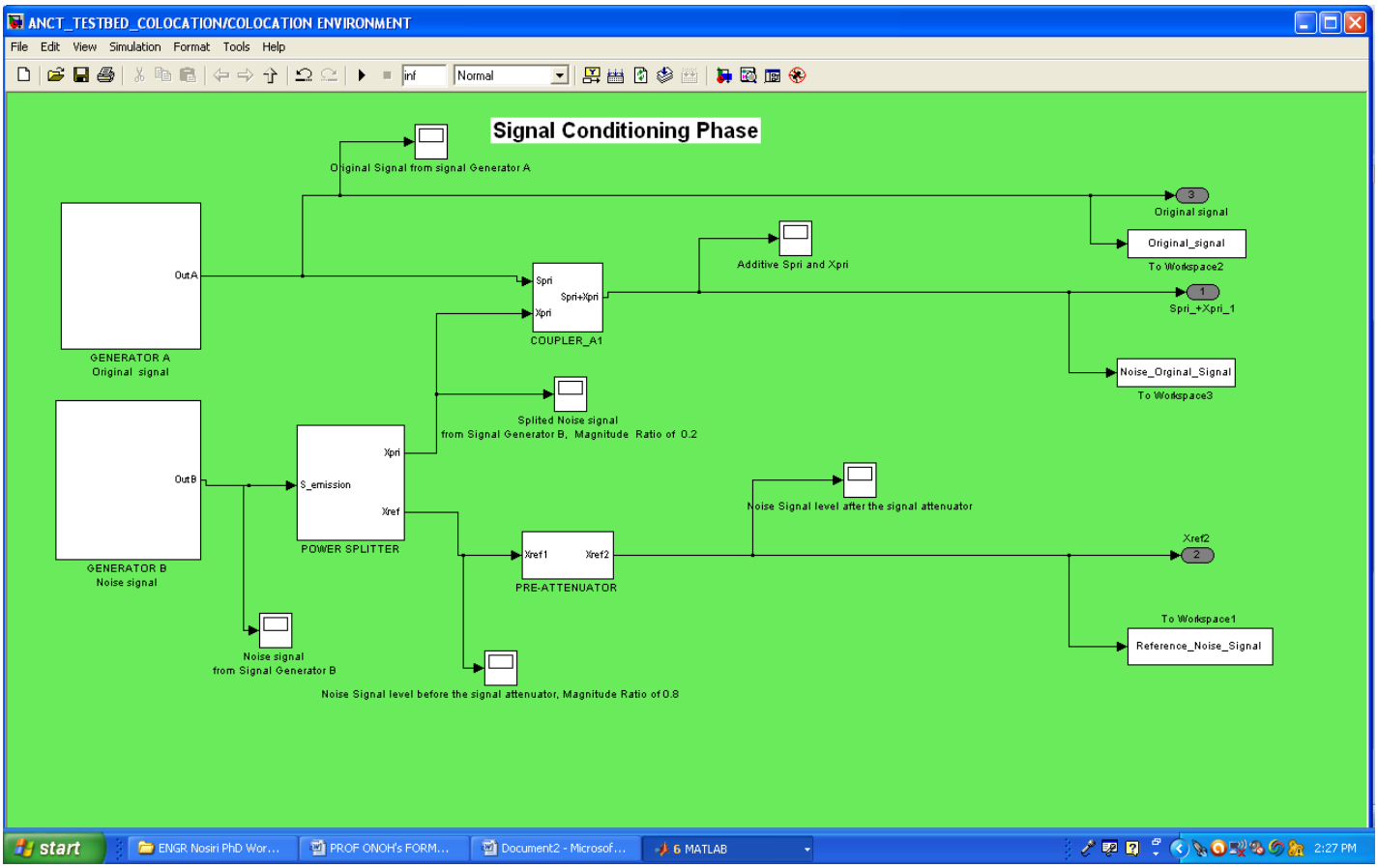

Figure 4.26 Signal Conditioning Phase

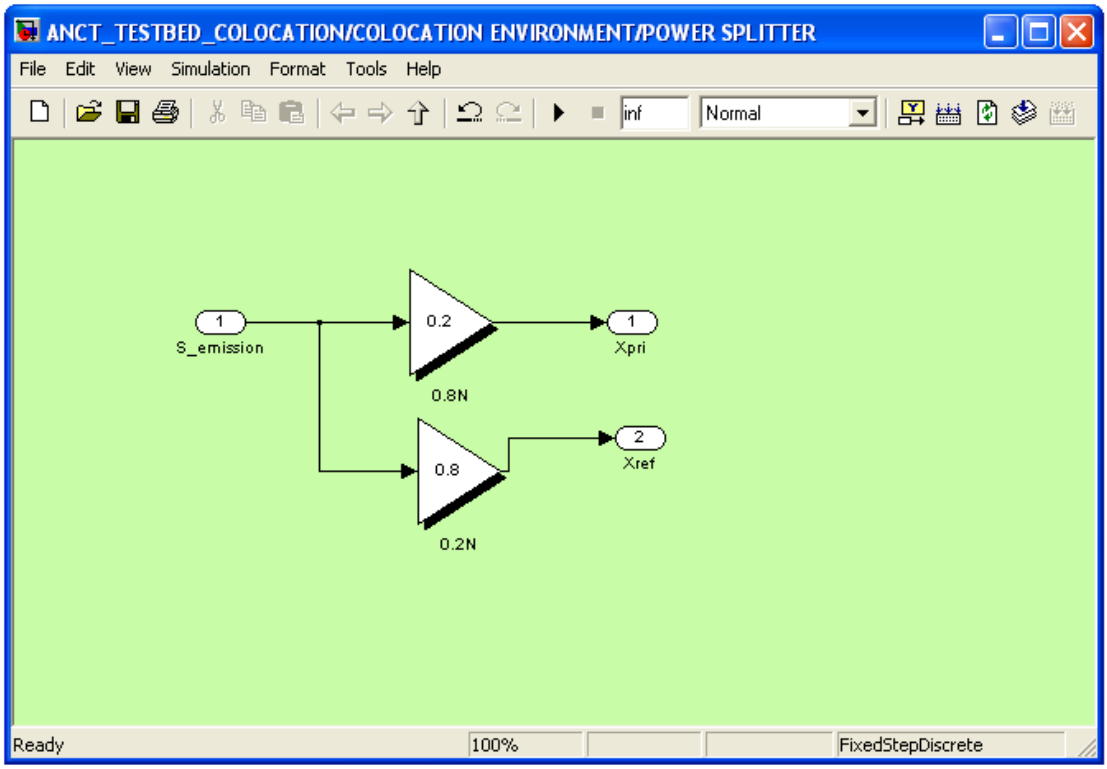

Figure 4.27 Power Splitter

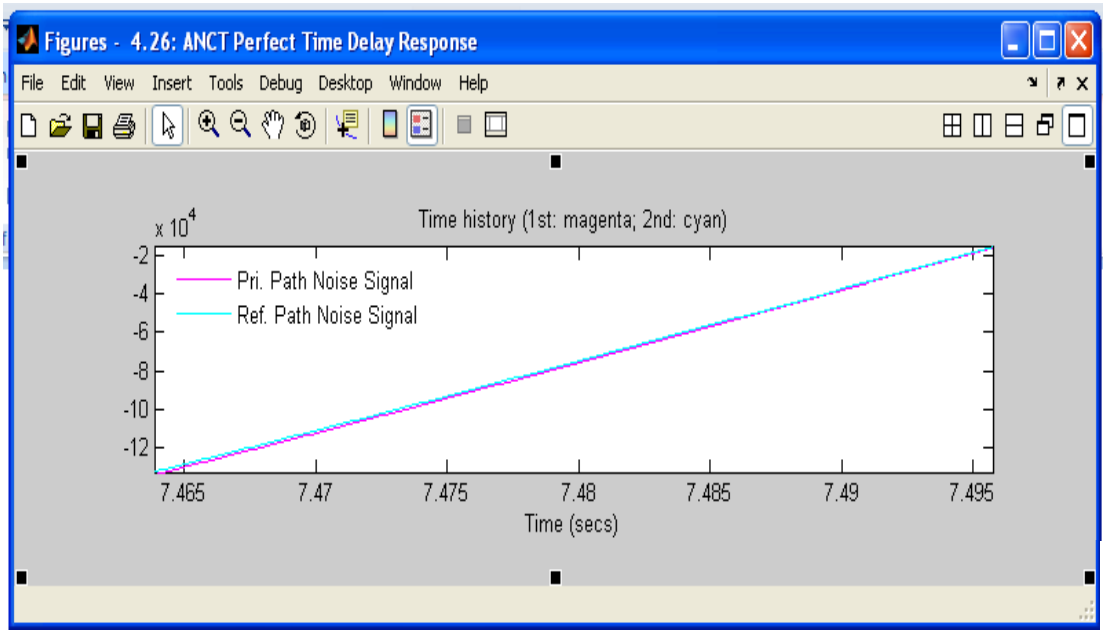

Figure 4.28 ANCT Perfect Time Delay Response

Figure 4.28 represented a time delay response for perfect cancellation. The two linear lines showed the primary signal and the reference signal, absolutely superimposed to each other given rise to absolute time delay match. Figures. 4.29-4.36 show the various noise and signal characteristics for the Matlab-Simulink Test-bed.

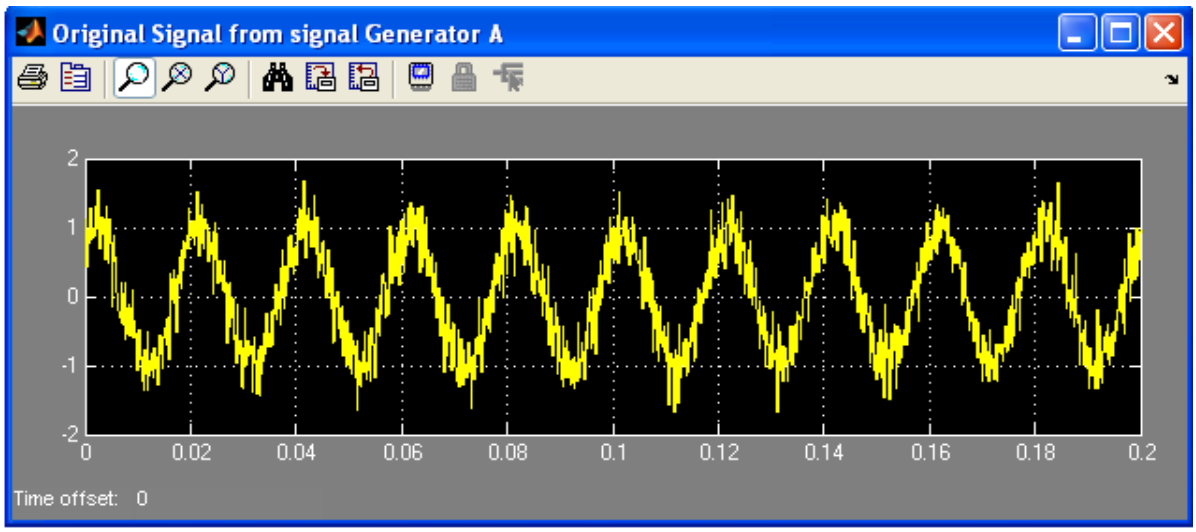

Figure 4.29 Original signal from Signal Generator A

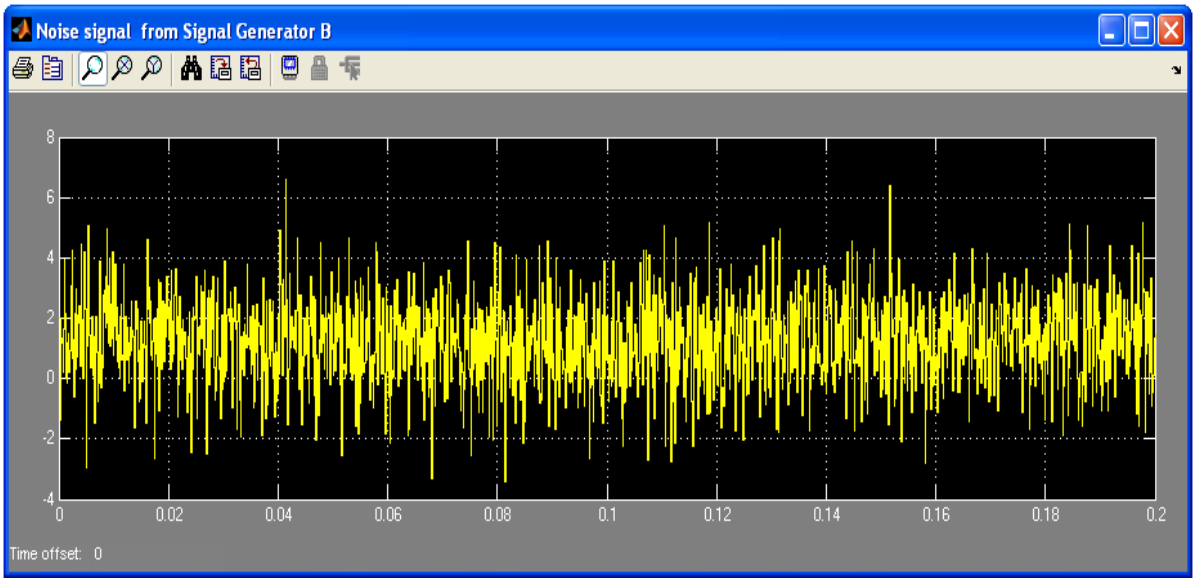

Figure 4.30 Noise signal from Signal Generator B

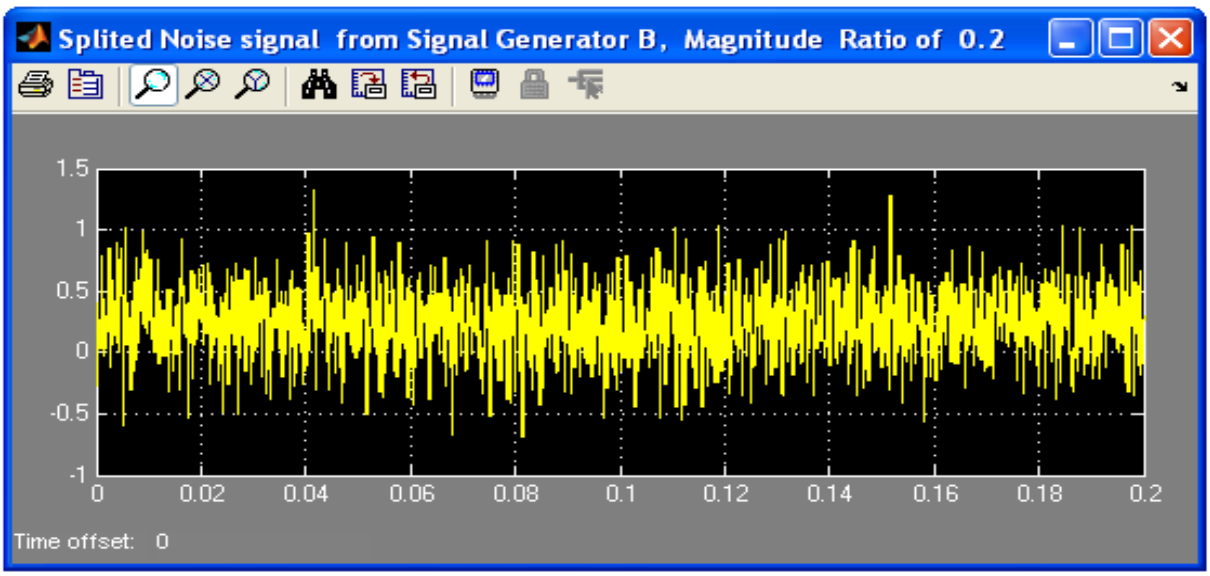

Figure 4.31 Splitted Noise signal from Signal Generator B, Magnitude Ratio of 0.2

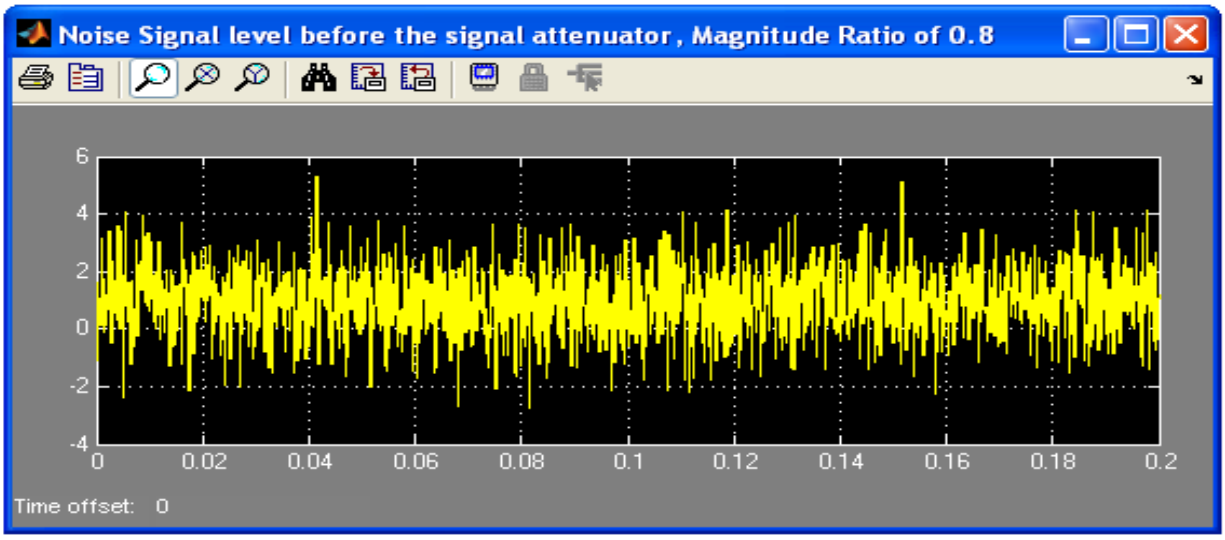

Figure 4.32 Noise signal level before the Signal attenuator, Magnitude Ratio of 0.8

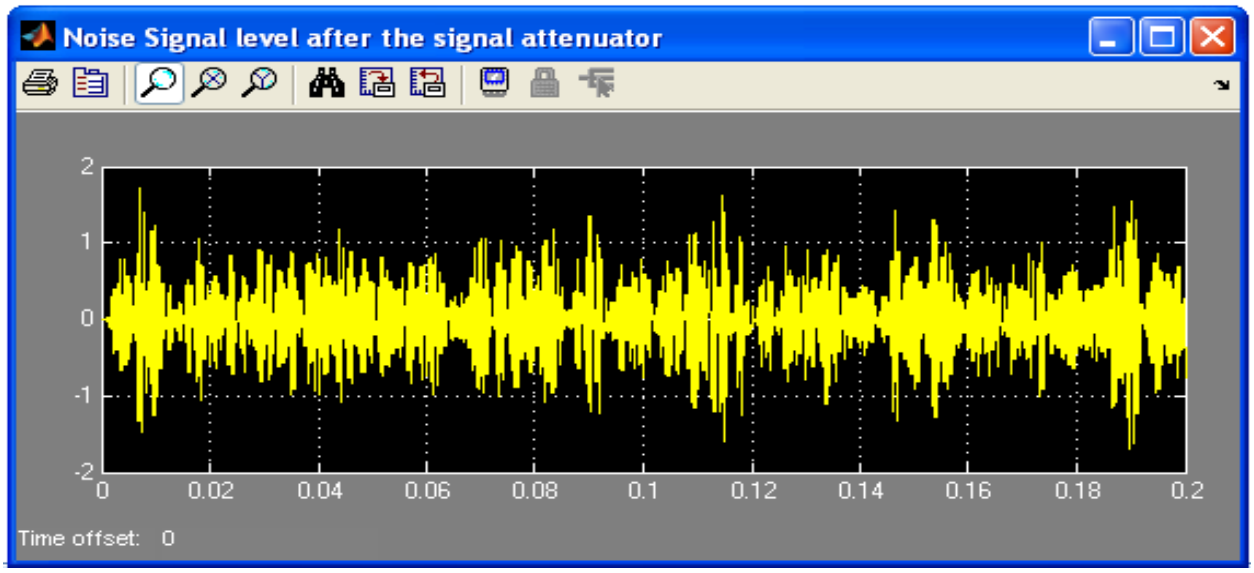

Figure 4.33 Noise signal level after the Signal Attenuator

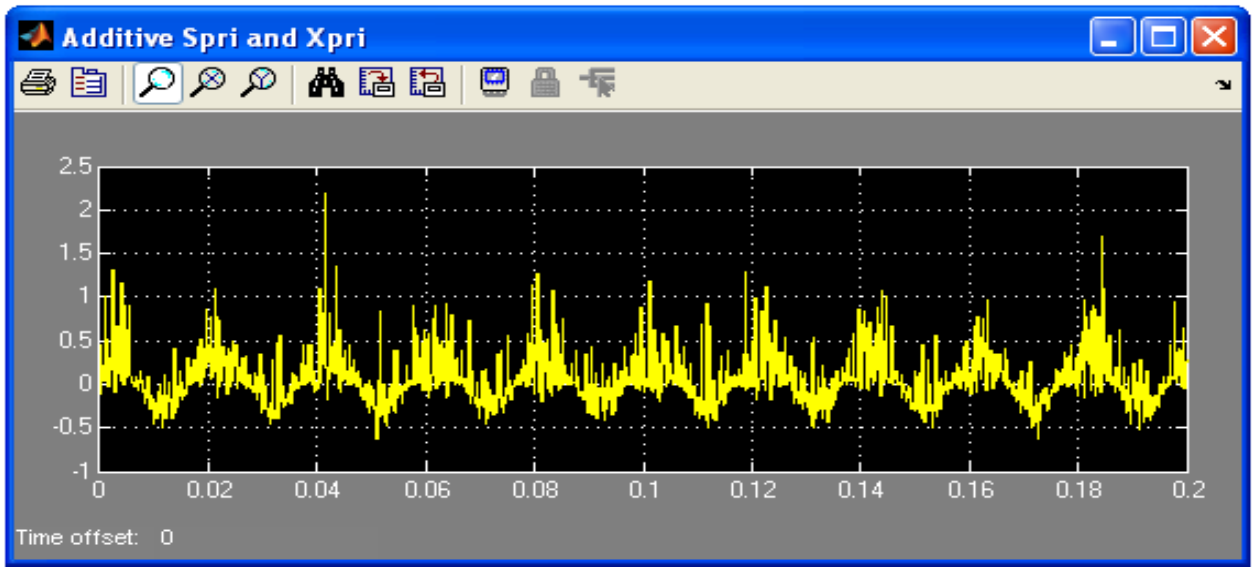

Figure 4.34 Additive Spri and Xpri

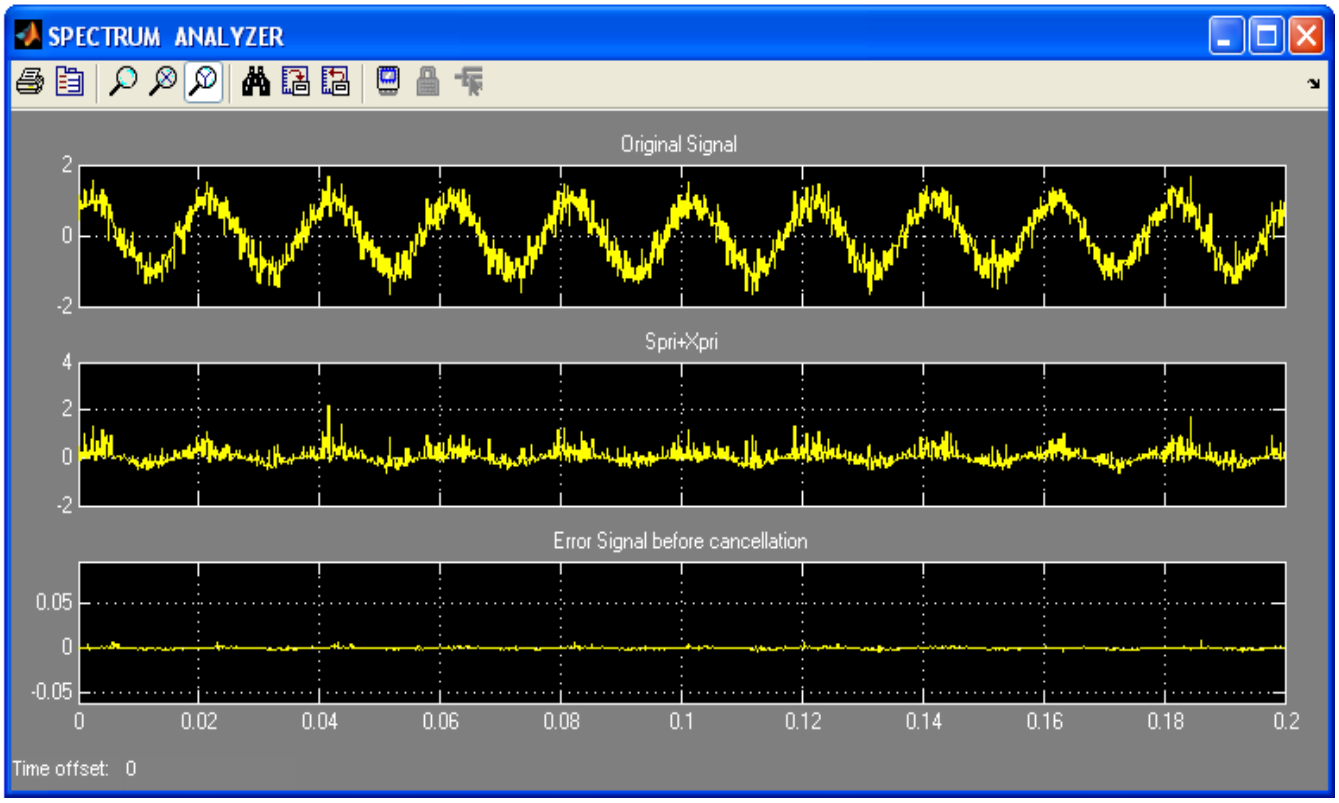

Figure 4.35 Error signal before Cancellation

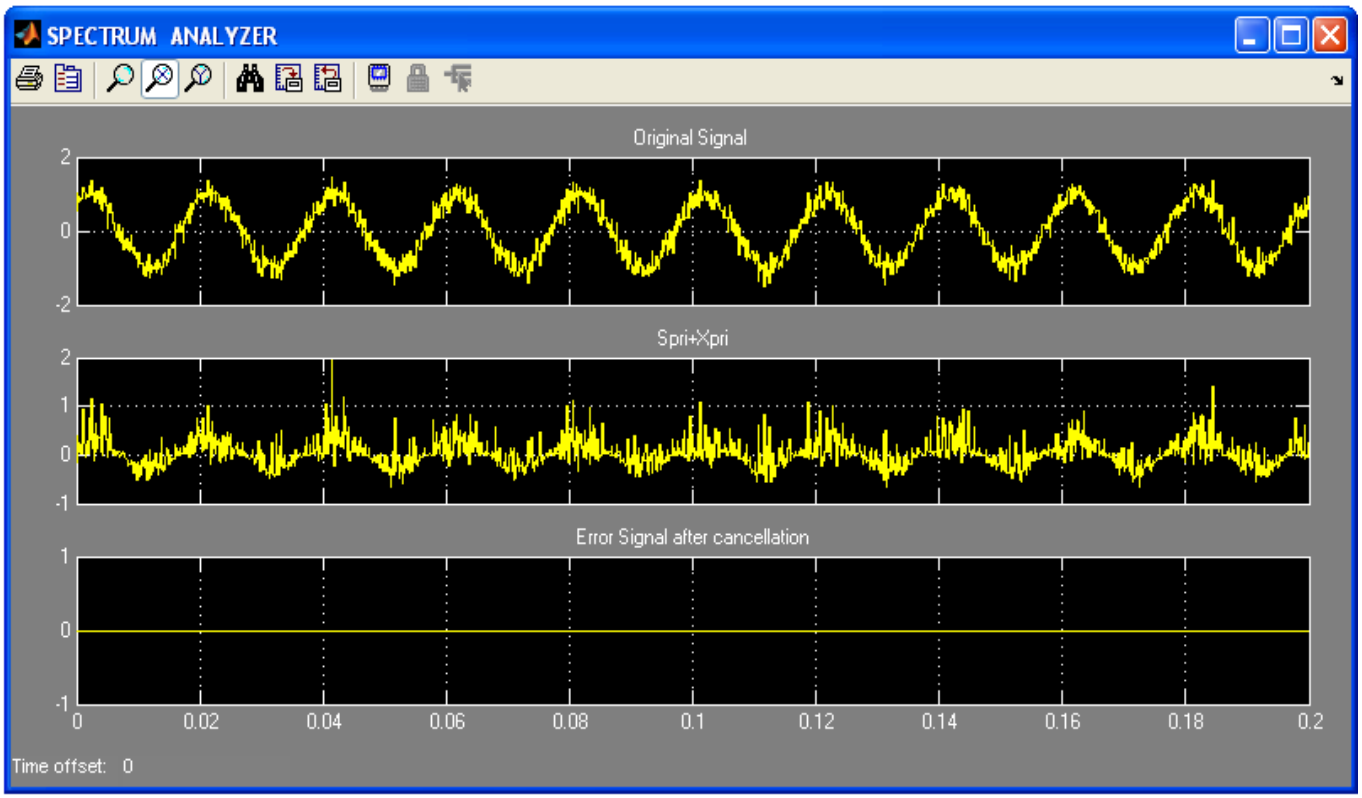

Figure 4.36 Error signal after Cancellation

4.10 Performance Evaluation Decisive Factors for the Proposed Techniques

It is necessary to evaluate the system performance of the proposed techniques using a method known as Noise Cancellation Performance (NCP). This is important to assess how best the performances of the designed system are. The NCP is a measure of the cancellation levels by which the noise signal power level in a certain bandwidth is reduced. It is mathematically defined as the power ratio of the residual error signal to the primary signal at the point of cancellation expressed in dB as shown in equation 4.17 [75].

$$NCP = 10\log(\frac{P_{err}}{P_{\Pr i}}) \tag{4.17}$$

where P_{err} is the error signal in terms of average power level and P_{pri} is the primary signals in terms of average power levels. Cancellation performance as a function of amplitude imbalance, phase error and delay mismatch are mathematically demonstrated.

4.10.1 Cancellation Performance as a Function of Amplitude Imbalance only

Let's assume that there is no phase error and no delay mismatch. The amplitude imbalance, expressed as the amplitude difference between the reference signal and the primary signal, normalized to the primary signal voltage has a normalized amplitude balance as [47].

$$\frac{V_{\Re f}}{V_{\Pr i}} = \frac{\Delta V + V_{\Pr i}}{V_{\Pr i}} \tag{4.18}$$

Let $\frac{V_{\mathrm{Re}f}}{V_{\mathrm{Pr}}} = \gamma$, hence $\gamma = \frac{\Delta V + V_{\mathrm{Pr}i}}{V_{\mathrm{Pr}i}}$ (4.19)

Eqn 4.18 is expressed in dB as

$$\gamma_{dB} = 20\log(\gamma) \tag{4.20}$$

Noise cancellation performance model for amplitude imbalance is given as

$$NCP_{dB} = 10\log\left\{1 - 2f + f^2\right\} \tag{4.21}$$

where f is the normalized amplitude. Substituting for γ gives

$$NCP_{dB} = 10\log\left\{1 - 2\gamma + \gamma^2\right\} \tag{4.22}$$

Therefore, the NCP in terms of amplitude imbalance is obtained as

$$NCP(\gamma_{dB}) = 10\log\left\{1 + 10^{\frac{2\gamma_{dB}}{20}} - 2.10^{\frac{\gamma_{dB}}{20}}\right\} = 10\log\left\{1 + 10^{0.1\gamma_{dB}} - 2.10^{0.05\gamma_{dB}}\right\} \tag{4.23}$$

4.10.2 Cancellation performance as a function of phase error only

Let's also assume that there is no amplitude imbalance and delay mismatch. Phase error which is defined as the phase deviation from perfect anti-phase between the reference signal and the primary signal, expressed in degrees(^{0}). Noise cancellation performance as a function of phase error in dB is given as [47].

$$NCP(\theta_{err}) = 10\log\left[2(1 - \cos(\theta_{err}))\right] \tag{4.24}$$

4.10.3 Effect of delay mismatch on signal cancellation

The delay difference between the primary and reference cancellation paths causes a linear phase response (constant delay) of the band of interest. The effect of delay mismatch between the primary signal and the reference signal

on cancellation performance is considered assuming perfect amplitude balance and no phase error ($\gamma = 0dB, \theta_{err} = 0^0$). The reference path and the primary path have different delay characteristics; this is because the two paths use different components as explained earlier. The mismatch between the delay characteristics (τ) of the primary path and reference path creates an important limitation on the cancellation performance. The modeling of the delay mismatch is shown in equation 4.25 [47].

$$NCP(\tau) = 10\log[2(1-\cos(B\pi\tau)] \tag{4.25}$$

Equations 4.23, 4.24, and 4.25 are used to plot the graph of Amplitude Imbalance versus Noise Cancellation Performance level, the graph of phase error against different levels of Noise Cancellation Performance and the graph of delay mismatch against Noise Cancellation Performance levels respectively, as shown in Figures. 4.37, 4.38 and 4.39. The cancellation performance levels (dB) are used to describe various levels achievable relative to the characteristic performances of the amplitude imbalance, phase error and delay mismatch.

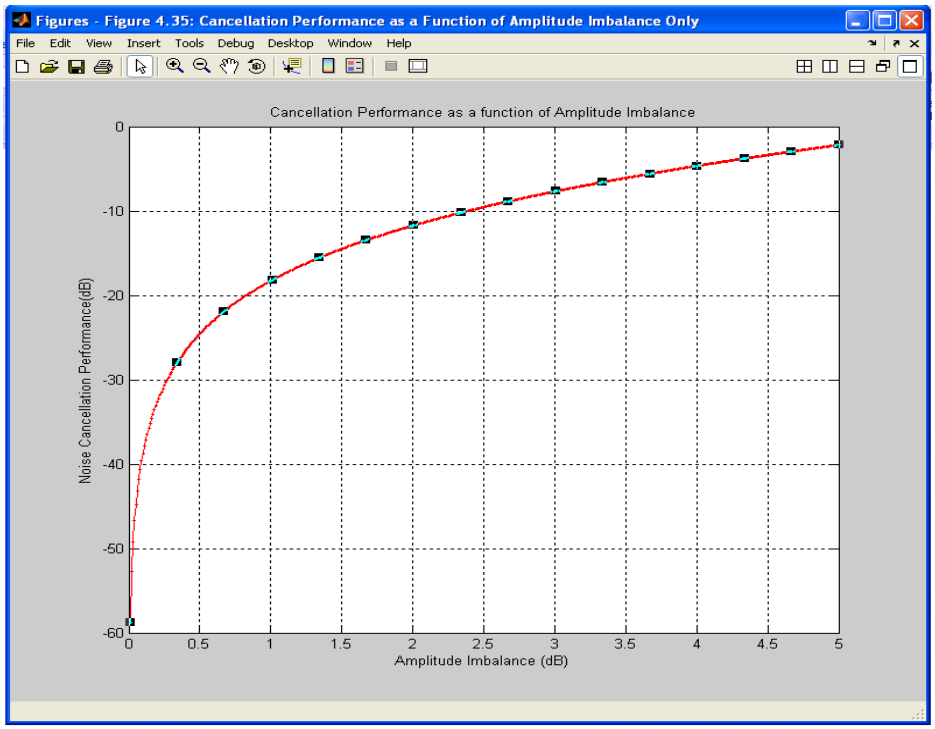

Figure 4.37: Amplitude Imbalance(dB) vs Noise Cancellation Performance(dB)

A graph of Noise Cancellation Performance (NCP) in the presence of different levels of Amplitude Imbalance attributable to noise cancellation between the primary and reference path at the point of cancellation is shown Figure 4.37. It can be observed that to achieve a 52dB cancellation, the amplitude imbalance must be below 0.03dB. Also to achieve above 60dB cancellation, the amplitude imbalance falls at zero decibel, given rise to perfect cancellation performance for the amplitude imbalance only. Hence, the higher the cancellation performance, the lower the amplitude imbalance.

The 52dB was applied in the ANCT as a comparative mechanism to what was achieved as the attenuation requirement for the BBPF. This was considered in order to evaluate the cancellation performance levels for the

amplitude imbalance, phase error and delay mismatch respectively. Hence, it showed the parametric requirements to achieve a 52dB using NCP approach. An improved feature of ANCT other than the advantages earlier enumerated is that ANCT can achieve a perfect cancellation by obtaining a zero level performance for the three defined parameters given rise to absolute recovery of the entire desired signals.

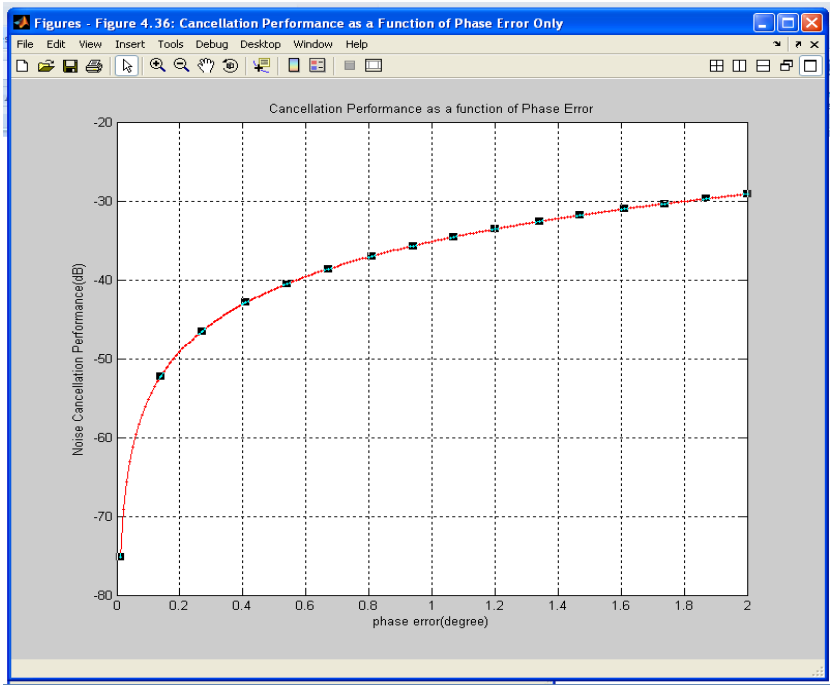

Figure 4.38: Phase Error(degrees) vs Noise Cancellation Performance(dB)

Noise performance cancellation in the presence of varying degrees of phase error at the point of cancellation between the noise at the primary signal and reference signal is shown in Figure 4.38. From the figure, to achieve a 52dB cancellation performance, the phase error (in degrees) required should be less than $0.14^{0.}$ Equally, to achieve a phase error of zero degrees (perfect cancelation), requires a noise cancellation performance above 75dB.

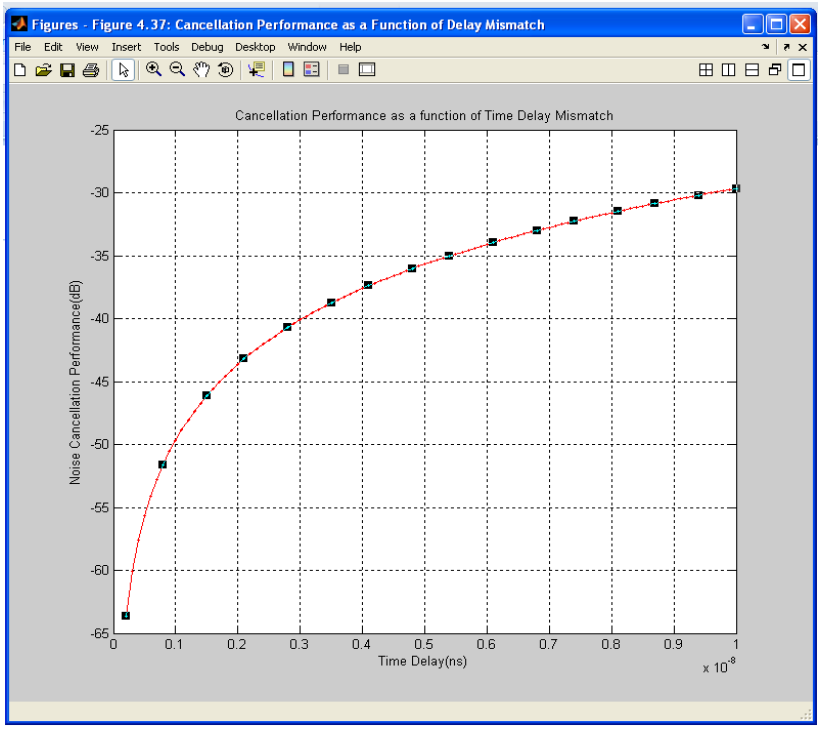

Figure 4.39 Time delay Mismatch (ns) vs Noise Cancellation Performance (dB)

As shown in Figure 4.39, to achieve a 52dB cancellation over a wider bandwidth, the delay mismatch should not exceed 0.07ns. To achieve a cancellation performance of above 65dB, gives rise to absolute zero time delay mismatch.

Figures 4.37, 4.38 and 4.39 showed that to achieve a noise cancellation performance of 52dB as used in the BBPF magnitude design, the amplitude imbalance, phase error and time delay mismatch must not be more than 0.03dB, 0.14^0 and 0.07ns respectively. Also to achieve a perfect cancellation, the cancellation performances are expected to be 60dB and above for amplitude imbalance, 75dB and above for phase error and 65dB and above for time delay mismatch, averaged at 67dB.

The generated matlab m-files for the graphs shown in Figures. 4.37-4.39 are specified in appendix E1-E5

Hence, in Figures 4.37-4.39, the minimum requirements necessary to obtain a 52dB noise cancellation performance are; Amplitude imbalance (γ) of less than 0.03dB, phase error (θ_{err}) of less than 0.14^0 and delay mismatch (τ) of 0.07ns. The three parametric values obtained validated the research result that the magnitude specification of 52dB rejection obtained for the BBPF design can substantially attenuate the sideband noise components present in the WCDMA receiver front end with lesser leakages considering the non-ideal characteristic of a fixed filter.

The ANCT technique, despite its capability to perform efficiently in a dynamic environment, has the potentials to achieve theoretical perfect cancellation above 67dB. This gave about 28% improvement relative to the cancellation performance of the BBPF.

CHAPTER FIVE

CONCLUSION AND RECOMMENDATIONS

5.1 Conclusion

The thesis was primarily aimed at providing a comprehensive solution to mitigate sideband noise which occurs when two networks involving downlink frequency of CDMA-2000 operating in the frequency range 1960-1990MHz and uplink WCDMA frequency in the range 1920-1980MHz are co-located on a single mast. Empirical analyses were conducted in two different scenarios to evaluate the degree of interference power effects on the victim receiver. The first scenario involved a standalone unco-located WCDMA while the second scenario involved a co-located setting. The general overview effects of the interfering noise power on the received signal stengthperformance and its degradation effects on the Carrier to Interference ratio performance including the noise floor levels were clearly enumerated using mathematical and graphical representations. From the measurements conducted, the interfering power was evaluated as -108.80dBm, which gave rise to 1.01dBm received signal strength degradation and 1.01dBm rise in total system noise floor, about 30% degradation in C/I ratio. The application of Butterworth Band pass filter was considered a classical technique to mitigate the sideband interference. A 52dB rejection band pass filter at 5MHz guard band offset from the low side edge of the pass band was designed to attenuate/reject the sideband noise.

To achieve a noise cancellation performance levels at 52dB required an amplitude imbalance of 0.03dB, phase error of 0.14^0 and time delay mismatch of 0.07ns. The three values obtained in the research findings showed that the magnitude specification of the 52dB rejection obtained for the BBPF design can to a larger extent attenuate the sideband noise components present in the WCDMA receiver front end.

The proposed adaptive noise cancellation technique was developed to improve the limitations of the band pass filter especially when operating in a time-varying environment. The technique was primarily focused on achieving perfect theoretical cancellations where the amplitude imbalance, phase error and delay mismatch are dynamically adjusted by the weight variables towards achieving zero cancellation performance. The simulated results obtained showed the noise cancellation performances at various levels. An experimental test-bed set-up was performed using Matlab-simulink environment to realize the error cancellation performances before and after cancellation, implemented using a self-developed algorithm.

5.2 Research Contributions to Knowledge

- A magnitude of 52dB rejection at 5MHz guard band was obtained from the empirical analysis as a unique design specification for the BBPF involving a co-located CDMA2000 and WCDMA network. Generated results were obtained which could serve as research reference point.
- ANCT was developed as an improvement over the fixed filter.
- Matlab-simulink experimental test-bed was actualized with graphical representations showing the error signals before and after cancellation. The result obtained using noise cancellation performance criteria, gave rise to about 28% improvement over the classical BBPF.
- This thesis has contributed also to four (4) journal papers published from highly reputable international technical journals (one in France, three in USA).

5.3 Recommendations

The proposed ANCT used a single cancellation loop comprised of a single primary and reference antennas and is only capable of mitigating interference signals radiating from a single co-located offending transmitting antenna. However, the recent campaign for co-located systems in Nigeria is to have more networks on the same tower as a palliative measure to improve the dwindling economic recession, which obviously will necessitate having more than one transmitting offender or jammer. Hence, future work would involve

the implementation of a Multi-Loop Adaptive Noise Cancellation Technique (MLANCT) other than the Single-Loop Adaptive Noise Cancellation Technique (SLANCT). The MLANCT will be capable of mitigating interfering jamming signals, blocking and intermodulation interference respectively on the receiver front ends from multiple co-located offending transmitters. It would also be of interest to look into the practicality of the controlled algorithm for the multi-loop cancellation and the distortion effects generated by the active components including the system thermal noise.

Following the findings in research study, it is recommended that:

1. The wireless network stakeholders' (e.g. IHS Vendor), should consider necessary the application of the designed BBPF and also the proposed ANCT for adequate cancellation performance especially in a dynamic environment.
2. The test-bed model for the ANCT should be developed using a hardware set-up and be implemented for optimal noise cancellation in a co-located setting.
3. In the practical implementation of the developed ANCT, it is important to evaluate the levels of insertion loss generated by the active components and provide adequate measures to reduce the insertion loss, to avoid forward coverage reduction of the desired signal amplitude.

4. The stakeholders in wireless networks need to support in sponsoring scholars and researchers in such a magnitude project especially in funding the relevant tools such as software (usually very expensive) that could provide the basic requirements to actualize the research goals which can ease the hardware design implementation.

REFERENCES

[1] Sadiq, O.M., Oyelade A.O., and Ukachukwu C.A.S., "Ten Years Of Telecommunication Infrastructure Development In Nigeria" *International Conference on Innovations in Engineering and Technology*, August 8th – 10th., 2011

[2] Allsebrook K. and Ripple C., "VHF co-site interference challenges and solutions for the united states marine corps expeditionary fighting vehicle program", *in Proc. IEEE Military Communication Conference*, 2004

[3] German F., Annamalai K., Young M., Miller M.C., "Simulations and Data Management for Co-site Interference Prediction", *in Proc. IEEE International symposium on Electromagnetic compatibility,* July 2010.

[4] Demirkiran I., Weiner D.D., Drozd A. and Kasperovich I., "Knowledge-based Approach to Interference Mitigation for EMC of Transceivers on Unmanned Aircraft," *in Proc. IEEE International Symposium on Electromagnetic Compatibility*, July 2010.

[5] Louay A. C., Bahjat E., Ghassan H., Mohamad M., "Telecom Infrastructure Sharing: Regulatory Enablers and Economic Benefits," *Booz Allen Hamilton*, 2007

[6] Opara S., Ituen I., "An option for Telecom operators during recession". *A journal paper*, pp 1.2, 2009

[7] Bhanu A., "Sharing of Telecom Infrastructure: Passive, Backhaul & Active", pp. 1 – 10, 2007

[8] Camila B.L. "Mobile Sharing", International Telecommunication Unions (ITU's) eighth Global Symposium for Regulators (GSR). Pp3-5, 2012

[9] Razavi B., "RF Microelectronics". *Upper Saddle River, NJ: Prentice Hall*, 1998,pp. 11-53.106

[10] Bala-Gbogbo E., "Telecom Industry Operators Opt for Infrastructure Sharing.", 2009

[11] *Nigeria Communication week*, The Threat of Multiple Regulations in Telecom,. Pg. 1, Mon, 2012-08-13.

[12] "NCC Guidelines on Collocation and Infrastructure Sharing" *Nigerian Communications Commission*, pp.1-13.2002.

[13] Robert S., Mawrey B., "Radio Frequency interference and antenna sites", *UNIsite, Inc* 3450 Buschwood Park Drive Suite 250. p 3, 2009

[14] Zhang H., Dai H., "Co-channel Interference Mitigation and Cooperative Processing In Downlink Multicell Multiuser MIMO networks," *European Journal on Wireless Communications and Networking*, 2004, no. 2, pp. 222-235, 2004

[15] Stavroulakis P., ''Interference Analysis of Communications Systems,'' *IEEE Press, New York, 1980*

[16] Infrastructure sharing and collocation services License by Nigerian Communications Commission Section 32 of the *Nigerian Communications Act*, 2003.

[17] Onuegbu C.I, "Co-location: An imperative for CAPEX Reduction". A Published paper, p1, 2009

[18] Onuzuruike E., "Telecom Infrastructure Sharing as a Strategy for Cost Optimization and Revenue Generation": A Case Study of MTN Nigeria/Zain Nigeria Collocation. *Blekinge Institute of Technology* p.10 (unpublished MBA thesis), 2009.

[19] Chen Z., Luk K.M., "Antennas for Base Stations in Wireless Communication", 2009.

[20] Chanab L.A., et al, "Telecom Infrastructure Sharing: Regulatory Enablers and Economic Benefits", *Booz Allen Hamilton Consulting*, December 2007, pp. 1 – 12, 2007.

[21] Compatibility between GSM MCBTS And Other Services (TRR, RSBN/PRMG, HC -SDMA, GSM-R, DME, MIDS, DECT) Operating In The 900 And 1800 MHz Frequency Bands. *Electronic Communications Committee (ECC) within the European Conference of Postal and Telecommunications Administrations (CEPT) ECC report* 146, 2010, pp 28-46.

[22] Lee, W. C. Y., "Elements of cellular mobile radio systems," *IEEE Transactions on Vehicular Technology*, vol. VT-35, no 2, pp. 48-56., May 1986.

[23] Rappaport , T.T.S., "Wireless Communications: Principles and Practice", 2nd ed. Singapore: *Pearson Education*, Inc., 2002.

[24] Trino G., *RF design Manager from Starcomms* "interference analysis between co-allocated networks in Nigeria", 2nd version, 2008.

[25] Macchiarella, G., Stracca , G.B., and Miglioli, L., "Experimental study of passive intermodulation in coaxial cavities for cellular base stations duplexers", *Microwave conference*, 2004.

[26] John P. "Market Mechanisms for Spectrum Management" *Spectrum Liberalization and Interference Management*, Transfinite System Ltd, pp1-7, 2006.

[27] Paul G. "Report for GSMA on the Coexistence of ISDB-T and LTE" *Advanced Topographic Development & Images* Limited, W1306L4205 p. 6, 2013

[28] Lee, W.C., "Mobile Communications Engineering", 2nd ed. New Delhi: *Tata McGraw-Hill*., 2006.

[29] Rappaport , T.S., "Wireless Communications: Principles and Practice", 2nd ed. Singapore: *Asoke K. Ghost Prentice hall of Indian Private limited, New Delhi* 110001, 2006.

[30] Carsello, R. et al., "IMT-2000 Standards: Radio Aspects, *IEEE Personal Communications*, 2002.

[31] Dalal, N., "A Comparative Study of UMTS (WCDMA) and CDMA-2000 Networks," *Award Solutions, Inc*., 2002.

[32] Kwansnicki, W., "Technological Substitution Processes-an Evolutionary Model", *Wroclaw University of Technology*, 2001.

[33] Carsello, R. et al., "IMT-2000 Standards: Radio Aspects", *IEEE Personal Communications*, PP. 30-40, 1997.

[34] Garg, V., "Wireless Network Evolution: 2G to 3G", *Prentice Hall Communications Engineering and Emerging Technology Series*, 2001.

[35] Report ITU-R M.2141 – Study of the isolation between VHF land mobile radio antennas in close proximity.

[36] Balanis, C. A., "Antenna Theory: Analysis and Design", – 2nd ed. *John Wiley & Sons, Inc*., 1997.

[37] Affanasiev, K. J., "Simplifications in the consideration of mutual effects between halfwave dipoles in collinear and parallel orientations", *Proc. IRE Wave*, 1946.

[38] ITU-R M.2244, "Isolation between antennas of IMT base stations in the land mobile service", *electronic publications Geneva*, pp 8-10, 2011.

[39] Chen X., "Analysis on co-site interference between different mobile communication system" *wireless technical support department, Huawei technologies* Co. Ltd, pg 9, 2008.

[40] Wiener N., "Extrapolation, Interpolation and Smoothing of Stationary Time Series, with Engineering Applications"**.** New York: *Wiley*, 1949.

[41] Kalman R., and Bucy R.,, "New results in linear filtering and pre-diction theory," *Trans. ASME, ser. D, J. Basic Eng***.,** vol. 83, pp. 95-107, DeC. 1961.

[42] Glover, Jr R. J.., 'Adaptive Noise Cancelling, Applied to Sinusoidal Interference", *IEEE Trans*. ASSP, Vol. ASSP-25, No. 6 pp 484-490, Dec,1977.

[43] Ghose R.N., and Suter W.A., "Interference cancellation system," *U.S. Patent* No.3,699,444, October 17, 1972.

[44] Ghose R.N., "Co-location of receivers and high power transmitters, *"IEEE trans*. Broadcasting, Vol. 34, No. 2 pp. 154-158, June 1988.

[45] Venskauskas K.K., and Bogomolov G.P., "some results on interference suppression on electromagnetically dense platforms", *IEEE international symposium on electromagnetic compatibility*, symposium record. Pp382-386, 1991

[46] Talwar A.K., "Antenna spacing consideration in an interference canceller", *IEEE Trans on Broadcasting*, Vol. 36, No. 3, pp. 203-206, September, 1990.

[47] Alain R., "Feedforward Interference Cancellation System applied to the 800MHz CDMA cellular band. A master thesis in electrical engineering *Ottawa-Carleton institute of Electrical Engineering*, may, 2003, pp. 20-39

[48] Lucyszyn S., and Robertson I.D., "Analog reflection Topology Building Blocks for Adaptive microwave signal processing applications", MTT, *IEEE Trans*. Vol.43, No.3 pp. 601-611, March, 1995.

[49] Daniel, V.P., Figueiredo, P. M., António R., Instituto Superior Técnico, "Impact of Adjacent Channel interference on the Capacity of WCDMA/FDD networks" *Technical University of Lisbon* Av. Rovisco Pais, Lisboa, Portugal, 2009.

[50] Jing, Z., Alan W., Xue Y., and Xingang G., "Multi radio coexistence: challenges and opportunities" *Communication technology Lab, Intel Corporation, Hillsboro,* USA, 2007.

[51] Vieri, V., Mustafa, S., and Jiang, J., "Frequency Coordination between UMTS and GSM systems at 900MHz" *Qualcomm Incorporated*, 5775 morehous Drive, San Diego, CA 92121, 2008.

[52] Paschos, G., Kotsopoulos, S.A., Zogas, D.A., "The Impact of Intermodulation interference in superimposed 2G and 3G wireless networks and optimization issues of the provided Q_OS", 2006.

[53] Muhammad S., Edward R. H., Dadana G. "The interference on WCDMA system in 3G coexistence network", *the 17th Annual IEEE International Symbosium on personal, indoor and mobile radio communication PIMRC* 2006.

[54] Jraifi, A., Laamara, R.A., Belhaj, A., and Saidi, E.H., "A proposal solution for interference inter-operators" *Progress in Electronagnetics Research* C, Vol 12, 15-25, 2010.

[55] Guthrie W., and Hanson D., "Co-Location Interference Mitigation". *White Paper*. Netcom Inc., USA, June 13, 2005 http://www.netcominc.com

[56] Alain R., Charles W. T. and Jim S. W., "Frequency Agile RF Feedforward Noise Cancellation System," in *Proc. IEEE Radio and Wireless Symposium,* 2008.

[57] Thomas H., Kodim W., Gloeckler R., Dingfelder H., "Transmitter Leakage Cancellation Circuit for Co-Located GPS Receiver," *European Patent 1 091497*, 11 April 2001.

[58] McConnell R. J., Tso R., "Method and Apparatus for Reducing GPS Receiver Jamming during Transmission in a Wireless Receiver," *U.S. Patent 6 961 019*, 1 Nov 2005.

[59] Raghavan A., Gebara E., Tentzeris E. M., and Laskar J., "Analysis and Design of an Interference Canceller for Collocated Radios," *IEEE Transactions on Microwave Theory and Techniques*, vol. 53, no. 11, November 2005.

[60] Kannangara S. and Faulkner M., "Adaptive Duplexer for Multiband Transreceiver," in *Proc. Radio and Wireless Conference (RAWCON)*, pp. 381-384,10-13 August, 2003.

[61] Charu S. and Monika B. "Active cancellation concept of the Tx/Rx feedthrough applying an auxiliary transmitter", *International Journal of Computer science Issues*, 2011

[62] "Compatibility Study for UMTS operating within the GSM 900 and GSM 1800 frequency bands" *Electronic Communications Committee (ECC) within the European Conference of Postal and Telecommunications Administrations* (CEPT), 2006.

[63] Chenung, T. C., *Virginia Tech*: ETD 122298, Chapter 4 "Radio Performance", pp 96-99, 2009.

[64] "Noise figure measurement accuracy, the Y-factor method". Application note 57-2, *Agilent Technologies*, p. 5.

[65] Sadeen P., "Receiver Noise figure sensitivity and dynamic range" *Ham Radio Magazine*, pp 1-18, 2008.

[66] 3GPP Technical Specification, "RF System Scenarios", TR 25.942

[67] Montegrotto T. "Practical Mechanism to Improve the Compatibility between GSM-R and Public Mobile Networks and Guidance on Practical Co-ordination", *ECC Report* 162, p. 40 May, 2011.

[68] Kabutz M.H., Langman A., and Inggs M.R., "Hardware Cancellation of the Direct Coupling in a Steeped CW Ground Penetrating Radar," IGARSS '94, Surface and Atmospheric Remote Sensing: *Technologies, Data Analysis and Interpretation*, Vol4. 1994.

[69] Ahmed S. and Faulkner M., "Optimized interference cancelling for co-located base station transceivers," *Vehicular technology, IEEE transactions on, Vol. 60. No. 9*, October 2011

[70] Kang S., Jung Y., and Lee I., "Novel Analysis of the Cancellation Performance of a Feed forward Amplifier," *Global Telecommunications Conference GLOBECOM '97*, Vol. 1 1997.

[71] Sander, J. W., "Spurious Emission Measurement on 3GPP Base station transmitters" *Rohde and Schwarz*. pp 2-6, 2002.

[72] Losada R.A., "Digital Filters with MATLAB", *The Mathworks Inc*. p 4, 2008.

[73] Jia-Sheng H., and Lancaster M.J., "Microstrip Filters for RF/Microwave Applications" *John Wiley and Sons Inc*, 2001.

[74] Cherniakov M., "An Introduction to Parametric Digital Filters and Oscillators" *John Willey and Sons Inc. Hoboken*, NJ 07030 USA, 2003.

[75] Ahmed S., "An adaptive Cancellation System for a Co-located Receiver and its Dynamic Range" *in Proc. IEEE Radio and Wireless Symposium*, January, 2011.

APPENDIX A

OBTAINED DATA

A1: Unco-located network: Reference received signal power

Table A1-1: Site Parameters and measurements for the unco-located network (dry season)

NE Name	G Cell ID	Longitude	Latitude	Address	Received Signal Power		
					Ch1(dBm)	Ch2(dBm)	Ch3(dBm)
HENB549	EN0099C	7.528694	6.44658	Independent Layout opposite Brown and Brown Hotel New Haven	-109.47	-109.40	-109.66
HENB549	EN0099C	7.528694	6.44658	Independent Layout opposite Brown and Brown Hotel New Haven	-109.83	-109.65	-109.65
HENB549	EN0099C	7.528694	6.44658	Independent Layout opposite Brown and Brown Hotel New Haven	-109.60	-109.38	-109.52
HENB549	EN0099C	7.528694	6.44658	Independent Layout opposite Brown and Brown Hotel New Haven	-109.71	-109.66	-109.58
HENB549	EN0099C	7.528694	6.44658	Independent Layout opposite Brown and Brown Hotel New Haven	-109.43	-109.46	-109.37

Source: Helios Towers Nigeria Plc 2013

Table A1-2: Site Parameters and measurements for the unco-located network (Rainy season)

NE Name	G Cell ID	Longitude	Latitude	Address	Received Signal Power		
					Ch1(dBm)	Ch2(dBm)	Ch3(dBm)
HENB549	EN0099C	7.528694	6.44658	Independent Layout opposite Brown and Brown Hotel New Haven	-109.64	-109.68	-109.82
HENB549	EN0099C	7.528694	6.44658	Independent Layout opposite Brown and Brown Hotel New Haven	-109.90	-109.77	-109.83
HENB549	EN0099C	7.528694	6.44658	Independent Layout opposite Brown and Brown Hotel New Haven	-109.97	-109.67	-110.12
HENB549	EN0099C	7.528694	6.44658	Independent Layout opposite Brown and Brown Hotel New Haven	-109.65	-109.97	-109.72
HENB549	EN0099C	7.528694	6.44658	Independent Layout opposite Brown and Brown Hotel New Haven	-110.07	-109.70	-109.81

Source: Helios Towers Nigeria Plc 2013

A2: Received signal power measurement for Co-located network (dry season)

DAY 1

Table A2-1: BTS RECEIVED SIGNAL POWER MEASUREMENT

TOWN	STATE	VISA ID	HIS ID	OPERATORS	ADDRESS	CH1 RSSI (dBm)	CH2 RSSI (dBm)	CH3 RSSI (dBm)	CH4 RSSI (dBm)
Abuja	Abuja	ABJ001	IHS_ABJ_060V	MTN-EMTS-VISAFONE-AIRTEL	Cellcom sites Garki	-107.12	-97.91	-94.67	NA
Abuja	Abuja	ABJ004	IHS_ABJ_062V	VISAFONE-MTN	Cellcom sites Kubwa	-108.5	-107.37	-107.3	NA
Abuja	Abuja	ABJ031	IHS_ABJ_066V	VISAFONE	PRPOPERTY NEAR POTTERY COTTAGE INDUSTRY,	-110.28	-110.11	-109.7	NA
Abuja	Abuja	ABJ033	IHS_ABJ_067V	AIRTEL-VISAFONE	GALADIMA HOUSE,NO.1,CHURCHROAD, OFF HAS	-109.46	-109.64	-108.8	NA
Abuja	Abuja	ABJ035	IHS_ABJ_068V	VISAFONE-EMTS	MAIALLA, CLOSE TO GLO & NITEL INSTALLATION,	-93.84	-90.21	-90.4	NA
Abuja	Abuja	ABJ037	IHS_ABJ_069V	AIRTEL-VISAFONE-MTN	PLOT NO. E10, BWARI AREA COUNCIL, KUBWA EX	-110.25	-108.08	-108.48	NA
Abuja	Abuja	ABJ038	IHS_ABJ_070V	AIRTEL-VISAFONE	PLOT AT TUDUN WADA, MARABAN GURKU, KARU	-108.8	-107.69	-107.5	NA
Abuja	Abuja	ABJ040	IHS_ABJ_072V	AIRTEL-VISAFONE	PLOT, NO. 401,JIKOYI,OFF ASO ESTATE ROAD, OF	-107.62	-107.66	-106.25	NA
Enugu	Enugu	ENU005	IHS_ENG_007	MTN-STARCOMMS-VISAFONE	Plot 5 peace Close Federal Housing Estate Trans	-110.66	-110.7	-109.82	NA
Kaduna	Kaduna	KAD018	IHS_KAD_026V	MTN-VISAFONE	No.1, Kargargo Str. Ugwan Kanawa,Kaduna.	-110.35	-110.76	NA	NA
Kaduna	Kaduna	KAD019	IHS_KAD_027V	MTN-EMTS-VISAFONE	10,Galadima Road,Badarawa,Kaduna.	-109.8	-109.4	NA	NA
Kaduna	Kaduna	KAD020	IHS_KAD_028V	AIRTEL-VISAFONE	Block DE 2,Nnamdi Azikwe Express Byepass, Kad	-110.21	-104.5	NA	NA
Kaduna	Kaduna	KAD027	IHS_KAD_033V	MTN-EMTS-VISAFONE	plot @ Apaka Village, Mando,Kaduna, Kaduna St	-105.75	-110.3	-109.43	NA
Lagos	Lagos	LS070	IHS_LAG_111V	MTN-VISAFONE-SWIFT	18, BENSTER CRESCENT, MAZA MAZA	-105.67	-104.9	-109.33	NA
Lagos	Lagos	LS078	IHS_LAG_115V	EMTS-VISAFONE-SWIFT	25/27, OLU ADEGBITE STREET, OFF OLADUN ROAD	-104.34	-105.2	NA	NA
Lagos	Lagos	LS116	IHS_LAG_142V	MTN-AIRTEL-VISAFONE	6, WILSON IJIEKHUAWEN STREET, OFF OBA AYOK	-106.69	-106.2	NA	NA
Lagos	Lagos	LS117	IHS_LAG_143V	MTN-VISAFONE	1/2 IBRAHIM KOSHEBINU STREET AKESAN LAGOS	-105.17	-106.3	NA	NA

Source: IHS Nigeria Plc 2013

DAY 2

Table A2-2: BTS RECEIVED SIGNAL POWER MEASUREMENT

TOWN	STATE	VISA ID	HIS ID	OPERATORS	ADDRESS	CH1 RSSI (dBm)	CH2 RSSI (dBm)	CH3 RSSI (dBm)	CH4 RSSI (dBm)
Abuja	Abuja	ABJ001	IHS_ABJ_060V	MTN-EMTS-VISAFONE-AIRTEL	Cellcom sites Garki	-109.24	-110.77	-110.2	NA
Abuja	Abuja	ABJ004	IHS_ABJ_062V	VISAFONE-MTN	Cellcom sites Kubwa	-109.44	-110.64	-107.3	NA
Abuja	Abuja	ABJ031	IHS_ABJ_066V	VISAFONE	PRPOPERTY NEAR POTTERY COTTAGE INDUSTRY,	-109.35	-110.88	-109.7	NA
Abuja	Abuja	ABJ033	IHS_ABJ_067V	AIRTEL-VISAFONE	GALADIMA HOUSE,NO.1,CHURCHROAD, OFF HAS	-109.58	-110.98	-108.8	NA
Abuja	Abuja	ABJ035	IHS_ABJ_068V	VISAFONE-EMTS	MAIALLA, CLOSE TO GLO & NITEL INSTALLATION,	-109.58	-109.7	-90.4	NA
Abuja	Abuja	ABJ037	IHS_ABJ_069V	AIRTEL-VISAFONE-MTN	PLOT NO. E10, BWARI AREA COUNCIL, KUBWA EX	-110.2	-109.76	-108.8	NA
Abuja	Abuja	ABJ038	IHS_ABJ_070V	AIRTEL-VISAFONE	PLOT AT TUDUN WADA, MARABAN GURKU, KARU	-110.47	-109.64	-107.5	NA
Abuja	Abuja	ABJ040	IHS_ABJ_072V	AIRTEL-VISAFONE	PLOT, NO. 401,JIKOYI,OFF ASO ESTATE ROAD, OF	-110.67	-109.8	-106.5	NA
Enugu	Enugu	ENU005	IHS_ENG_007	MTN-STARCOMMS-VISAFONE	Plot 5 peace Close Federal Housing Estate Trans	-110.62	-110.54	-110.58	NA
Kaduna	Kaduna	KAD018	IHS_KAD_026V	MTN-VISAFONE	No.1, Kargargo Str. Ugwan Kanawa,Kaduna.	-110.3	-110.6	NA	NA
Kaduna	Kaduna	KAD019	IHS_KAD_027V	MTN-EMTS-VISAFONE	10,Galadima Road,Badarawa,Kaduna.	-109.8	-109.4	-109.88	NA
Kaduna	Kaduna	KAD020	IHS_KAD_028V	AIRTEL-VISAFONE	Block DE 2,Nnamdi Azikwe Express Byepass, Kad	-110.67	-108.66	-109.37	NA
Kaduna	Kaduna	KAD027	IHS_KAD_033V	MTN-EMTS-VISAFONE	plot @ Apaka Village, Mando,Kaduna, Kaduna St	-110.54	-108.46	-109.24	NA
Lagos	Lagos	LS070	IHS_LAG_111V	MTN-VISAFONE-SWIFT	18, BENSTER CRESCENT, MAZA MAZA	-107.87	-108.89	-109.44	NA
Lagos	Lagos	LS078	IHS_LAG_115V	EMTS-VISAFONE-SWIFT	25/27, OLU ADEGBITE STREET, OFF OLADUN ROAD	-108.35	-109.11	NA	NA
Lagos	Lagos	LS116	IHS_LAG_142V	MTN-AIRTEL-VISAFONE	6, WILSON IJIEKHUAWEN STREET, OFF OBA AYOK	-109.58	-108.36	NA	NA
Lagos	Lagos	LS117	IHS_LAG_143V	MTN-VISAFONE	1/2 IBRAHIM KOSHEBINU STREET AKESAN LAGOS	-108.35	-107.27	-109.44	NA

Source: IHS Nigeria Plc 2013

DAY 3

Table A2-3: BTS RECEIVED SIGNAL POWER MEASUREMENT

TOWN	STATE	VISA ID	HIS ID	OPERATORS	ADDRESS	CH1 RSSI (dBm)	CH2 RSSI (dBm)	CH3 RSSI (dBm)	CH4 RSSI (dBm)
Abuja	Abuja	ABJ001	IHS_ABJ_060V	MTN-EMTS-VISAFONE-AIRTEL	Cellcom sites Garki	-107.2	-110.88	-110.43	NA
Abuja	Abuja	ABJ004	IHS_ABJ_062V	VISAFONE-MTN	Cellcom sites Kubwa	-108.5	-107.7	-110.5	NA
Abuja	Abuja	ABJ031	IHS_ABJ_066V	VISAFONE	PRPOPERTY NEAR POTTERY COTTAGE INDUSTRY,	-110.2	-110.1	-110.5	NA
Abuja	Abuja	ABJ033	IHS_ABJ_067V	AIRTEL-VISAFONE	GALADIMA HOUSE,NO.1,CHURCHROAD, OFF HAS	-109.6	-109.6	-110.52	NA
Abuja	Abuja	ABJ035	IHS_ABJ_068V	VISAFONE-EMTS	MAIALLA, CLOSE TO GLO & NITEL INSTALLATION,	-109.11	-108.46	-110.54	NA
Abuja	Abuja	ABJ037	IHS_ABJ_069V	AIRTEL-VISAFONE-MTN	PLOT NO. E10, BWARI AREA COUNCIL, KUBWA EX	-110.2	-108.8	-108.8	NA
Abuja	Abuja	ABJ038	IHS_ABJ_070V	AIRTEL-VISAFONE	PLOT AT TUDUN WADA, MARABAN GURKU, KARU	-108.8	-110.81	-107.5	NA
Abuja	Abuja	ABJ040	IHS_ABJ_072V	AIRTEL-VISAFONE	PLOT, NO. 401,JIKOYI,OFF ASO ESTATE ROAD, OF	-107.4	-107.6	-106.5	NA
Enugu	Enugu	ENU005	IHS_ENG_007	MTN-STARCOMMS-VISAFONE	Plot 5 peace Close Federal Housing Estate Trans	-110.68	-110.7	-110.66	NA
Kaduna	Kaduna	KAD018	IHS_KAD_026V	MTN-VISAFONE	No.1, Kargargo Str. Ugwan Kanawa,Kaduna.	-110.3	-109.77	-110.98	NA
Kaduna	Kaduna	KAD019	IHS_KAD_027V	MTN-EMTS-VISAFONE	10,Galadima Road,Badarawa,Kaduna.	-109.8	-109.77	-109.7	NA
Kaduna	Kaduna	KAD020	IHS_KAD_028V	AIRTEL-VISAFONE	Block DE 2,Nnamdi Azikwe Express Byepass, Kad	-110.1	-109.98	-109.76	NA
Kaduna	Kaduna	KAD027	IHS_KAD_033V	MTN-EMTS-VISAFONE	plot @ Apaka Village, Mando,Kaduna, Kaduna St	-108.82	-110.63	-109.64	NA
Lagos	Lagos	LS070	IHS_LAG_111V	MTN-VISAFONE-SWIFT	18, BENSTER CRESCENT, MAZA MAZA	-109.37	-110.47	-109.8	NA
Lagos	Lagos	LS078	IHS_LAG_115V	EMTS-VISAFONE-SWIFT	25/27, OLU ADEGBITE STREET, OFF OLADUN ROAD	-108.66	-110.67	-109.45	NA
Lagos	Lagos	LS116	IHS_LAG_142V	MTN-AIRTEL-VISAFONE	6, WILSON IJIEKHUAWEN STREET, OFF OBA AYOK	-108.46	-110.54	-109.53	NA
Lagos	Lagos	LS117	IHS_LAG_143V	MTN-VISAFONE	1/2 IBRAHIM KOSHEBINU STREET AKESAN LAGOS	-108.89	-110.88	NA	NA

Source: IHS Nigeria Plc 2013

DAY 4

Table A2-4: BTS RECEIVED SIGNAL POWER MEASUREMENT

TOWN	STATE	VISA ID	HIS ID	OPERATORS	ADDRESS	CH1 RSSI (dBm)	CH2 RSSI (dBm)	CH3 RSSI (dBm)	CH4 RSSI (dBm)
Abuja	Abuja	ABJ001	IHS_ABJ_060V	MTN-EMTS-VISAFONE-AIRTEL	Cellcom sites Garki	-110.72	-110.83	-110.73	NA
Abuja	Abuja	ABJ004	IHS_ABJ_062V	VISAFONE-MTN	Cellcom sites Kubwa	-110.73	-110.77	-110.24	NA
Abuja	Abuja	ABJ031	IHS_ABJ_066V	VISAFONE	PRPOPERTY NEAR POTTERY COTTAGE INDUSTRY,	-110.24	-110.64	-109.77	NA
Abuja	Abuja	ABJ033	IHS_ABJ_067V	AIRTEL-VISAFONE	GALADIMA HOUSE,NO.1,CHURCHROAD, OFF HAS	-110.99	-110.88	-109.77	NA
Abuja	Abuja	ABJ035	IHS_ABJ_068V	VISAFONE-EMTS	MAIALLA, CLOSE TO GLO & NITEL INSTALLATION,	-110.81	-110.98	-109.98	NA
Abuja	Abuja	ABJ037	IHS_ABJ_069V	AIRTEL-VISAFONE-MTN	PLOT NO. E10, BWARI AREA COUNCIL, KUBWA EX	-110.4	-109.7	-110.63	NA
Abuja	Abuja	ABJ038	IHS_ABJ_070V	AIRTEL-VISAFONE	PLOT AT TUDUN WADA, MARABAN GURKU, KARU	-110.8	-109.76	-107.5	NA
Abuja	Abuja	ABJ040	IHS_ABJ_072V	AIRTEL-VISAFONE	PLOT, NO. 401,JIKOYI,OFF ASO ESTATE ROAD, OF	-107.4	-109.64	-106.5	NA
Enugu	Enugu	ENU005	IHS_ENG_007	MTN-STARCOMMS-VISAFONE	Plot 5 peace Close Federal Housing Estate Trans	-110.55	-109.8	-110.56	NA
Kaduna	Kaduna	KAD018	IHS_KAD_026V	MTN-VISAFONE	No.1, Kargargo Str. Ugwan Kanawa,Kaduna.	-109.98	-110.6	-110.43	NA
Kaduna	Kaduna	KAD019	IHS_KAD_027V	MTN-EMTS-VISAFONE	10,Galadima Road,Badarawa,Kaduna.	-110.63	-109.84	-110.5	NA
Kaduna	Kaduna	KAD020	IHS_KAD_028V	AIRTEL-VISAFONE	Block DE 2,Nnamdi Azikwe Express Byepass, Kad	-110.47	-110.5	-110.5	NA
Kaduna	Kaduna	KAD027	IHS_KAD_033V	MTN-EMTS-VISAFONE	plot @ Apaka Village, Mando,Kaduna, Kaduna St	-110.67	-110.3	-110.52	NA
Lagos	Lagos	LS070	IHS_LAG_111V	MTN-VISAFONE-SWIFT	18, BENSTER CRESCENT, MAZA MAZA	-110.54	-110.44	-110.6	NA
Lagos	Lagos	LS078	IHS_LAG_115V	EMTS-VISAFONE-SWIFT	25/27, OLU ADEGBITE STREET, OFF OLADUN ROAD	-110.88	-110.46	-110.83	NA
Lagos	Lagos	LS116	IHS_LAG_142V	MTN-AIRTEL-VISAFONE	6, WILSON IJIEKHUAWEN STREET, OFF OBA AYOK	-110.81	-110.83	-110.47	NA
Lagos	Lagos	LS117	IHS_LAG_143V	MTN-VISAFONE	1/2 IBRAHIM KOSHEBINU STREET AKESAN LAGOS	-110.7	-110.3	-110.72	NA

Source: IHS Nigeria Plc 2013

DAY 5

Table A2-5: BTS RECEIVED SIGNAL POWER MEASUREMENT

TOWN	STATE	VISA ID	HIS ID	OPERATORS	ADDRESS	CH1 RSSI (dBm)	CH2 RSSI (dBm)	CH3 RSSI (dBm)	CH4 RSSI (dBm)
Abuja	Abuja	ABJ001	IHS_ABJ_060V	MTN-EMTS-VISAFONE-AIRTEL	Cellcom sites Garki	-109.11	-108.46	-110.54	NA
Abuja	Abuja	ABJ004	IHS_ABJ_062V	VISAFONE-MTN	Cellcom sites Kubwa	-108.36	-108.89	-110.88	NA
Abuja	Abuja	ABJ031	IHS_ABJ_066V	VISAFONE	PRPOPERTY NEAR POTTERY COTTAGE INDUSTRY,	-107.27	-109.11	-110.81	NA
Abuja	Abuja	ABJ033	IHS_ABJ_067V	AIRTEL-VISAFONE	GALADIMA HOUSE,NO.1,CHURCHROAD, OFF HAS	-108.66	-108.36	-110.88	NA
Abuja	Abuja	ABJ035	IHS_ABJ_068V	VISAFONE-EMTS	MAIALLA, CLOSE TO GLO & NITEL INSTALLATION,	-107.34	-107.27	-110.43	NA
Abuja	Abuja	ABJ037	IHS_ABJ_069V	AIRTEL-VISAFONE-MTN	PLOT NO. E10, BWARI AREA COUNCIL, KUBWA EX	-108.34	-108.66	-110.5	NA
Abuja	Abuja	ABJ038	IHS_ABJ_070V	AIRTEL-VISAFONE	PLOT AT TUDUN WADA, MARABAN GURKU, KARU	-108.8	-107.6	-107.5	NA
Abuja	Abuja	ABJ040	IHS_ABJ_072V	AIRTEL-VISAFONE	PLOT, NO. 401,JIKOYI,OFF ASO ESTATE ROAD, OF	-107.4	-107.6	-106.5	NA
Enugu	Enugu	ENU005	IHS_ENG_007	MTN-STARCOMMS-VISAFONE	Plot 5 peace Close Federal Housing Estate Trans	-110.5	-110.65	-110.65	NA
Kaduna	Kaduna	KAD018	IHS_KAD_026V	MTN-VISAFONE	No.1, Kargargo Str. Ugwan Kanawa,Kaduna.	-109.55	-110.47	-109.54	NA
Kaduna	Kaduna	KAD019	IHS_KAD_027V	MTN-EMTS-VISAFONE	10,Galadima Road,Badarawa,Kaduna.	-109.47	-110.72	-109.02	NA
Kaduna	Kaduna	KAD020	IHS_KAD_028V	AIRTEL-VISAFONE	Block DE 2,Nnamdi Azikwe Express Byepass, Kad	-109.36	-110.73	-109.98	NA
Kaduna	Kaduna	KAD027	IHS_KAD_033V	MTN-EMTS-VISAFONE	plot @ Apaka Village, Mando,Kaduna, Kaduna St	-109.37	-110.47	-109.77	NA
Lagos	Lagos	LS070	IHS_LAG_111V	MTN-VISAFONE-SWIFT	18, BENSTER CRESCENT, MAZA MAZA	-108.66	-110.67	-109.83	NA
Lagos	Lagos	LS078	IHS_LAG_115V	EMTS-VISAFONE-SWIFT	25/27, OLU ADEGBITE STREET, OFF OLADUN ROAD	-108.46	-110.54	-109.74	NA
Lagos	Lagos	LS116	IHS_LAG_142V	MTN-AIRTEL-VISAFONE	6, WILSON IJIEKHUAWEN STREET, OFF OBA AYOK	-108.89	-110.88	-109.67	NA
Lagos	Lagos	LS117	IHS_LAG_143V	MTN-VISAFONE	1/2 IBRAHIM KOSHEBINU STREET AKESAN LAGOS	-108.82	-110.63	-109.9	NA

Source: IHS Nigeria Plc 2013

B3: Received signal power measurement for Co-located network (Rainy season)

DAY 1

Table A3-1: BTS RECEIVED SIGNAL POWER MEASUREMENT

TOWN	STATE	VISA ID	HIS ID	OPERATORS	ADDRESS	CH1 RSSI (dBm)	CH2 RSSI (dBm)	CH3 RSSI (dBm)	CH4 RSSI (dBm)
Abuja	Abuja	ABJ001	IHS_ABJ_060V	MTN-EMTS-VISAFONE-AIRTEL	Cellcom sites Garki	-110.98	-110.97	NA	NA
Abuja	Abuja	ABJ004	IHS_ABJ_062V	VISAFONE-MTN	Cellcom sites Kubwa	-110.67	-111	-109.72	NA
Abuja	Abuja	ABJ031	IHS_ABJ_066V	VISAFONE	PRPOPERTY NEAR POTTERY COTTAGE INDUSTRY,	-110.2	-110.1	-109.7	NA
Abuja	Abuja	ABJ033	IHS_ABJ_067V	AIRTEL-VISAFONE	GALADIMA HOUSE,NO.1,CHURCHROAD, OFF HAS	-110.88	-109.6	-110.64	NA
Abuja	Abuja	ABJ035	IHS_ABJ_068V	VISAFONE-EMTS	MAIALLA, CLOSE TO GLO & NITEL INSTALLATION,	-110.99	-110.34	-110.55	NA
Abuja	Abuja	ABJ037	IHS_ABJ_069V	AIRTEL-VISAFONE-MTN	PLOT NO. E10, BWARI AREA COUNCIL, KUBWA EX	-110.2	-109.86	-108.98	NA
Abuja	Abuja	ABJ038	IHS_ABJ_070V	AIRTEL-VISAFONE	PLOT AT TUDUN WADA, MARABAN GURKU, KARU	-110.89	-110.82	-110.89	NA
Abuja	Abuja	ABJ040	IHS_ABJ_072V	AIRTEL-VISAFONE	PLOT, NO. 401,JIKOYI,OFF ASO ESTATE ROAD, OF	-110.92	-111.05	-111.2	NA
Enugu	Enugu	ENU005	IHS_ENG_007	MTN-STARCOMMS-VISAFONE	Plot 5 peace Close Federal Housing Estate Trans	-110.67	-110.68	-110.75	NA
Kaduna	Kaduna	KAD018	IHS_KAD_026V	MTN-VISAFONE	No.1, Kargargo Str. Ugwan Kanawa,Kaduna.	-109.78	-110.6	-110.09	NA
Kaduna	Kaduna	KAD019	IHS_KAD_027V	MTN-EMTS-VISAFONE	10,Galadima Road,Badarawa,Kaduna.	-110.54	-110.52	-109.77	NA
Kaduna	Kaduna	KAD020	IHS_KAD_028V	AIRTEL-VISAFONE	Block DE 2,Nnamdi Azikwe Express Byepass, Kad	-110.88	-110.6	-109.83	NA
Kaduna	Kaduna	KAD027	IHS_KAD_033V	MTN-EMTS-VISAFONE	plot @ Apaka Village, Mando,Kaduna, Kaduna St	-110.81	-110.83	-109.74	NA
Lagos	Lagos	LS070	IHS_LAG_111V	MTN-VISAFONE-SWIFT	18, BENSTER CRESCENT, MAZA MAZA	-110.88	-110.47	-109.67	NA
Lagos	Lagos	LS078	IHS_LAG_115V	EMTS-VISAFONE-SWIFT	25/27, OLU ADEGBITE STREET, OFF OLADUN ROAD	-110.43	-110.72	-109.32	NA
Lagos	Lagos	LS116	IHS_LAG_142V	MTN-AIRTEL-VISAFONE	6, WILSON IJIEKHUAWEN STREET, OFF OBA AYOK	-106.9	-110.73	-109.47	NA
Lagos	Lagos	LS117	IHS_LAG_143V	MTN-VISAFONE	1/2 IBRAHIM KOSHEBINU STREET AKESAN LAGOS	-105.7	-106.3	-109.33	NA

Source: IHS Nigeria Plc 2013

DAY 2

Table A3-2: BTS RECEIVED SIGNAL POWER MEASUREMENT

TOWN	STATE	VISA ID	HIS ID	OPERATORS	ADDRESS	CH1 RSSI (dBm)	CH2 RSSI (dBm)	CH3 RSSI (dBm)	CH4 RSSI (dBm)
Abuja	Abuja	ABJ001	IHS_ABJ_060V	MTN-EMTS-VISAFONE-AIRTEL	Cellcom sites Garki	-109.77	-110.24	-110.46	NA
Abuja	Abuja	ABJ004	IHS_ABJ_062V	VISAFONE-MTN	Cellcom sites Kubwa	-109.98	-110.99	-110.44	NA
Abuja	Abuja	ABJ031	IHS_ABJ_066V	VISAFONE	PRPOPERTY NEAR POTTERY COTTAGE INDUSTRY,	-110.63	-110.1	-110.46	NA
Abuja	Abuja	ABJ033	IHS_ABJ_067V	AIRTEL-VISAFONE	GALADIMA HOUSE,NO.1,CHURCHROAD, OFF HAS	-110.47	-110.67	-110.83	NA
Abuja	Abuja	ABJ035	IHS_ABJ_068V	VISAFONE-EMTS	MAIALLA, CLOSE TO GLO & NITEL INSTALLATION,	-110.67	-110.68	-110.77	NA
Abuja	Abuja	ABJ037	IHS_ABJ_069V	AIRTEL-VISAFONE-MTN	PLOT NO. E10, BWARI AREA COUNCIL, KUBWA EX	-110.54	-110.99	-110.64	NA
Abuja	Abuja	ABJ038	IHS_ABJ_070V	AIRTEL-VISAFONE	PLOT AT TUDUN WADA, MARABAN GURKU, KARU	-110.88	-110.65	-110.88	NA
Abuja	Abuja	ABJ040	IHS_ABJ_072V	AIRTEL-VISAFONE	PLOT, NO. 401,JIKOYI,OFF ASO ESTATE ROAD, OF	-110.81	-110.78	-110.98	NA
Enugu	Enugu	ENU005	IHS_ENG_007	MTN-STARCOMMS-VISAFONE	Plot 5 peace Close Federal Housing Estate Trans	-110.76	-110.76	-109.7	NA
Kaduna	Kaduna	KAD018	IHS_KAD_026V	MTN-VISAFONE	No.1, Kargargo Str. Ugwan Kanawa,Kaduna.	-110.5	-110.6	-109.76	NA
Kaduna	Kaduna	KAD019	IHS_KAD_027V	MTN-EMTS-VISAFONE	10,Galadima Road,Badarawa,Kaduna.	-110.5	-109.98	-109.64	NA
Kaduna	Kaduna	KAD020	IHS_KAD_028V	AIRTEL-VISAFONE	Block DE 2,Nnamdi Azikwe Express Byepass, Kad	-110.52	-110.5	NA	NA
Kaduna	Kaduna	KAD027	IHS_KAD_033V	MTN-EMTS-VISAFONE	plot @ Apaka Village, Mando,Kaduna, Kaduna St	-110.6	-110.3	NA	NA
Lagos	Lagos	LS070	IHS_LAG_111V	MTN-VISAFONE-SWIFT	18, BENSTER CRESCENT, MAZA MAZA	-110.83	-110.9	-110.44	NA
Lagos	Lagos	LS078	IHS_LAG_115V	EMTS-VISAFONE-SWIFT	25/27, OLU ADEGBITE STREET, OFF OLADUN ROAD	-110.47	-110.2	-110.65	NA
Lagos	Lagos	LS116	IHS_LAG_142V	MTN-AIRTEL-VISAFONE	6, WILSON IJIEKHUAWEN STREET, OFF OBA AYOK	-110.72	-109.88	NA	NA
Lagos	Lagos	LS117	IHS_LAG_143V	MTN-VISAFONE	1/2 IBRAHIM KOSHEBINU STREET AKESAN LAGOS	-110.73	-109.96	NA	NA

Source: IHS Nigeria Plc 2013

DAY 3

Table A3-3: BTS RECEIVED SIGNAL POWER MEASUREMENT

TOWN	STATE	VISA ID	HIS ID	OPERATORS	ADDRESS	CH1 RSSI (dBm)	CH2 RSSI (dBm)	CH3 RSSI (dBm)	CH4 RSSI (dBm)
Abuja	Abuja	ABJ001	IHS_ABJ_060V	MTN-EMTS-VISAFONE-AIRTEL	Cellcom sites Garki	-110.66	-110.78	-111	NA
Abuja	Abuja	ABJ004	IHS_ABJ_062V	VISAFONE-MTN	Cellcom sites Kubwa	-110.66	-110.34	-110.48	NA
Abuja	Abuja	ABJ031	IHS_ABJ_066V	VISAFONE	PRPOPERTY NEAR POTTERY COTTAGE INDUSTRY,	-110.2	-110.1	-110.31	NA
Abuja	Abuja	ABJ033	IHS_ABJ_067V	AIRTEL-VISAFONE	GALADIMA HOUSE,NO.1,CHURCHROAD, OFF HAS	-110.01	-109.99	-109.8	NA
Abuja	Abuja	ABJ035	IHS_ABJ_068V	VISAFONE-EMTS	MAIALLA, CLOSE TO GLO & NITEL INSTALLATION,	111.02	-110.88	-110.92	NA
Abuja	Abuja	ABJ037	IHS_ABJ_069V	AIRTEL-VISAFONE-MTN	PLOT NO. E10, BWARI AREA COUNCIL, KUBWA EX	-110.62	-110.81	-110.8	NA
Abuja	Abuja	ABJ038	IHS_ABJ_070V	AIRTEL-VISAFONE	PLOT AT TUDUN WADA, MARABAN GURKU, KARU	-110.46	-110.44	-110.78	NA
Abuja	Abuja	ABJ040	IHS_ABJ_072V	AIRTEL-VISAFONE	PLOT, NO. 401,JIKOYI,OFF ASO ESTATE ROAD, OF	-110.83	-110.65	-110.92	NA
Enugu	Enugu	ENU005	IHS_ENG_007	MTN-STARCOMMS-VISAFONE	Plot 5 peace Close Federal Housing Estate Trans	-110.98	-110.8	-111.01	NA
Kaduna	Kaduna	KAD018	IHS_KAD_026V	MTN-VISAFONE	No.1, Kargargo Str. Ugwan Kanawa,Kaduna.	-110.47	-110.6	-111.09	NA
Kaduna	Kaduna	KAD019	IHS_KAD_027V	MTN-EMTS-VISAFONE	10,Galadima Road,Badarawa,Kaduna.	-110.67	-110.46	-110.45	NA
Kaduna	Kaduna	KAD020	IHS_KAD_028V	AIRTEL-VISAFONE	Block DE 2,Nnamdi Azikwe Express Byepass, Kad	-110.54	-110.83	-110.32	NA
Kaduna	Kaduna	KAD027	IHS_KAD_033V	MTN-EMTS-VISAFONE	plot @ Apaka Village, Mando,Kaduna, Kaduna St	-110.88	-110.77	NA	NA
Lagos	Lagos	LS070	IHS_LAG_111V	MTN-VISAFONE-SWIFT	18, BENSTER CRESCENT, MAZA MAZA	-110.81	-110.64	-110.88	NA
Lagos	Lagos	LS078	IHS_LAG_115V	EMTS-VISAFONE-SWIFT	25/27, OLU ADEGBITE STREET, OFF OLADUN ROAD	-104.3	-110.88	-110.81	NA
Lagos	Lagos	LS116	IHS_LAG_142V	MTN-AIRTEL-VISAFONE	6, WILSON IJIEKHUAWEN STREET, OFF OBA AYOK	-106.9	-110.98	-110.88	NA
Lagos	Lagos	LS117	IHS_LAG_143V	MTN-VISAFONE	1/2 IBRAHIM KOSHEBINU STREET AKESAN LAGOS	-105.7	-109.7	-110.43	NA

Source: IHS Nigeria Plc 2013

DAY 4

Table A3-4: BTS RECEIVED SIGNAL POWER MEASUREMENT

TOWN	STATE	VISA ID	HIS ID	OPERATORS	ADDRESS	CH1 RSSI (dBm)	CH2 RSSI (dBm)	CH3 RSSI (dBm)	CH4 RSSI (dBm)
Abuja	Abuja	ABJ001	IHS_ABJ_060V	MTN-EMTS-VISAFONE-AIRTEL	Cellcom sites Garki	-109.88	-110.77	NA	NA
Abuja	Abuja	ABJ004	IHS_ABJ_062V	VISAFONE-MTN	Cellcom sites Kubwa	-109.37	-110.64	-110.3	NA
Abuja	Abuja	ABJ031	IHS_ABJ_066V	VISAFONE	PRPOPERTY NEAR POTTERY COTTAGE INDUSTRY,	-110.83	-110.1	-109.7	NA
Abuja	Abuja	ABJ033	IHS_ABJ_067V	AIRTEL-VISAFONE	GALADIMA HOUSE,NO.1,CHURCHROAD, OFF HAS	-110.77	-110.6	-100.8	NA
Abuja	Abuja	ABJ035	IHS_ABJ_068V	VISAFONE-EMTS	MAIALLA, CLOSE TO GLO & NITEL INSTALLATION,	-110.64	-110.78	-111.05	NA
Abuja	Abuja	ABJ037	IHS_ABJ_069V	AIRTEL-VISAFONE-MTN	PLOT NO. E10, BWARI AREA COUNCIL, KUBWA EX	-110.88	-110.98	-111.12	NA
Abuja	Abuja	ABJ038	IHS_ABJ_070V	AIRTEL-VISAFONE	PLOT AT TUDUN WADA, MARABAN GURKU, KARU	-110.98	-111.2	-109.87	NA
Abuja	Abuja	ABJ040	IHS_ABJ_072V	AIRTEL-VISAFONE	PLOT, NO. 401,JIKOYI,OFF ASO ESTATE ROAD, OF	-110.45	-110.76	-110.42	NA
Enugu	Enugu	ENU005	IHS_ENG_007	MTN-STARCOMMS-VISAFONE	Plot 5 peace Close Federal Housing Estate Trans	-110.69	-110.7	-110.8	NA
Kaduna	Kaduna	KAD018	IHS_KAD_026V	MTN-VISAFONE	No.1, Kargargo Str. Ugwan Kanawa,Kaduna.	-110.6	-110.6	-110.93	NA
Kaduna	Kaduna	KAD019	IHS_KAD_027V	MTN-EMTS-VISAFONE	10,Galadima Road,Badarawa,Kaduna.	-110.46	-110.44	-110.32	NA
Kaduna	Kaduna	KAD020	IHS_KAD_028V	AIRTEL-VISAFONE	Block DE 2,Nnamdi Azikwe Express Byepass, Kad	-110.54	-110.88	-110.67	NA
Kaduna	Kaduna	KAD027	IHS_KAD_033V	MTN-EMTS-VISAFONE	plot @ Apaka Village, Mando,Kaduna, Kaduna St	-110.82	-111	-110.99	NA
Lagos	Lagos	LS070	IHS_LAG_111V	MTN-VISAFONE-SWIFT	18, BENSTER CRESCENT, MAZA MAZA	-110.4	-110	-110.29	NA
Lagos	Lagos	LS078	IHS_LAG_115V	EMTS-VISAFONE-SWIFT	25/27, OLU ADEGBITE STREET, OFF OLADUN ROAD	-110.43	-110.43	-110.28	NA
Lagos	Lagos	LS116	IHS_LAG_142V	MTN-AIRTEL-VISAFONE	6, WILSON IJIEKHUAWEN STREET, OFF OBA AYOK	-110.33	-109.97	-109.77	NA
Lagos	Lagos	LS117	IHS_LAG_143V	MTN-VISAFONE	1/2 IBRAHIM KOSHEBINU STREET AKESAN LAGOS	-109.62	-110.83	-110.66	NA

Source: IHS Nigeria Plc 2013

DAY 5

Table A3-5: BTS RECEIVED SIGNAL POWER MEASUREMENT

TOWN	STATE	VISA ID	HIS ID	OPERATORS	ADDRESS	CH1 RSSI (dBm)	CH2 RSSI (dBm)	CH3 RSSI (dBm)	CH4 RSSI (dBm)
Abuja	Abuja	ABJ001	IHS_ABJ_060V	MTN-EMTS-VISAFONE-AIRTEL	Cellcom sites Garki	-110.63	-109.9	-109.9	NA
Abuja	Abuja	ABJ004	IHS_ABJ_062V	VISAFONE-MTN	Cellcom sites Kubwa	-110.47	-109.77	-110.23	NA
Abuja	Abuja	ABJ031	IHS_ABJ_066V	VISAFONE	PRPOPERTY NEAR POTTERY COTTAGE INDUSTRY,	-110.67	-109.83	-109.81	NA
Abuja	Abuja	ABJ033	IHS_ABJ_067V	AIRTEL-VISAFONE	GALADIMA HOUSE,NO.1,CHURCHROAD, OFF HAS	-109.6	-110.77	-109.54	NA
Abuja	Abuja	ABJ035	IHS_ABJ_068V	VISAFONE-EMTS	MAIALLA, CLOSE TO GLO & NITEL INSTALLATION,	-110.44	-110.64	-110.21	NA
Abuja	Abuja	ABJ037	IHS_ABJ_069V	AIRTEL-VISAFONE-MTN	PLOT NO. E10, BWARI AREA COUNCIL, KUBWA EX	-110.46	-110.88	-110.67	NA
Abuja	Abuja	ABJ038	IHS_ABJ_070V	AIRTEL-VISAFONE	PLOT AT TUDUN WADA, MARABAN GURKU, KARU	-110.44	-110.98	-110.98	NA
Abuja	Abuja	ABJ040	IHS_ABJ_072V	AIRTEL-VISAFONE	PLOT, NO. 401,JIKOYI,OFF ASO ESTATE ROAD, OF	-110.46	-110.6	-110.33	NA
Enugu	Enugu	ENU005	IHS_ENG_007	MTN-STARCOMMS-VISAFONE	Plot 5 peace Close Federal Housing Estate Trans	-110.77	-110.8	-110.68	NA
Kaduna	Kaduna	KAD018	IHS_KAD_026V	MTN-VISAFONE	No.1, Kargargo Str. Ugwan Kanawa,Kaduna.	-110.43	-110.33	-110.67	NA
Kaduna	Kaduna	KAD019	IHS_KAD_027V	MTN-EMTS-VISAFONE	10,Galadima Road,Badarawa,Kaduna.	-110.5	-110.49	-110.54	NA
Kaduna	Kaduna	KAD020	IHS_KAD_028V	AIRTEL-VISAFONE	Block DE 2,Nnamdi Azikwe Express Byepass, Kad	-110.47	-109.77	-110.88	NA
Kaduna	Kaduna	KAD027	IHS_KAD_033V	MTN-EMTS-VISAFONE	plot @ Apaka Village, Mando,Kaduna, Kaduna St	-110.67	-110.83	-110.81	NA
Lagos	Lagos	LS070	IHS_LAG_111V	MTN-VISAFONE-SWIFT	18, BENSTER CRESCENT, MAZA MAZA	-110.54	-109.74	-110.88	NA
Lagos	Lagos	LS078	IHS_LAG_115V	EMTS-VISAFONE-SWIFT	25/27, OLU ADEGBITE STREET, OFF OLADUN ROAD	-110.88	-109.67	-110.43	NA
Lagos	Lagos	LS116	IHS_LAG_142V	MTN-AIRTEL-VISAFONE	6, WILSON IJIEKHUAWEN STREET, OFF OBA AYOK	-110.81	-110.32	-110.47	NA
Lagos	Lagos	LS117	IHS_LAG_143V	MTN-VISAFONE	1/2 IBRAHIM KOSHEBINU STREET AKESAN LAGOS	-110.88	-110.47	-110.98	NA

Source: IHS Nigeria Plc 2013

A4: Effective radiated power measurement for Co-located network (dry season)

DAY 1

Table A4-1: BTS POWER MEASUREMENT

TOWN	STATE	VISA ID	HIS ID	OPERATORS	ADDRESS	CH1 Output (dBm)	CH2 Output (dBm)	CH3 Output (dBm)
Abuja	Abuja	ABJ001	IHS_ABJ_060V	MTN-EMTS-VISAFONE-AIRTEL	Cellcom sites Garki	39.2	40.1	42.8
Abuja	Abuja	ABJ004	IHS_ABJ_062V	VISAFONE-MTN	Cellcom sites Kubwa	36.5	38.8	38.2
Abuja	Abuja	ABJ031	IHS_ABJ_066V	VISAFONE	PRPOPERTY NEAR POTTERY COTTAGE INDUSTRY, KWALI, ABUJA	38.8	39	NA
Abuja	Abuja	ABJ033	IHS_ABJ_067V	AIRTEL-VISAFONE	GALADIMA HOUSE,NO.1,CHURCHROAD, OFF HASSAN DALHATTU ROAD, SULEJA	37.1	38.4	NA
Abuja	Abuja	ABJ035	IHS_ABJ_068V	VISAFONE-EMTS	MAIALLA,CLOSE TO GLO & NITEL INSTALLATION, MAIALLA, ABUJA.	36.1	39.1	37.1
Abuja	Abuja	ABJ037	IHS_ABJ_069V	AIRTEL-VISAFONE-MTN	PLOT NO. E10, BWARI AREA COUNCIL, KUBWA EXTENTION LAYOUT, KUBWA PHASE IV, ABUJA	38.5	36.4	NA
Abuja	Abuja	ABJ038	IHS_ABJ_070V	AIRTEL-VISAFONE	PLOT AT TUDUN WADA, MARABAN GURKU, KARU, KARU LGA, NASARAWA.	35	35	35
Abuja	Abuja	ABJ040	IHS_ABJ_072V	AIRTEL-VISAFONE	PLOT, NO. 401,JIKOYI,OFF ASO ESTATE ROAD, OFF KARISHI OZORO ROAD, JIKOYI LAYOUT, ABUJA.	37.6	39.1	39.1
Enugu	Enugu	ENU005	IHS_ENG_007	MTN-STARCOMMS-VISAFONE	Plot 5 peace Close Federal Housing Estate Trans Ekulu Enugu State	39.8	38.1	38.2
Kaduna	Kaduna	KAD018	IHS_KAD_026V	MTN-VISAFONE	No.1, Kargargo Str. Ugwan Kanawa,Kaduna.	38.5	38.5	NA
Kaduna	Kaduna	KAD019	IHS_KAD_027V	MTN-EMTS-VISAFONE	10,Galadima Road,Badarawa,Kaduna.	38.6	38.8	38.1
Kaduna	Kaduna	KAD020	IHS_KAD_028V	AIRTEL-VISAFONE	Block DE 2,Nnamdi Azikwe Express Byepass, Kaduna.	38.5	38.6	NA
Kaduna	Kaduna	KAD027	IHS_KAD_033V	MTN-EMTS-VISAFONE	plot @ Apaka Village, Mando,Kaduna, Kaduna State.	38.7	38.9	NA
Lagos	Lagos	LS070	IHS_LAG_111V	MTN-VISAFONE-SWIFT	18, BENSTER CRESCENT, MAZA MAZA	41.9	43.1	42.8
Lagos	Lagos	LS078	IHS_LAG_115V	EMTS-VISAFONE-SWIFT	25/27, OLU ADEGBITE STREET, OFF OLADUN ROAD, ISHERI	37.9	39.8	NA
Lagos	Lagos	LS116	IHS_LAG_142V	MTN-AIRTEL-VISAFONE	6, WILSON IJIEKHUAWEN STREET, OFF OBA AYOKA ROAD, IBA TOWN	38.1	38.1	NA
Lagos	Lagos	LS117	IHS_LAG_143V	MTN-VISAFONE	1/2 IBRAHIM KOSHEBINU STREET AKESAN LAGOS	38.8	40.1	40.1

Source: IHS Nigeria Plc 2013

DAY 2

Table A4-2: BTS POWER MEASUREMENT

TOWN	STATE	VISA ID	HIS ID	OPERATORS	ADDRESS	CH1 Output (dBm)	CH2 Output (dBm)	CH3 Output (dBm)
Abuja	Abuja	ABJ001	IHS_ABJ_060V	MTN-EMTS-VISAFONE-AIRTEL	Cellcom sites Garki	38.4	40.1	42.8
Abuja	Abuja	ABJ004	IHS_ABJ_062V	VISAFONE-MTN	Cellcom sites Kubwa	38.4	38.8	NA
Abuja	Abuja	ABJ031	IHS_ABJ_066V	VISAFONE	PRPOPERTY NEAR POTTERY COTTAGE INDUSTRY, KWALI, ABUJA	38.6	39	40.1
Abuja	Abuja	ABJ033	IHS_ABJ_067V	AIRTEL-VISAFONE	GALADIMA HOUSE,NO.1,CHURCHROAD, OFF HASSAN DALHATTU ROAD, SULEJA	39.1	38.4	41.9
Abuja	Abuja	ABJ035	IHS_ABJ_068V	VISAFONE-EMTS	MAIALLA,CLOSE TO GLO & NITEL INSTALLATION, MAIALLA, ABUJA.	37.9	37.1	38.7
Abuja	Abuja	ABJ037	IHS_ABJ_069V	AIRTEL-VISAFONE-MTN	PLOT NO. E10, BWARI AREA COUNCIL, KUBWA EXTENTION LAYOUT, KUBWA PHASE IV, ABUJA	38.9	39.5	38.5
Abuja	Abuja	ABJ038	IHS_ABJ_070V	AIRTEL-VISAFONE	PLOT AT TUDUN WADA, MARABAN GURKU, KARU, KARU LGA, NASARAWA.	38.6	35	38.5
Abuja	Abuja	ABJ040	IHS_ABJ_072V	AIRTEL-VISAFONE	PLOT, NO. 401,JIKOYI,OFF ASO ESTATE ROAD, OFF KARISHI OZORO ROAD, JIKOYI LAYOUT, ABUJA.	38.7	39.1	39.1
Enugu	Enugu	ENU005	IHS_ENG_007	MTN-STARCOMMS-VISAFONE	Plot 5 peace Close Federal Housing Estate Trans Ekulu Enugu State	38.6	38	38.2
Kaduna	Kaduna	KAD018	IHS_KAD_026V	MTN-VISAFONE	No.1, Kargargo Str. Ugwan Kanawa,Kaduna.	39.8	38.5	38.2
Kaduna	Kaduna	KAD019	IHS_KAD_027V	MTN-EMTS-VISAFONE	10,Galadima Road,Badarawa,Kaduna.	40.1	38.8	38.2
Kaduna	Kaduna	KAD020	IHS_KAD_028V	AIRTEL-VISAFONE	Block DE 2,Nnamdi Azikwe Express Byepass, Kaduna.	NA	38.6	37.3
Kaduna	Kaduna	KAD027	IHS_KAD_033V	MTN-EMTS-VISAFONE	plot @ Apaka Village, Mando,Kaduna, Kaduna State.	41.6	38.9	38.6
Lagos	Lagos	LS070	IHS_LAG_111V	MTN-VISAFONE-SWIFT	18, BENSTER CRESCENT, MAZA MAZA	38	43.1	NA
Lagos	Lagos	LS078	IHS_LAG_115V	EMTS-VISAFONE-SWIFT	25/27, OLU ADEGBITE STREET, OFF OLADUN ROAD, ISHERI	38.1	39.8	38.4
Lagos	Lagos	LS116	IHS_LAG_142V	MTN-AIRTEL-VISAFONE	6, WILSON IJIEKHUAWEN STREET, OFF OBA AYOKA ROAD, IBA TOWN	36.5	38.1	38.6
Lagos	Lagos	LS117	IHS_LAG_143V	MTN-VISAFONE	1/2 IBRAHIM KOSHEBINU STREET AKESAN LAGOS	38.1	NA	39.1

Source: IHS Nigeria Plc 2013

DAY 3

Table A4-3: BTS POWER MEASUREMENT

TOWN	STATE	VISA ID	HIS ID	OPERATORS	ADDRESS	CH1 Output (dBm)	CH2 Output (dBm)	CH3 Output (dBm)
Abuja	Abuja	ABJ001	IHS_ABJ_060V	MTN-EMTS-VISAFONE-AIRTEL	Cellcom sites Garki	40	39.3	42.8
Abuja	Abuja	ABJ004	IHS_ABJ_062V	VISAFONE-MTN	Cellcom sites Kubwa	38.9	40.5	38.2
Abuja	Abuja	ABJ031	IHS_ABJ_066V	VISAFONE	PRPOPERTY NEAR POTTERY COTTAGE INDUSTRY, KWALI, ABUJA	40	38.9	NA
Abuja	Abuja	ABJ033	IHS_ABJ_067V	AIRTEL-VISAFONE	GALADIMA HOUSE,NO.1,CHURCHROAD, OFF HASSAN DALHATTU ROAD, SULEJA	39.2	38.9	38.6
Abuja	Abuja	ABJ035	IHS_ABJ_068V	VISAFONE-EMTS	MAIALLA,CLOSE TO GLO & NITEL INSTALLATION, MAIALLA, ABUJA.	39	38.3	37.1
Abuja	Abuja	ABJ037	IHS_ABJ_069V	AIRTEL-VISAFONE-MTN	PLOT NO. E10, BWARI AREA COUNCIL, KUBWA EXTENTION LAYOUT, KUBWA PHASE IV, ABUJA	38.5	40.9	NA
Abuja	Abuja	ABJ038	IHS_ABJ_070V	AIRTEL-VISAFONE	PLOT AT TUDUN WADA, MARABAN GURKU, KARU, KARU LGA, NASARAWA.	35	36.2	35
Abuja	Abuja	ABJ040	IHS_ABJ_072V	AIRTEL-VISAFONE	PLOT, NO. 401,JIKOYI,OFF ASO ESTATE ROAD, OFF KARISHI OZORO ROAD, JIKOYI LAYOUT, ABUJA.	38.7	41.1	39.1
Enugu	Enugu	ENU005	IHS_ENG_007	MTN-STARCOMMS-VISAFONE	Plot 5 peace Close Federal Housing Estate Trans Ekulu Enugu State	38.9	38	38.2
Kaduna	Kaduna	KAD018	IHS_KAD_026V	MTN-VISAFONE	No.1, Kargargo Str. Ugwan Kanawa,Kaduna.	39.6	40.4	38.6
Kaduna	Kaduna	KAD019	IHS_KAD_027V	MTN-EMTS-VISAFONE	10,Galadima Road,Badarawa,Kaduna.	38.6	39.9	39
Kaduna	Kaduna	KAD020	IHS_KAD_028V	AIRTEL-VISAFONE	Block DE 2,Nnamdi Azikwe Express Byepass, Kaduna.	38.4	40.9	37.9
Kaduna	Kaduna	KAD027	IHS_KAD_033V	MTN-EMTS-VISAFONE	plot @ Apaka Village, Mando,Kaduna, Kaduna State.	40.1	37.1	30.8
Lagos	Lagos	LS070	IHS_LAG_111V	MTN-VISAFONE-SWIFT	18, BENSTER CRESCENT, MAZA MAZA	39.5	39.4	42.8
Lagos	Lagos	LS078	IHS_LAG_115V	EMTS-VISAFONE-SWIFT	25/27, OLU ADEGBITE STREET, OFF OLADUN ROAD, ISHERI	38.5	38.5	34.5
Lagos	Lagos	LS116	IHS_LAG_142V	MTN-AIRTEL-VISAFONE	6, WILSON IJIEKHUAWEN STREET, OFF OBA AYOKA ROAD, IBA TOWN	38.4	38.1	38.6
Lagos	Lagos	LS117	IHS_LAG_143V	MTN-VISAFONE	1/2 IBRAHIM KOSHEBINU STREET AKESAN LAGOS	38.8	40.1	NA

Source: IHS Nigeria Plc 2013

DAY 4

Table A4-4: BTS POWER MEASUREMENT

TOWN	STATE	VISA ID	HIS ID	OPERATORS	ADDRESS	CH1 Output (dBm)	CH2 Output (dBm)	CH3 Output (dBm)
Abuja	Abuja	ABJ001	IHS_ABJ_060V	MTN-EMTS-VISAFONE-AIRTEL	Cellcom sites Garki	39.2	40.1	42.8
Abuja	Abuja	ABJ004	IHS_ABJ_062V	VISAFONE-MTN	Cellcom sites Kubwa	36.5	38.8	38.2
Abuja	Abuja	ABJ031	IHS_ABJ_066V	VISAFONE	PRPOPERTY NEAR POTTERY COTTAGE INDUSTRY, KWALI, ABUJA	37.9	39	37.9
Abuja	Abuja	ABJ033	IHS_ABJ_067V	AIRTEL-VISAFONE	GALADIMA HOUSE,NO.1,CHURCHROAD, OFF HASSAN DALHATTU ROAD, SULEJA	38.9	38.4	NA
Abuja	Abuja	ABJ035	IHS_ABJ_068V	VISAFONE-EMTS	MAIALLA,CLOSE TO GLO & NITEL INSTALLATION, MAIALLA, ABUJA.	39.1	37.1	37.1
Abuja	Abuja	ABJ037	IHS_ABJ_069V	AIRTEL-VISAFONE-MTN	PLOT NO. E10, BWARI AREA COUNCIL, KUBWA EXTENTION LAYOUT, KUBWA PHASE IV, ABUJA	38.6	NA	NA
Abuja	Abuja	ABJ038	IHS_ABJ_070V	AIRTEL-VISAFONE	PLOT AT TUDUN WADA, MARABAN GURKU, KARU, KARU LGA, NASARAWA.	40.2	35	38.9
Abuja	Abuja	ABJ040	IHS_ABJ_072V	AIRTEL-VISAFONE	PLOT, NO. 401,JIKOYI,OFF ASO ESTATE ROAD, OFF KARISHI OZORO ROAD, JIKOYI LAYOUT, ABUJA.	39.5	39.1	39.1
Enugu	Enugu	ENU005	IHS_ENG_007	MTN-STARCOMMS-VISAFONE	Plot 5 peace Close Federal Housing Estate Trans Ekulu Enugu State	38.2	39.1	38.9
Kaduna	Kaduna	KAD018	IHS_KAD_026V	MTN-VISAFONE	No.1, Kargargo Str. Ugwan Kanawa,Kaduna.	37.7	38.5	NA
Kaduna	Kaduna	KAD019	IHS_KAD_027V	MTN-EMTS-VISAFONE	10,Galadima Road,Badarawa,Kaduna.	38	38.8	NA
Kaduna	Kaduna	KAD020	IHS_KAD_028V	AIRTEL-VISAFONE	Block DE 2,Nnamdi Azikwe Express Byepass, Kaduna.	38.1	38.6	39.2
Kaduna	Kaduna	KAD027	IHS_KAD_033V	MTN-EMTS-VISAFONE	plot @ Apaka Village, Mando,Kaduna, Kaduna State.	37.7	NA	39.2
Lagos	Lagos	LS070	IHS_LAG_111V	MTN-VISAFONE-SWIFT	18, BENSTER CRESCENT, MAZA MAZA	41.9	43.1	39.2
Lagos	Lagos	LS078	IHS_LAG_115V	EMTS-VISAFONE-SWIFT	25/27, OLU ADEGBITE STREET, OFF OLADUN ROAD, ISHERI	37.9	39.8	40.5
Lagos	Lagos	LS116	IHS_LAG_142V	MTN-AIRTEL-VISAFONE	6, WILSON IJIEKHUAWEN STREET, OFF OBA AYOKA ROAD, IBA TOWN	38.1	38.1	40.1
Lagos	Lagos	LS117	IHS_LAG_143V	MTN-VISAFONE	1/2 IBRAHIM KOSHEBINU STREET AKESAN LAGOS	38.8	40.1	NA

Source: IHS Nigeria Plc 2013

DAY 5 **Table A4-5: BTS POWER MEASUREMENT**

STATE	VISA ID	HIS ID	OPERATORS	ADDRESS	CH1 Output (dBm)	CH2 Output (dBm)	CH3 Output (dBm)
Abuja	ABJ001	IHS_ABJ_060V	MTN-EMTS-VISAFONE-AIRTEL	Cellcom sites Garki	38.5	40.1	42.8
Abuja	ABJ004	IHS_ABJ_062V	VISAFONE-MTN	Cellcom sites Kubwa	38.6	38.8	38.2
Abuja	ABJ031	IHS_ABJ_066V	VISAFONE	PRPOPERTY NEAR POTTERY COTTAGE INDUSTRY, KWALI, ABUJA	38.5	39	NA
Abuja	ABJ033	IHS_ABJ_067V	AIRTEL-VISAFONE	GALADIMA HOUSE,NO.1,CHURCHROAD, OFF HASSAN DALHATTU ROAD, SULEJA	38.7	38.4	38.8
Abuja	ABJ035	IHS_ABJ_068V	VISAFONE-EMTS	MAIALLA,CLOSE TO GLO & NITEL INSTALLATION, MAIALLA, ABUJA.	41.9	37.1	37.1
Abuja	ABJ037	IHS_ABJ_069V	AIRTEL-VISAFONE-MTN	PLOT NO. E10, BWARI AREA COUNCIL, KUBWA EXTENTION LAYOUT, KUBWA PHASE IV, ABUJA	37.9	37.6	NA
Abuja	ABJ038	IHS_ABJ_070V	AIRTEL-VISAFONE	PLOT AT TUDUN WADA, MARABAN GURKU, KARU, KARU LGA, NASARAWA.	38.1	35	35
Abuja	ABJ040	IHS_ABJ_072V	AIRTEL-VISAFONE	PLOT, NO. 401,JIKOYI,OFF ASO ESTATE ROAD, OFF KARISHI OZORO ROAD, JIKOYI LAYOUT, ABUJA.	38.8	39.1	39.1
Enugu	ENU005	IHS_ENG_007	MTN-STARCOMMS-VISAFONE	Plot 5 peace Close Federal Housing Estate Trans Ekulu Enugu State	39.2	38.7	38.5
Kaduna	KAD018	IHS_KAD_026V	MTN-VISAFONE	No.1, Kargargo Str. Ugwan Kanawa,Kaduna.	39.2	38.5	38.8
Kaduna	KAD019	IHS_KAD_027V	MTN-EMTS-VISAFONE	10,Galadima Road,Badarawa,Kaduna.	36.5	38.8	39
Kaduna	KAD020	IHS_KAD_028V	AIRTEL-VISAFONE	Block DE 2,Nnamdi Azikwe Express Byepass, Kaduna.	38.8	38.6	38.4
Kaduna	KAD027	IHS_KAD_033V	MTN-EMTS-VISAFONE	plot @ Apaka Village, Mando,Kaduna, Kaduna State.	37.1	38.9	37.1
Lagos	LS070	IHS_LAG_111V	MTN-VISAFONE-SWIFT	18, BENSTER CRESCENT, MAZA MAZA	36.1	43.1	42.8
Lagos	LS078	IHS_LAG_115V	EMTS-VISAFONE-SWIFT	25/27, OLU ADEGBITE STREET, OFF OLADUN ROAD, ISHERI	38.5	39.8	36.5
Lagos	LS116	IHS_LAG_142V	MTN-AIRTEL-VISAFONE	6, WILSON IJIEKHUAWEN STREET, OFF OBA AYOKA ROAD, IBA TOWN	35	38.1	38.8
Lagos	LS117	IHS_LAG_143V	MTN-VISAFONE	1/2 IBRAHIM KOSHEBINU STREET AKESAN LAGOS	38.8	40.1	37.1

Source: IHS Nigeria Plc 2013

A5: Effective radiated power measurement for Co-located network (rainy season)

DAY 1 **Table A5-1: BTS POWER MEASUREMENT**

TOWN	STATE	VISA ID	HIS ID	OPERATORS	ADDRESS	CH1 Output (dBm)	CH2 Output (dBm)	CH3 Output (dBm)
Abuja	Abuja	ABJ001	IHS_ABJ_060V	MTN-EMTS-VISAFONE-AIRTEL	Cellcom sites Garki	39.2	40.2	42.8
Abuja	Abuja	ABJ004	IHS_ABJ_062V	VISAFONE-MTN	Cellcom sites Kubwa	36.5	37.7	38.2
Abuja	Abuja	ABJ031	IHS_ABJ_066V	VISAFONE	PRPOPERTY NEAR POTTERY COTTAGE INDUSTRY, KWALI, ABUJA	38.8	38	NA
Abuja	Abuja	ABJ033	IHS_ABJ_067V	AIRTEL-VISAFONE	GALADIMA HOUSE,NO.1,CHURCHROAD, OFF HASSAN DALHATTU ROAD, SULEJA	37.1	38.1	NA
Abuja	Abuja	ABJ035	IHS_ABJ_068V	VISAFONE-EMTS	MAIALLA,CLOSE TO GLO & NITEL INSTALLATION, MAIALLA, ABUJA.	36.1	37.7	37.1
Abuja	Abuja	ABJ037	IHS_ABJ_069V	AIRTEL-VISAFONE-MTN	PLOT NO. E10, BWARI AREA COUNCIL, KUBWA EXTENTION LAYOUT, KUBWA PHASE IV, ABUJA	38.5	38	NA
Abuja	Abuja	ABJ038	IHS_ABJ_070V	AIRTEL-VISAFONE	PLOT AT TUDUN WADA, MARABAN GURKU, KARU, KARU LGA, NASARAWA.	35	38.5	35
Abuja	Abuja	ABJ040	IHS_ABJ_072V	AIRTEL-VISAFONE	PLOT, NO. 401,JIKOYI,OFF ASO ESTATE ROAD, OFF KARISHI OZORO ROAD, JIKOYI LAYOUT, ABUJA.	37.6	38.4	39.1
Enugu	Enugu	ENU005	IHS_ENG_007	MTN-STARCOMMS-VISAFONE	Plot 5 peace Close Federal Housing Estate Trans Ekulu Enugu State	39.7	38.6	38.2
Kaduna	Kaduna	KAD018	IHS_KAD_026V	MTN-VISAFONE	No.1, Kargargo Str. Ugwan Kanawa,Kaduna.	38.5	39.2	37.2
Kaduna	Kaduna	KAD019	IHS_KAD_027V	MTN-EMTS-VISAFONE	10,Galadima Road,Badarawa,Kaduna.	38.6	39.2	37.3
Kaduna	Kaduna	KAD020	IHS_KAD_028V	AIRTEL-VISAFONE	Block DE 2,Nnamdi Azikwe Express Byepass, Kaduna.	38.5	39.2	37.8
Kaduna	Kaduna	KAD027	IHS_KAD_033V	MTN-EMTS-VISAFONE	plot @ Apaka Village, Mando,Kaduna, Kaduna State.	38.7	39.2	40.1
Lagos	Lagos	LS070	IHS_LAG_111V	MTN-VISAFONE-SWIFT	18, BENSTER CRESCENT, MAZA MAZA	41.9	40.5	41.9
Lagos	Lagos	LS078	IHS_LAG_115V	EMTS-VISAFONE-SWIFT	25/27, OLU ADEGBITE STREET, OFF OLADUN ROAD, ISHERI	37.9	39.8	38.7
Lagos	Lagos	LS116	IHS_LAG_142V	MTN-AIRTEL-VISAFONE	6, WILSON IJIEKHUAWEN STREET, OFF OBA AYOKA ROAD, IBA TOWN	38.1	38.1	NA
Lagos	Lagos	LS117	IHS_LAG_143V	MTN-VISAFONE	1/2 IBRAHIM KOSHEBINU STREET AKESAN LAGOS	38.8	40.1	NA

Source: IHS Nigeria Plc 2013

DAY 2

Table A5-2: BTS POWER MEASUREMENT

TOWN	STATE	VISA ID	HIS ID	OPERATORS	ADDRESS	CH1 Output (dBm)	CH2 Output (dBm)	CH3 Output (dBm)
Abuja	Abuja	ABJ001	IHS_ABJ_060V	MTN-EMTS-VISAFONE-AIRTEL	Cellcom sites Garki	39.2	39.5	42.8
Abuja	Abuja	ABJ004	IHS_ABJ_062V	VISAFONE-MTN	Cellcom sites Kubwa	36.5	40.2	38.2
Abuja	Abuja	ABJ031	IHS_ABJ_066V	VISAFONE	PRPOPERTY NEAR POTTERY COTTAGE INDUSTRY, KWALI, ABUJA	38.8	37.7	NA
Abuja	Abuja	ABJ033	IHS_ABJ_067V	AIRTEL-VISAFONE	GALADIMA HOUSE,NO.1,CHURCHROAD, OFF HASSAN DALHATTU ROAD, SULEJA	37.1	38	NA
Abuja	Abuja	ABJ035	IHS_ABJ_068V	VISAFONE-EMTS	MAIALLA,CLOSE TO GLO & NITEL INSTALLATION, MAIALLA, ABUJA.	36.1	38.1	37.1
Abuja	Abuja	ABJ037	IHS_ABJ_069V	AIRTEL-VISAFONE-MTN	PLOT NO. E10, BWARI AREA COUNCIL, KUBWA EXTENTION LAYOUT, KUBWA PHASE IV, ABUJA	38.5	37.7	NA
Abuja	Abuja	ABJ038	IHS_ABJ_070V	AIRTEL-VISAFONE	PLOT AT TUDUN WADA, MARABAN GURKU, KARU, KARU LGA, NASARAWA.	35	35	35
Abuja	Abuja	ABJ040	IHS_ABJ_072V	AIRTEL-VISAFONE	PLOT, NO. 401,JIKOYI,OFF ASO ESTATE ROAD, OFF KARISHI OZORO ROAD, JIKOYI LAYOUT, ABUJA.	37.6	39.1	39.1
Enugu	Enugu	ENU005	IHS_ENG_007	MTN-STARCOMMS-VISAFONE	Plot 5 peace Close Federal Housing Estate Trans Ekulu Enugu State	38.1	39.2	38.4
Kaduna	Kaduna	KAD018	IHS_KAD_026V	MTN-VISAFONE	No.1, Kargargo Str. Ugwan Kanawa,Kaduna.	39.5	39.2	37.5
Kaduna	Kaduna	KAD019	IHS_KAD_027V	MTN-EMTS-VISAFONE	10,Galadima Road,Badarawa,Kaduna.	40.2	39.2	37.2
Kaduna	Kaduna	KAD020	IHS_KAD_028V	AIRTEL-VISAFONE	Block DE 2,Nnamdi Azikwe Express Byepass, Kaduna.	37.7	39.2	37.3
Kaduna	Kaduna	KAD027	IHS_KAD_033V	MTN-EMTS-VISAFONE	plot @ Apaka Village, Mando,Kaduna, Kaduna State.	38	39.2	37.8
Lagos	Lagos	LS070	IHS_LAG_111V	MTN-VISAFONE-SWIFT	18, BENSTER CRESCENT, MAZA MAZA	38.1	40.5	40.1
Lagos	Lagos	LS078	IHS_LAG_115V	EMTS-VISAFONE-SWIFT	25/27, OLU ADEGBITE STREET, OFF OLADUN ROAD, ISHERI	37.7	40.1	41.9
Lagos	Lagos	LS116	IHS_LAG_142V	MTN-AIRTEL-VISAFONE	6, WILSON IJIEKHUAWEN STREET, OFF OBA AYOKA ROAD, IBA TOWN	38	38.1	38.7
Lagos	Lagos	LS117	IHS_LAG_143V	MTN-VISAFONE	1/2 IBRAHIM KOSHEBINU STREET AKESAN LAGOS	38.5	40.1	38.5

Source: IHS Nigeria Plc 2013

DAY 3

Table A5-3: BTS POWER MEASUREMENT

TOWN	STATE	VISA ID	HIS ID	OPERATORS	ADDRESS	CH1 Output (dBm)	CH2 Output (dBm)	CH3 Output (dBm)
Abuja	Abuja	ABJ001	IHS_ABJ_060V	MTN-EMTS-VISAFONE-AIRTEL	Cellcom sites Garki	39.2	40.1	42.8
Abuja	Abuja	ABJ004	IHS_ABJ_062V	VISAFONE-MTN	Cellcom sites Kubwa	36.5	38.8	38.2
Abuja	Abuja	ABJ031	IHS_ABJ_066V	VISAFONE	PRPOPERTY NEAR POTTERY COTTAGE INDUSTRY, KWALI, ABUJA	38.8	39	37.6
Abuja	Abuja	ABJ033	IHS_ABJ_067V	AIRTEL-VISAFONE	GALADIMA HOUSE,NO.1,CHURCHROAD, OFF HASSAN DALHATTU ROAD, SULEJA	37.1	38.4	38
Abuja	Abuja	ABJ035	IHS_ABJ_068V	VISAFONE-EMTS	MAIALLA,CLOSE TO GLO & NITEL INSTALLATION, MAIALLA, ABUJA.	36.1	39.8	36.7
Abuja	Abuja	ABJ037	IHS_ABJ_069V	AIRTEL-VISAFONE-MTN	PLOT NO. E10, BWARI AREA COUNCIL, KUBWA EXTENTION LAYOUT, KUBWA PHASE IV, ABUJA	38.7	38.8	NA
Abuja	Abuja	ABJ038	IHS_ABJ_070V	AIRTEL-VISAFONE	PLOT AT TUDUN WADA, MARABAN GURKU, KARU, KARU LGA, NASARAWA.	38.2	35	35
Abuja	Abuja	ABJ040	IHS_ABJ_072V	AIRTEL-VISAFONE	PLOT, NO. 401,JIKOYI,OFF ASO ESTATE ROAD, OFF KARISHI OZORO ROAD, JIKOYI LAYOUT, ABUJA.	38.2	39.1	39.1
Enugu	Enugu	ENU005	IHS_ENG_007	MTN-STARCOMMS-VISAFONE	Plot 5 peace Close Federal Housing Estate Trans Ekulu Enugu State	38.3	38	38.6
Kaduna	Kaduna	KAD018	IHS_KAD_026V	MTN-VISAFONE	No.1, Kargargo Str. Ugwan Kanawa,Kaduna.	38.6	38.5	NA
Kaduna	Kaduna	KAD019	IHS_KAD_027V	MTN-EMTS-VISAFONE	10,Galadima Road,Badarawa,Kaduna.	38.4	38.8	NA
Kaduna	Kaduna	KAD020	IHS_KAD_028V	AIRTEL-VISAFONE	Block DE 2,Nnamdi Azikwe Express Byepass, Kaduna.	38.4	38.6	38.9
Kaduna	Kaduna	KAD027	IHS_KAD_033V	MTN-EMTS-VISAFONE	plot @ Apaka Village, Mando,Kaduna, Kaduna State.	38.6	38.9	NA
Lagos	Lagos	LS070	IHS_LAG_111V	MTN-VISAFONE-SWIFT	18, BENSTER CRESCENT, MAZA MAZA	39.1	43.1	42.8
Lagos	Lagos	LS078	IHS_LAG_115V	EMTS-VISAFONE-SWIFT	25/27, OLU ADEGBITE STREET, OFF OLADUN ROAD, ISHERI	37.9	39.8	37.8
Lagos	Lagos	LS116	IHS_LAG_142V	MTN-AIRTEL-VISAFONE	6, WILSON IJIEKHUAWEN STREET, OFF OBA AYOKA ROAD, IBA TOWN	38.9	38.1	NA
Lagos	Lagos	LS117	IHS_LAG_143V	MTN-VISAFONE	1/2 IBRAHIM KOSHEBINU STREET AKESAN LAGOS	38.8	40.1	37.9

Source: IHS Nigeria Plc 2013

DAY 4

Table A5-4: BTS POWER MEASUREMENT

TOWN	STATE	VISA ID	HIS ID	OPERATORS	ADDRESS	CH1 Output (dBm)	CH2 Output (dBm)	CH3 Output (dBm)
Abuja	Abuja	ABJ001	IHS_ABJ_060V	MTN-EMTS-VISAFONE-AIRTEL	Cellcom sites Garki	37.3	NA	37.2
Abuja	Abuja	ABJ004	IHS_ABJ_062V	VISAFONE-MTN	Cellcom sites Kubwa	38.6	38.8	37.3
Abuja	Abuja	ABJ031	IHS_ABJ_066V	VISAFONE	PRPOPERTY NEAR POTTERY COTTAGE INDUSTRY, KWALI, ABUJA	NA	39	37.8
Abuja	Abuja	ABJ033	IHS_ABJ_067V	AIRTEL-VISAFONE	GALADIMA HOUSE,NO.1,CHURCHROAD, OFF HASSAN DALHATTU ROAD, SULEJA	38.4	38.4	40.1
Abuja	Abuja	ABJ035	IHS_ABJ_068V	VISAFONE-EMTS	MAIALLA,CLOSE TO GLO & NITEL INSTALLATION, MAIALLA, ABUJA.	38.6	37.1	41.9
Abuja	Abuja	ABJ037	IHS_ABJ_069V	AIRTEL-VISAFONE-MTN	PLOT NO. E10, BWARI AREA COUNCIL, KUBWA EXTENTION LAYOUT, KUBWA PHASE IV, ABUJA	39.1	NA	38.7
Abuja	Abuja	ABJ038	IHS_ABJ_070V	AIRTEL-VISAFONE	PLOT AT TUDUN WADA, MARABAN GURKU, KARU, KARU LGA, NASARAWA.	37.9	35	38.5
Abuja	Abuja	ABJ040	IHS_ABJ_072V	AIRTEL-VISAFONE	PLOT, NO. 401,JIKOYI,OFF ASO ESTATE ROAD, OFF KARISHI OZORO ROAD, JIKOYI LAYOUT, ABUJA.	38.9	39.1	38.5
Enugu	Enugu	ENU005	IHS_ENG_007	MTN-STARCOMMS-VISAFONE	Plot 5 peace Close Federal Housing Estate Trans Ekulu Enugu State	38.8	38.6	38.2
Kaduna	Kaduna	KAD018	IHS_KAD_026V	MTN-VISAFONE	No.1, Kargargo Str. Ugwan Kanawa,Kaduna.	38.7	38.5	38.2
Kaduna	Kaduna	KAD019	IHS_KAD_027V	MTN-EMTS-VISAFONE	10,Galadima Road,Badarawa,Kaduna.	38.1	38.8	38.2
Kaduna	Kaduna	KAD020	IHS_KAD_028V	AIRTEL-VISAFONE	Block DE 2,Nnamdi Azikwe Express Byepass, Kaduna.	39.8	38.6	37.3
Kaduna	Kaduna	KAD027	IHS_KAD_033V	MTN-EMTS-VISAFONE	plot @ Apaka Village, Mando,Kaduna, Kaduna State.	40.1	38.9	38.6
Lagos	Lagos	LS070	IHS_LAG_111V	MTN-VISAFONE-SWIFT	18, BENSTER CRESCENT, MAZA MAZA	39.8	NA	38.4
Lagos	Lagos	LS078	IHS_LAG_115V	EMTS-VISAFONE-SWIFT	25/27, OLU ADEGBITE STREET, OFF OLADUN ROAD, ISHERI	41.6	39.8	38.4
Lagos	Lagos	LS116	IHS_LAG_142V	MTN-AIRTEL-VISAFONE	6, WILSON IJIEKHUAWEN STREET, OFF OBA AYOKA ROAD, IBA TOWN	38	38.1	38.6
Lagos	Lagos	LS117	IHS_LAG_143V	MTN-VISAFONE	1/2 IBRAHIM KOSHEBINU STREET AKESAN LAGOS	38.1	40.1	39.1

Source: IHS Nigeria Plc 2013

DAY 5

Table A5-5: BTS POWER MEASUREMENT

TOWN	STATE	VISA ID	HIS ID	OPERATORS	ADDRESS	CH1 Output (dBm)	CH2 Output (dBm)	CH3 Output (dBm)
Abuja	Abuja	ABJ001	IHS_ABJ_060V	MTN-EMTS-VISAFONE-AIRTEL	Cellcom sites Garki	39.2	40.1	42.8
Abuja	Abuja	ABJ004	IHS_ABJ_062V	VISAFONE-MTN	Cellcom sites Kubwa	36.5	38.8	38.2
Abuja	Abuja	ABJ031	IHS_ABJ_066V	VISAFONE	PRPOPERTY NEAR POTTERY COTTAGE INDUSTRY, KWALI, ABUJA	38.8	39	39.8
Abuja	Abuja	ABJ033	IHS_ABJ_067V	AIRTEL-VISAFONE	GALADIMA HOUSE,NO.1,CHURCHROAD, OFF HASSAN DALHATTU ROAD, SULEJA	37.1	38.4	NA
Abuja	Abuja	ABJ035	IHS_ABJ_068V	VISAFONE-EMTS	MAIALLA,CLOSE TO GLO & NITEL INSTALLATION, MAIALLA, ABUJA.	36.1	40.1	38.9
Abuja	Abuja	ABJ037	IHS_ABJ_069V	AIRTEL-VISAFONE-MTN	PLOT NO. E10, BWARI AREA COUNCIL, KUBWA EXTENTION LAYOUT, KUBWA PHASE IV, ABUJA	38.5	40.1	NA
Abuja	Abuja	ABJ038	IHS_ABJ_070V	AIRTEL-VISAFONE	PLOT AT TUDUN WADA, MARABAN GURKU, KARU, KARU LGA, NASARAWA.	37.2	35	35
Abuja	Abuja	ABJ040	IHS_ABJ_072V	AIRTEL-VISAFONE	PLOT, NO. 401,JIKOYI,OFF ASO ESTATE ROAD, OFF KARISHI OZORO ROAD, JIKOYI LAYOUT, ABUJA.	37.3	39.1	39.1
Enugu	Enugu	ENU005	IHS_ENG_007	MTN-STARCOMMS-VISAFONE	Plot 5 peace Close Federal Housing Estate Trans Ekulu Enugu State	38.1	38.7	39.9
Kaduna	Kaduna	KAD018	IHS_KAD_026V	MTN-VISAFONE	No.1, Kargargo Str. Ugwan Kanawa,Kaduna.	40.1	38.5	NA
Kaduna	Kaduna	KAD019	IHS_KAD_027V	MTN-EMTS-VISAFONE	10,Galadima Road,Badarawa,Kaduna.	41.9	38.8	38.8
Kaduna	Kaduna	KAD020	IHS_KAD_028V	AIRTEL-VISAFONE	Block DE 2,Nnamdi Azikwe Express Byepass, Kaduna.	38.7	38.6	37.1
Kaduna	Kaduna	KAD027	IHS_KAD_033V	MTN-EMTS-VISAFONE	plot @ Apaka Village, Mando,Kaduna, Kaduna State.	38.5	38.9	36.1
Lagos	Lagos	LS070	IHS_LAG_111V	MTN-VISAFONE-SWIFT	18, BENSTER CRESCENT, MAZA MAZA	38.5	43.1	42.8
Lagos	Lagos	LS078	IHS_LAG_115V	EMTS-VISAFONE-SWIFT	25/27, OLU ADEGBITE STREET, OFF OLADUN ROAD, ISHERI	38.7	39.8	NA
Lagos	Lagos	LS116	IHS_LAG_142V	MTN-AIRTEL-VISAFONE	6, WILSON IJIEKHUAWEN STREET, OFF OBA AYOKA ROAD, IBA TOWN	38.2	38.1	38.6
Lagos	Lagos	LS117	IHS_LAG_143V	MTN-VISAFONE	1/2 IBRAHIM KOSHEBINU STREET AKESAN LAGOS	38.2	40.1	NA

Source: IHS Nigeria Plc 2013

APPENDIX B

Computation Procedure for Unco-located and Co-located Networks

- **For Unco-located Network**

Thermal noise power is given as KT_0B in Watts,

Where;

k is the Boltzmann's constant given as $1.38x10^{-23}\ J/k$

T_0 is the absolute temperature in Kelvin, i.e. $T_0 = K = 273 + {}^0C = 290k$ where ${}^0C$ is given as $16.85^0C \approx 17^0C$,which is the ambient temperature for Noise Figure (NF), B is the measurement or signal bandwidth. For WCDMA, the signal bandwidth is given as 3.84MHz.

Solving for KT_o

$$\therefore KT_0 = 1.38x10^{-23}x290 = 4.002x10^{-21}(W) \quad \text{(B-1)}$$

Converting power in Watt to dBm, equation (C-2) is applied

$$P(dBm) = 10\log\left\{\frac{P(W)}{1W}\right\} + 30dB = \quad \text{(B-2)}$$

$$P(dBm) = 10\log\left\{4.002x10^{-21})\right\} + 30dB = -173.97 \approx -174dBm$$

Therefore Thermal Noise power for WCDMA in dBm is calculated as;

$$P_N = kT_0B = -174dBm + 10\log\left(3.84x10^6\right)dB = -108dBm \quad \text{(B-3)}$$

To evaluate the noise figure using the Minimum detectable signal given by protocol as -102dBm for WCDMA network. The mathematical model is given as:

$$NF(dB) = MDS(dBm) - (-174(dBm) - 10\log B(dB) \quad \text{(B-.4)}$$

where B is the channel bandwidth for the WCDMA given as 5MHz .

$$\therefore NF(dB) = -102(dBm) - (-174(dBm) - 10\log 5x10^6(dB) = 5.02 \approx 5dB$$

The noise floor of the standalone WCDMA is given as :

$$N_{floor} = 10^{\frac{KT_0B + NF}{10}} mw$$

$$N_{floor} = KT_0B + NF(dBm) = -103dBm \quad \text{(B-5)}$$

To compute the Minimum Demodulation Carrier to Interference $\left(\frac{C}{I}\right)_m$ ratio, is given as;

$$\left(\frac{C}{I}\right)_m = s_{0u} - N_{floor} \quad \text{(B-6)}$$

Where S_{0u} is the average received signal power for the unco-located WCDMA network

$$\therefore \left(\frac{C}{I}\right)_m = -6.69$$

- **For Co-located Network**

The average measured received signal power for the standalone WCDMA was obtained as $-109.69dBm$ and the average measured received signal power for the co-located WCDMA network was obtained as $-110.70dBm$. The received signal strength degradation (η) is evaluated as: $-109.69-(-110.70)=1.01dBm$, $\therefore \eta = 1.01dBm$

To calculate the Total Noise Floor (N_{FT}) level when interfered is obtained as;

$$N_{FT} = N_{floor} + \eta = 10^{\frac{KT_0B + NF}{10}} 10^{\frac{\eta}{10}} mw \quad \text{(B-7)}$$

$$\therefore N_{FT}(dBm) = (N_{floor} + \eta)dBm = KT_0B + NF + \eta(dBm) = -101.99$$

The interfering power at the receiver input denoted as (γ) is obtained as

$$\gamma = 10\log_{10}\left\{10^{\frac{KTB + NF + \eta}{10}} \text{ or } -10^{\frac{KTB + NF}{10}}\right\}dBm$$

$$\gamma = (KT_0B + NF) + 10\log_{10}\left\{10^{\frac{\eta}{10}} - 1\right\}dBm = -103 + 10\log\left\{10^{\frac{1.01}{10}} - 1\right\} = -108.8dBm \quad \text{(C-8)}$$

The Minimum Demodulation Carrier to Interference $\left(\frac{C}{I}\right)_m$ ratio, in the presence of the interference is obtained as;

$$S_{0c} = (N_{floor} + \eta) + \left(\frac{C}{I}\right) \quad \text{(B-9)}$$

$$\therefore \left(\frac{C}{I}\right)_m = -8.71$$

Where S_{0c} the average is received signal power for the co-located WCDMA network

Thus, the $\frac{C}{I}$ degradation is obtained as: $= 2.02dB$

Therefore percentage reduction is obtained as:

$$\frac{2.02}{6.69} x100\% = 30.19\% \approx 30\%$$

APPENDIX C

GENERATED VALUES AND MATLAB CODES

C1: Rise in Noise Floor level vs Recieved signal strength degradation

```
RiseinNoisefloor = [
0.01 0.10 0.19 0.28 0.37 0.46 0.55 0.64 0.73 0.82 0.91 1.00 1.01 1.09 1.18
1.27 1.36 1.45 1.54 1.63 1.72 1.81 1.90 1.99 2.08 2.17 2.26 2.35 2.44 2.53
2.62 2.71 2.80 2.89 2.98 3.003.07
];

recieversensitivitydegradation = [
0.01 0.10 0.19 0.28 0.37 0.46 0.55 0.64 0.73 0.82 0.91 1.00 1.01 1.09 1.18
1.27 1.36 1.45 1.54 1.63 1.72 1.81 1.90 1.99 2.08 2.17 2.26 2.35 2.44 2.53
2.62 2.71 2.80 2.89 2.98 3.00 3.07
];

plot(riseinNoisefloor,recieversensitivitydegradation,'-sr')
xlabel('Rise in Noise Level after the system is interfered (dBm)')
ylabel('Recieved signal strength degradation (dB)')
```

C2: Interfering Power level Vs Recieved signal strength degradation

```
InterferingPower = [
-129.37 -119.32 -116.39 -114.7  -113.50 -112.52  -111.70 -110.99 -110.40
-109.8    -109.32 -108.87 -108.80 -108.45 -108.06 -107.69 -107.34 -107.02
-106.70 -106.40 -106.13 -105.86 -105.61 -105.36 -105.12 -104.88 -104.66
-104.44 -104.23 -104.02  -103.82 -103.62 -103.43 -103.24 -103.10 -103.02
-102.88
  ];

receiversensitivitydegradation = [
 0.01 0.10 0.19 0.28 0.37 0.46 0.55 0.64 0.73 0.82 0.91 1.00 1.01 1.09 1.18
1.27 1.36 1.45 1.54 1.63 1.72 1.81 1.90 1.99 2.08 2.17 2.26 2.35 2.44 2.53
2.62 2.71 2.80 2.89 2.98 3.00 3.07
 ];

plot(InterferingPower,degradation,'-sr')
xlabel('Interfering Power level (dBm)')
ylabel('Recieved signal strength degradation (dB)')
```

C3: Minimum Demodulation C/I Ratio Vs Received signal stength Degradation

```
minimumDemod = [
-6.71 -6.89 -7.07 -7.25 -7.43 -7.61 -7.79 -7.97 -8.15 -8.33 -8.51 -8.69 -8.70
-8.7 -8.96 -9.14 -9.32 -9.5 -9.68 -9.86 -10.04 -10.22 -10.4 -10.58 -10.76 -10.94
-11.12 -11.3 -11.48 -11.66 -11.84 -12.02 -12.2 -12.38 -12.56 -12.60 -12.74
 ];

receiversensitivitydegradation = [
0.01  0.10  0.19  0.28  0.37  0.46  0.55  0.64  0.73  0.82  0.91  1.00 1.01 1.09
1.18 1.2  1.36 1.45 1.54 1.63 1.72 1.81 1.90 1.99 2.08 2.17 2.26 2.35 2.44 2.53
2.62 2.71 2.8 2.89 2.98 3.00 3.07
];

plot(minimumDemod,degradation,'-sr')
xlabel('Minimum Demodulation C/I ratio')
ylabel('Recieved signal strength degradation (dB)')
```

C4: Percentage C/I Ratio Vs Recieved signal strength degradation

```
percentCIdegrad = [
0.3% 3% 6% 8.4% 11% 14% 16.4% 19% 22% 25% 27% 30%  31% 34% 37%
39% 42% 45% 47% 50% 53% 56% 58% 61% 64% 66% 69% 72% 74% 77%
80% 82% 85% 88% 88.3% 90%
];

recieversensitivitydegradation = [
0.01 0.10 0.19 0.28 0.37 0.46 0.55 0.64 0.73 0.82 0.91 1.00 1.01 1.09 1.18
1.27 1.36 1.45 1.54 1.63 1.72 1.81 1.90 1.99 2.08 2.17 2.26 2.35 2.44 2.53
2.62 2.71 2.80 2.89 2.98 3.00 3.07

];
plot(percentCIdegrad,degradation,'-sr')
xlabel('% C/I ratio degradation')
ylabel('Recieved signal strength degradation (dB)')
```

C5: Recieved signal strength degradation Vs Interfering Power and Rise in noise level

```
recieversensitivitydegradation = [
0.01  0.10  0.19  0.28  0.37  0.46  0.55  0.64 0.73 0.82 0.91 1.00 1.01 1.09 1.18
1.27 1.36 1.45 1.54  1.63  1.72  1.81  1.90  1.99  2.08  2.17 2.26 2.35 2.44 2.53
2.62  2.71  2.80  2.89 2.98  3.00 3.07
];

InterferingPower = [
-129.37 -119.32 -116.39 -114.76 -113.50 -112.52 -111.70 -110.9  -110.40
-109.82   -109.32 -108.87 -108.80 -108.45 -108.06 -107.69 -107.34 -107.02
-106.70 -106.40 -106.13 -105.86 -105.61 -105.36 -105.12 -104.88 -104.66
-104.44 -104.23 -104.02-103.82 -103.62 -103.43 -103.24 -103.10 -103.02
 -102.88
 ];

  riseinNoise = [
0.01 0.10 0.19 0.28 0.37 0.46 0.55 0.64 0.73 0.82 0.9 1.00 1.01 1.09 1.18 1.27
1.36  1.45  1.54  1.63  1.72  1.81  1.90  1.99  2.08  2.17  2.26  2.35  2.44  2.53  2.62
2.71 2.80 2.89 2.98 3.00 3.07
 ];

[AX, H1, H2] = plotyy(degradation,InterferingPower,...
    degradation,riseinNoise);
    %degradation,minimumDemod,%degradation,percentCIdegrad,...
grid on
set(get(AX(1),'Ylabel'),'String','Interfering Power(dBm)')
set(get(AX(2),'Ylabel'),'String','Rise in Noise floor(dBm)')
set(get(AX(1),'xlabel'),'String','Recieved signal strength degradation(dBm)')

set(H1,'linestyle','-','marker','s')
set(H2,'linestyle','-','marker','d')
```

C6: Rise in Noise floor level after the system is interfered Vs Interfering Power

```
riseinNoise = [
0.01  0.10  0.19  0.28  0.37  0.46  0.55  0.64  0.73 0.82 0.91 1.00 1.01  1.09
1.18  1.27  1.36  1.45  1.54  1.63 1.72 1.81 1.90 1.99 2.08 2.17 2.26 2.35 2.44
2.53 2.62 2.71 2.80 2.89 2.98 3.00 3.07
];
```

```
InterferingPower = [
-129.37 -119.32 -116.39 -114.76 -113.50 -112.52 -111.70 -110.99 -110.40
-109.82 -109.32 -108.87 -108.80 -108.45 -108.06 -107.69 -107.34 -107.02
 -106.70 -106.40 -106.13 -105.86 -105.61 -105.36 -105.12 -104.88 -104.66
-104.44 -104.23 -104.02 -103.82 -103.62 -103.43 -103.24 -103.10 -103.02
-102.88
 ];

plot(riseinNoise,InterferingPower,'-sr')
ylabel('Interfering Power level (dBm)')
xlabel('Rise in Noise Level after the system is interfered (dBm)')
```

C7: Interfering Power levels vs Minimum demodulation C/I ratio

```
InterferingPower = [
-129.37 -119.32 -116.39 -114.76 -113.50 -112.52 -111.70 -110.99 -110.40
-109.82 -109.32 -108.87 -108.80 -108.45 -108.06 -107.69 -107.34 -107.02
-106.70 -106.40 -106.13 -105.86 -105.61 -105.36 -105.12 -104.88 -104.66
-104.44 -104.23 -104.02 -103.82 -103.62 -103.43 -103.24 -103.10 -103.02
-102.88
 ];

minimumDemod = [
-6.71 -6.89 -7.07 -7.25 -7.43 -7.61 -7.79 -7.97 -8.15 -8.33  -8.51 -8.69 -8.70
-8.78  -8.96 -9.14 -9.32 -9.50 -9.68 -9.86 -10.04 -10.22 -10.4 -10.58 -10.76
-10.94 -11.12 -11.3 -11.48 -11.66 -11.84 -12.02 -12.2 -12.38 -12.56 -12.60
-12.74
 ];

plot(interfering power,Minimum demodulation,'-sr')
xlabel('Interfering Power level (dBm)')
ylabel('Minimum demodulationC/I ')
```

C8: Interfering Power Vs % C/I Ratio Degradation

```
InterferingPower = [
-129.37 -119.32 -116.39 -114.76 -113.50 -112.52 -111.70 -110.99 -110.40
-109.82   -109.32 -108.87 -108.80 -108.45 -108.06 -107.69 -107.34 -107.0
-106.70  -106.40 -106.13 -105.86 -105.61 -105.36 -105.12 -104.88 -104.66
-104.44 -104.23 -104.02 -103.82 -103.62 -103.43 -103.24 -103.10 -103.02
-102.88
  ];
```

```
percentCIdegrad = [
0.3% 3% 6% 8.4% 11% 14% 16.4% 19% 22% 25% 27% 30% 30% 31% 34%
37% 39% 42% 45% 47% 50% 53% 56% 58% 61% 64% 66% 69% 72% 74%
77% 80% 82% 85% 88% 88.3% 90%
];

plot(InterferingPower,percentCIdegrad,'-sr')
xlabel('interfering noise power (dBm)')
ylabel('% C/I ratio degradation')
```

C9: Decrease in interfering power level compared to the original noise level Vs Interfering Power

```
decreaseinInterfLevel = [
26.37  16.32  13.49 11.76  10.50  9.52  8.70 7.99  7.37  6.82  6.32  5.87 5.80
5.45  5.06  4.69  4.34  4.02  3.71  3.42  3.13  2.86  2.61  2.36  2.12 1.88 1.66
1.44 1.23 1.02 0.82 0.62 0.43 0.24 0.10 0.02 -0.12
];

InterferingPower = [
-129.37 -119.32 -116.39 -114.76 -113.50 -112.52 -111.70 -110.99 -110.40
-109.82  -109.32 -108.87 -108.80 -108.45 -108.06 -107.69 -107.34 -107.02
-106.70 -106.40 -106.13 -105.86 -105.61 -105.36 -105.12 -104.88 -104.66
-104.44 -104.23 -104.02 -103.82 -103.62 -103.43 -103.24 -103.10 -103.02
-102.88
 ];

plot(decreaseinInterfLevel,InterferingPower,'-sr')
xlabel('Decrease in interfering level compare to the original noise level (dB)')
ylabel('Interfering Power level (dBm)')
```

C10: Interfering Power Level Vs Minimum demodulation C/I Ratio and Decrease in interfering power level compared to the original noise level

```
InterferingPower = [
-129.37 -119.32 -116.39 -114.76 -113.50 -112.52 -111.70 -110.99 -110.40
-109.82 -109.32 -108.87 -108.80 -108.45 -108.06 -107.69 -107.34 -107.02
-106.70 -106.40 -106.13 -105.86 -105.61 -105.36 -105.12 -104.88 -104.66
-104.44 -104.23 -104.02 -103.82 -103.62 -103.43 -103.24 -103.10 -103.02
-102.88
  ];
```

```
minimumDemod = [
-6.71 -6.89 -7.07 -7.25 -7.43 -7.61 -7.79  -7.97 -8.15 -8.33 -8.51 -8.69 -8.70
-8.78 -8.96 -9.14 -9.32 -9.5 -9.68 -9.86 -10.04 -10.22 -10.4 -10.58 -10.76
-10.94 -11.12 -11.3 -11.48 -11.66 -11.84 -12.02 -12.2 -12.38 -12.56 -12.60
 -12.74
  ];

decreaseinInterfLevel = [
26.37  16.32 13.49  11.76  10.50  9.52  8.70 7.99 7.37 6.82 6.32 5.87 5.80 5.45
5.06 4.69 4.34 4.02 3.71 3.42 3.13 2.86 2.61 2.36 2.12 1.88 1.66 1.44 1.23
1.02 0.82 0.62 0.43 0.240.10 0.02 -0.12
];

[AX, H1, H2] = plotyy(InterferingPower,decreaseinInterfLevel,...
                    InterferingPower,minimumDemod);
    %degradation,minimumDemod,%degradation,percentCIdegrad,...
grid on
set(get(AX(1),'Ylabel'),'String','Decrease in interfering level compare to the
original noise level (dB)')
set(get(AX(2),'Ylabel'),'String','Minimum Demodulation C/I ratio')
set(get(AX(1),'xlabel'),'String','Interfering power level (dBm)')

set(H1,'linestyle','-','marker','s')
set(H2,'linestyle','-','marker','d')
```

C11: **<u>Rise in noise floor level after the system is interfered vs Minimum demodulation C/I Ratio</u>**

```
riseinNoise = [
0.01   0.10   0.19   0.28   0.37 0.46   0.55 0.64   0.73   0.82 0.91 1.00 1.01   1.09
1.18 1.27 1.36 1.45 1.54 1.63 1.72 1.81 1.90 1.99 2.08 2.17 2.26 2.35 2.44
2.53 2.62 2.712.80 2.89 2.98 3.00 3.07
];


minimumDemod = [
-6.71 -6.89 -7.07 -7.25 -7.43 -7.6  -7.79 -7.97 -8.15 -8.33 -8.51 -8.69 -8.70
-8.78   -8.96 -9.14 -9.32 -9.5 -9.68 -9.8 -10.04 -10.22  -10.4  -10.58 -10.76
-10.94 -11.12 -11.3 -11.48 -11.66 -11.8 -12.02 -12.2 -12.38 -12.56 -12.60
-12.74
 ];
```

C12: Magnitude response, phase response, Group delay response, Impulse and Pole/Zero plot for the BBPF design

```
% M-File generated by MATLAB(R) 7.5 and the Signal Processing Toolbox 6.8.
%
% Generated on: 19-Sep-2013 04:12:30
%

% Butterworth Bandpass filter designed using FDESIGN.BANDPASS.

% All frequency values are normalized to 1.

Fstop1 = 0.4912;      % First Stopband Frequency
Fpass1 = 0.4924;      % First Passband Frequency
Fpass2 = 0.5;         % Second Passband Frequency
Fstop2 = 0.5012;      % Second Stopband Frequency
Astop1 = 52;          % First Stopband Attenuation (dB)
Apass  = 0.1;         % Passband Ripple (dB)
Astop2 = 52;          % Second Stopband Attenuation (dB)
match  = 'passband';  % Band to match exactly

% Construct an FDESIGN object and call its BUTTER method.
h  = fdesign.bandpass(Fstop1, Fpass1, Fpass2, Fstop2, Astop1, Apass, ...
                      Astop2);
Hd = design(h, 'butter', 'MatchExactly', match);

% [EOF]

#Filter information
Discrete-Time IIR Filter (real)
-------------------------------
Filter Structure    : Direct-Form II, Second-Order Sections
Number of Sections  : 29
Stable              : Yes
Linear Phase        : No

Design Method Information
Design Algorithm : butter

Design Options
MatchExactly                : passband
SOSScaleNorm                : Linf
```

SOSScaleOpts.sosReorder : bandpass
SOSScaleOpts.MaxNumerator : 2
SOSScaleOpts.NumeratorConstraint : unit
SOSScaleOpts.OverflowMode : wrap
SOSScaleOpts.ScaleValueConstraint : none
SOSScaleOpts.MaxScaleValue : 1

Design Specifications
Sampling Frequency : N/A (normalized frequency)
Response : Bandpass
Specification : Fst1,Fp1,Fp2,Fst2,Ast1,Ap,Ast2
First Stopband Edge : 0.4912
First Passband Edge : 0.4924
Second Passband Edge : 0.5
Second Stopband Edge : 0.5012
First Stopband Atten. : 52 dB
Passband Ripple : 0.1 dB
Second Stopband Atten. : 52 dB

Measurements
Sampling Frequency : N/A (normalized frequency)
First Stopband Edge : 0.4912
First 6-dB Point : 0.49207
First 3-dB Point : 0.49215
First Passband Edge : 0.4924
Second Passband Edge : 0.5
Second 3-dB Point : 0.50025
Second 6-dB Point : 0.50033
Second Stopband Edge : 0.5012
First Stopband Atten. : 52.8191 dB
Passband Ripple : 0.1 dB
Second Stopband Atten. : 52.7992 dB
First Transition Width : 0.0012
Second Transition Width : 0.0012

Implementation Cost
Number of Multipliers : 88
Number of Adders : 87
Number of States : 58
MultPerInputSample : 88
AddPerInputSample : 87

C13: Function Block parameters for the BBPF design

Coefficients marked with positive symbol overflowed toward positive infinity while coefficients marked with negative symbol overflowed toward negative infinity. Coefficients marked with zero symbol under flowed to zero.

#Filter coefficient

Section #1

Numerator:
1
0
-1
Denominator:
1
-0.048253430904941053
0.99320954186801114
Gain:
0.0033956106518762954

Section #2

Numerator:
1
0
-1
Denominator:
1
0.00066825928899200832
0.99320755828789409
Gain:
0.024467344171416328

Section #3

Numerator:
1
0
-1
Denominator:
1
-0.042936375574382235

0.98364533582181179
Gain:
0.0083942742584337694

Section #4

Numerator:
1
0
-1
Denominator:
1
-0.0044231246038912431
0.98364157496117488
Gain:
0.022304200374437141

Section #5

Numerator:
1
0
-1
Denominator:
1
-0.034178457793863304
0.97714472695927002
Gain:
0.012557694779022794

Section #6

Numerator:
1
0
-1
Denominator:
1
-0.013028928682037394
0.97714184093594836
Gain:
0.018809886925653382

Section #7

Numerator:
 1
 0
-1
Denominator:
 1
-0.02357691289991698
 0.97484419455059035
Gain:
0.013959859717606412

Section #8

Numerator:
 1
 0
-1
Denominator:
 1
-0.028993043649925609
 0.97542607236850465
Gain:
0.012346774076670685

Section #9

Numerator:
 1
 0
-1
Denominator:
 1
-0.018174307447886284
 0.97542448510006075
Gain:
0.01282098674456815

Section #10

Numerator:
 1

0
-1
Denominator:
1
-0.038898224285684069
0.97992515414022963
Gain:
0.011712678131706534

Section #11

Numerator:
1
0
-1
Denominator:
1
-0.008374095860581493
0.97992149549375362
Gain:
0.013575859758269802

Section #12

Numerator:
1
0
-1
Denominator:
1
-0.04610513249318815
0.98814056971545139
Gain:
0.010542552083389648

Section #13

Numerator:
1
0
-1
Denominator:
1

-0.0013601597434932389
 0.98813740122997429
Gain:
0.015206864340102329

Section #14

Numerator:
 1
 0
-1
Denominator:
 1
-0.049274421792857404
 0.99862212643627568
Gain:
0.0033853790907577255

Section #15

Numerator:
 1
 0
-1
Denominator:
1
0.0015605636660074307
0.9986217081978469
Gain:
0.024895189739308713

Section #16

Numerator:
 1
 0
-1
Denominator:
 1
-0.047314632603032813
 0.99061714908280496
Gain:
0.004785885022468764

```
------------------------
Section #17
------------------------
Numerator:
 1
 0
-1
Denominator:
 1
-0.0002091526227674112
 0.99061450999990519
Gain:
0.024144455279940202
------------------------
Section #18
------------------------
Numerator:
 1
 0
-1
Denominator:
 1
-0.041015002757798458
 0.98167713179538529
Gain:
0.0098869788903386199
------------------------
Section #19
------------------------
Numerator:
 1
 0
-1
Denominator:
 1
-0.0062983316201869199
 0.98167333373398891
Gain:
0.022652519683290386
------------------------
Section #20
------------------------
Numerator:
```

1
0
-1
Denominator:
1
-0.031629606323991144
0.9761468495769382
Gain:
0.014437890481112981

Section #21

Numerator:
1
0
-1
Denominator:
1
-0.015554524582587048
0.97614456026462559
Gain:
0.020034675989301767

Section #22

Numerator:
1
0
-1
Denominator:
1
-0.026298655960504846
0.97499026789877685
Gain:
0.012997352181100735

Section #23

Numerator:
1
0
-1
Denominator:

1
-0.020858559627864814
0.97498945561473194
Gain:
0.012677324157751432

Section #24

Numerator:
1
0
-1
Denominator:
1
-0.036610600223644318
0.97840878546255705
Gain:
0.01189442872739415

Section #25

Numerator:
1
0
-1
Denominator:
1
-0.010626282698070338
0.97840543575098105
Gain:
0.013348209062319094

Section #26

Numerator:
1
0
-1
Denominator:
1
-0.044639824141550655
0.98580787835084971
Gain:

0.010951934141651343

Section #27

Numerator:
 1
 0
-1
Denominator:
 1
-0.0027705088397145111
 0.98580433035558979
Gain:
0.01460437043087129

Section #28

Numerator:
 1
 0
-1
Denominator:
 1
-0.048909612811667891
 0.99588814321768193
Gain:
0.0066553253920284021

Section #29

Numerator:
 1
 0
-1
Denominator:
1
0.0012608440023456624
0.99588691142689001
Gain:
0.02427607786194684

Output Gain:
0.99999999999626032

APPENDIX D

Codes for the ANCT (Perfect Cancellation)

***Part 1*: /*Define Co-location Environment for User*/**

Initialize:

/*Signal generator A*/ *sources* G_a= desired signal S (-109.69dBm).
/*Signal generator B*/ *sources* G_b= sideband noise X (-108.8dBm).

/ perfect _Cancellation = /
For I =*1* to *N+1;*
Check for valid signal sources G_a *and* $G_{b;}$
***If** Valid, **then** Check for Valid Generator sources* $G_{b;}$
If** Ok, **Then G_b*= Set Amplitude, Freq, Phase Offset;*
Signal_Converter = Set;
Initialize Power Splitter (S_emission);
***If** (S_emission (*X_a*)) = Set **Then** Noise_Sig = OutB;*

/X_A *and* X_B *is split in the ratio of 0.8:0.2 relative to distance with the power splitter to the primary and reference paths respectively. The gain-phase adjuster is realized with the use of a vector modulator and amplifier*/*

Pre-Attenuator (Regulator) = F(X_{pri}*&&*X_{ref}*): *X_{pri}*=0.8 &&* X_{ref}= 0.2 //
Call Regulator_Ref ();
S_emission(X_{ref}*) = Pre-Attenuator;*
Pre-Attenuator = input Port_1(X_{ref1}*;)*
Xref =output Port_1(X_{ref2}*);*
***Call** Coupler_B;*

*/*Using a -20dB coupler in coupler 2 to couple out the error sample from the cancellation output, also a -10dB is used for the cancellation coupler while -20dB coupler is also used to couple the input generated signal from the signal generator A and the splitter power signals from the signal generator B*/*

G_a *(*Desired) ➔ *Spri;*
Coupler_A:
Spri_Xpri ← Spri+ Xpri;
/ ***No Call*** *Delay (12Secs) */;*
Call *Xref;*
Return;

Define // variables for ANC DSP
Vector_mod, gain_Amp ➔ ANC DSP /* Use Vector Modulator ,gain Amplifier as the core of ANC DSP*/
Begin:
Input: *Ref.noise_I/P; Spri_Xpri; Opt_Adapt; Adapt_Fb_I/P; Rst_Enable;* /*Input Variables*/
Output*: Error_Out;Fitr_Sig; Wts* /*Output Variables*/
Conditions

***Part II*:** */* Set ANC iteration ID*/*

If *no signal sources G_a && G_b is present;* ***Then*** *Add a new count N;*
Specify its iteration ID;
Set signal sources G_a and G_b priority to zero;
Else
if *signal sources G_a && G_b already exists;****Then*** *replace the iteration ID with the specified value;*
*Call I****nput*** *();*
Call ***Procedure_ANC(perfect);***
Map ***Procedure_ANC(perfect);***
End
End

Part III: ***ANC DSP*** **Algorithm for Perfect Cancellation**

/ Adapts the filter weights based on the ANC algorithm for filtering of the input signals*/*
*/*Select the Adapt port check box to create an Adapt port on the block*/*
*/*When the input to this port is nonzero, the block continuously updates the filter weights*/*
*/*When the input to this port is zero, the filter weights remain constant*/*
/*If the Reset port is enabled and a reset event occurs, the block resets the filter weights to their initial values*/*
*Procedure_ANC(perfect): DSP_Controller : Public { **(Input)** 1:N}*
At above 70dB cancellation (perfect):
Begin:
{
Set
Normalization (ANC DSP)UiXi ==0
RateController ==0
/ Port Initialization/
Define Abitration Input {Ports}==0;
Vector_mod, gain_Amp,transferScheduled(True) { }
Define error_Signal (Err_Sig)
Addports(Weight_Varibports);
Signal_Process: ➔ perfect _Cancellation()

feedback error ε ← Cancellation_O/p;
Vector_mod ← Mod_adjustments;
ANC ➔ Cancellation residual power level{True}.
Display ➔ Output;
/*Next iteration*/*
/Tracks the perfect cancellation levels/
int uploadData() const { perfect_Canc_Address};
setUploadLimit(int dB Per Second)
upLimit ()

/*The original signal, the signal plus noise and the error cancellation levels captured at the spectrum analyzer*/*
/*Graph_1: original signal only, Graph_2: Signal+Noise level and Graph_3: error signal before cancellation*/;*

If *(Amplitude imbalance obtained = = 0 dB)* ***Then*** *DSP_Controller = = (True),* ***/***** perfect cancellation*/*
Elseif

```
        If (Phase error = = 0)  Then , DSP_Controller  = = (True), /*Perfect perfect */
      Elseif
            If (Delay mismatch = = 0), Then  DSP_Controller  = = (True), /* perfect
   cancellation*/.
        Elseif
          Return
      Call output ();    /*Display Signal_Process  */
     Display ←: Output
                        Assign Data bytes: ➔ signal analyzers (L);
          {
            Normalize(PortContention)
                  Signal(readyToTransfer()),
           DSP_Controller  ➔ setReadBufferSize(0);
         }
                  ScheduleTransfer(workspace);
       };
    If  (Sim_time i == N+1)
     {
               Connect(output.data (readyToTransfer());
              Complete Scheduled Transfert->setReadBufferSize();
            Output. buffer(port);
            ScheduleTransfer(workspace);
  }
     For (i =0;i++)
    Display ()

            End.
        End
    End
End
```

APPENDIX E

GENERATED MATLAB M-FILES FOR THE ANCT

E1 M-files for perfect time response

```
function createfigure(X1, YMatrix1, X2, Y1, Y2)
%CREATEFIGURE(X1,YMATRIX1,X2,Y1,Y2)
%  X1:  vector of x data
%  YMATRIX1:  matrix of y data
%  X2:  vector of x data
%  Y1:  vector of y data
%  Y2:  vector of y data

%  Auto-generated by MATLAB on 15-Sep-2014 06:19:38

% Create figure
figure1 = figure('Name','perfectcanceller/Spectrum_Analyzer');

% Create subplot
subplot1 = subplot(3,1,1,'Parent',figure1);
% Uncomment the following line to preserve the X-limits of the axes
% xlim([7.464 7.496]);
% Uncomment the following line to preserve the Y-limits of the axes
% ylim([-1.325e+005 -1.614e+004]);
box('on');
hold('all');

% Create multiple lines using matrix input to plot
plot1 = plot(X1,YMatrix1,'Parent',subplot1);
set(plot1(1),'Color',[1 0 1]);
set(plot1(2),'Color',[0 1 1]);

% Create title
title('Time history (1st: magenta; 2nd: cyan)');

% Create xlabel
xlabel('Time (secs)');

% Create subplot
subplot2 = subplot(3,1,2,'Parent',figure1);
% Uncomment the following line to preserve the X-limits of the axes
% xlim([0 2.513e+004]);
% Uncomment the following line to preserve the Y-limits of the axes
```

```
% ylim([0.9782 1]);
box('on');
hold('all');

% Create plot
plot(X2,Y1,'Parent',subplot2);

function createlegend(axes1)
%CREATELEGEND(AXES1)
%  AXES1:  legend axes

%  Auto-generated by MATLAB on 15-Sep-2014 06:35:51

% Create legend
legend1 = legend(axes1,'show');
set(legend1,'YColor',[1 1 1],'XColor',[1 1 1],...
    'Position',[0.1508 0.8287 0.3975 0.084]);
```

E2: **Cancellation Performance as a function of Amplitude Imbalance only**

```
% cancellation performance as a function of amplitude imbalance only

y = 0.01:0.01:5;    % amplitude imbalance
NCP = 10.*log10(1 + 10.^(0.1*y) - 2*10.^(0.05*y));   % cancellation
performance

%semilogx(y,NCP)
plot(y,NCP,'-dr','markersize',1.8)
grid on
%axis([0 5 -60 10])

xlabel('Amplitude Imbalance (dB)')
ylabel('Noise Cancellation Performance(dB)')
```

E3: **Cancellation Performance as a function of Phase error only**

```
% cancellation performance as a function of phase error only
phaseErr = 0.01:0.01:2;    % phase error
NCP = 10.*log10(2*(1 - cosd(phaseErr)));   % cancellation performance

%semilogx(y,NCP)
plot(phaseErr,NCP,'-dr','markersize',1.8)
```

```
grid on
%axis([0 5 -60 10])

xlabel('phase error(degree)')
ylabel('Noise Cancellation Performance(dB)')
```

E4: **Cancellation Performance as a function of Time delay Mismatch only**

```
% cancellation performance as a function of time delay only

B = 60e6;            % constant bandwidth
tau = 10e-9*(0.02:0.01:1);    % time delay
NCP = 10.*log10(2*(1 - cosd(B*pi*tau)));   % cancellation performance

%semilogx(y,NCP)
plot(tau,NCP,'-dr','markersize',1.8)
grid on
%axis([0 5 -60 10])
xlabel('Time Delay(ns)')
ylabel('Noise Cancellation Performance(dB)')
```

E5: **ANCT Model Manifest Report:**

ANCT_main

Analysis performed:
08-Sep-2014 11:29:50
Dependency analysis settings:

Analyze files in MathWorks toolboxes:
false

Analyze files in user-defined toolboxes:
true

Analyze M-files:
true

Find model references:
true

Find library links:
true

Find S-functions:
true

Analyze model and block callbacks:
true

Find code-generation files:
true

Find data files:
true

Analyze Stateflow charts:
true

Analyze Embedded MATLAB code:
true

Find Requirements documents:
false

Model Reference and Library Link hierarchy

ANCT_main

C:\Documents and Settings\ENG BUCHI\Desktop\ANCT TO USE FOR PHD\ANCT_main.mdl

(open)

72983 bytes
2014-09-08 11:26:16
true

Toolboxes required by this model

Communications Blockset (3.6)
MATLAB (7.5)
Signal Processing Blockset (6.6)
Simulink (7.0)

APPENDIX F:

Brief Theory of the Designed Digital Butterworth Band Pass Filter

The foremost design specification of the BBPF is to remove sideband noise emission from a co-located CDMA2000 on the WCDMA receiver front end. This requires eliminating the emissions above a certain cutoff frequency which involves specific amount of pass band ripples, stop band attenuation or transition width.

The major design requirement is to achieve a stable filter. The research work considered the application of Infinite Impulse Response (IIR) filter more suitable than the counterpart Finite Impulse Response filter (FIR) owing to the following considerations: (a) They typically meet a given set of specifications with a much lower filter order which has a cost implementation advantage, (b) They posses much better frequency response than the FIR of the same order and Exhibit small group delay of the same order with FIR with a short transient response to input stimuli.

Butterworth band pass filter was considered in the research in lieu to Chebyshev I, Chebyshev II, Elliptic and Bessel filters, which belong to the family of IIR due to its attributes to the least amount of phase distortion. Other enhanced features include; maximally flat response with no ripples both at the

pass band and stop band and provides the best Taylor series approximation to the filter response frequencies where $\Omega = 0$ and $\Omega = \infty$.

The output of the BBPF is expected to contain mostly the desired information. Hence, the filter design was centered predominantly on the magnitude response regarding other responses secondary. Consequently, for such condition to be achieved, required a sharp roll-off space for the filter. The research considered a guard band of 5MHz, taking into consideration the operating bandwidth of research interest to avoid wastage of the scarce resource. A 52dB rejection was the required magnitude specification for the BBPF design. The output result vividly interprets that any undesired signal (noise) that comes out of the filter must be 52dB lower than its original input signal.

The designed digital BBPF is characterized with the first 3-dB point at $0.49215\pi rad/sample$ and $0.50025\pi rad/sample$. The centre frequency was also significant in the study which demonstrates the point at which the filter achieves its maximum gain obtained as $0.4962\pi rad/sample$. The phase response of the desired filter showed no ripple or distortion both at the pass band and stop band edge frequencies. It is important to note that non-linear phase response in audio systems can cause noticeable phase distortion for the listener which may not be tolerable by the user. The filter showed relatively a constant

group delay towards the mid pass-band frequencies which implied that the waveform distortion of the designed filter was at its minimal level. Also the system showed symmetrical characteristics of the poles which did not fall outside the unit circle signifying the system stability. The designed filter consists of a cascaded 29 sections and a low filter order of 58. Implementation of the designed filter as a cascade of quadratic factor adequately provided a better control stability of the filter. On that note, the desired BBPF for sideband noise mitigation is a stable direct form II second order.

Evaluation of the optimal performance of the designed BBPF was obtained using the noise cancellation performance model which graphically illustrated the cancellation performance at 52dB in terms of amplitude imbalance; phase error and delay mismatch. It clearly demonstrated a minimal amplitude imbalance of 0.03, phase error of 0.14^0 and delay mismatch of 0.07ns. The hardware implementation of the designed filter should be installed at the CDMA2000 antenna front end to attenuate the presence of the undesired sideband noise that affects the WCDMA received signal power.